N88-16629

A REVIEW OF RESEARCH IN ROTOR LOADS

William G. Bousman
Research Scientist
U.S. Army Aeroflightdynamics Directorate
Moffett Field, California 94035

and

Wayne R. Mantay
Aeromechanics Division Chief
U.S. Army Aerostructures Directorate
Hampton, Virginia

ABSTRACT

The research accomplished in the area of rotor loads over the last 13 to 14 years is reviewed. The start of the period examined is defined by the 1973 AGARD Milan conference and the 1974 hypothetical rotor comparison. The major emphasis of the review is research performed by the U.S. Army and NASA at their laboratories, and/or by the industry under government contract. Important independent work is included in the review to keep an appropriate perspective on the field. For the purpose of this review, two main topics are addressed: rotor loads prediction and means of rotor loads reduction. A limited discussion of research in gust loads and maneuver loads is included. In the area of rotor loads predictions, the major problem areas are reviewed including dynamic stall, wake induced flows, blade tip effects, fuselage induced effects, blade structural modeling, hub impedance, and solution methods. It is concluded that the capability to predict rotor loads has not significantly improved in the time frame of the paper. Future progress will require more extensive correlation of measurements and predictions to better understand the causes of the problems, and a recognition that differences between theory and measurement have multiple sources, yet must be treated as a whole.

The development of comprehensive models for rotor loads must be the first priority of the government, but this development should be the responsibility of the government laboratories instead of their contractors. There is a need for high-quality data to support future research in rotor loads, but the resulting data base must not be seen as an end it itself. It will be useful only if it is integrated into firm long-range plans for use of the data.

Research in reducing rotor loads has sometimes been successful in the time frame of this paper, but the reasons have not always been understood. This research area should be productive in the future The major emphasis should be placed on understanding the fundamental mechanisms of vibration, and this should be accompanied by careful experimentation.

Presented at NASA/Army Rotorcraft Technology Conference, March 14-16, 1987, NASA Ames Research Center.

INTRODUCTION

"Instead of running into unexpectedly high loads almost everywhere the first time the full flight envelope is explored, we now only run into them occasionally, at some extreme flight condition." - Loewy, 1973

Rotor Loads Problem

The rotor of a vehicle in trimmed flight provides the necessary lift and propulsive force to sustain flight. The aerodynamic loads on the rotor will cause the blade to deform which will induce additional aeroelastic loads and deflections, and will affect the trim of the rotorcraft. The motions and deformations of the individual rotor blades will combine to impart shears and moments at the rotor hub. In turn, the fuselage will respond to these shears and moments, and modify the blade airloads and stresses. The complete problem of the loads and stresses on a helicopter is very complex; however, substantial progress has been made in the past by reducing the problem into smaller pieces. The aerodynamics of the rotor and its associated performance in forward flight can be understood to a substantial degree without considering the elastic deformation of the blades. In turn, the distribution of moments and stresses in the rotor blade and control system can normally be treated without considering the impedance of the rotor hub. And, lastly, the problem of the treatment of vibration within the fuselage can be approached even when the vibratory source in the rotor is not well understood. These three divisions--aerodynamics, rotor loads, and fuselage vibration--are useful in the design and analysis of a flight vehicle, but, to a degree, such divisions remain arbitrary. The scope of the present paper is the second division, rotor loads. For the purpose of this paper, rotor loads is meant to include both the aerodynamic loading of the rotor and its structural response.

The loads on a rotor include both a steady component and an oscillatory component that appears at harmonics of the rotor rotational frequency; that is, 1/rev, 2/rev, and so forth. The oscillatory component is sometimes referred to in the literature as the alternating load or half peak-to-peak load, but for this paper, the term oscillatory will be used to describe loads that have had the steady or mean value removed. In general, the rotor loads are dominated by the steady component and the first one or two harmonics. These are the loads that generally determine the fatigue life of the blade and controls, and are the primary interest of the rotor designer. At harmonics above the second, the loads become progressively smaller and often have little influence on the rotor structural design. However, it is these higher harmonic loads that are the source of vibration in the fuselage and their understanding is fundamental for progress in rotor loads predictive capability. For the purposes of this paper, the loads at the third harmonic and above will be termed the vibratory loads.

The characteristic behavior of rotor loads with increasing harmonic is illustrated in figure 1 using data obtained on a CH-34 rotor tested in the Ames 40- by 80-Foot Wind Tunnel (ref. 1). In this example, the airload at $r/R = 0.85$ is largest in the first and second harmonics and decreases quite rapidly as the harmonic number is increased. The flap and chord bending moments measured at $r/R = 0.375$ also decrease with the harmonic number, but show the influence of the blade elastic modes. This is particularly clear in this example for the chord bending moment, where the second chord mode is between 3 and 4/rev and the third chord mode is near 8/rev. In terms of blade design, what is of most interest is the fatigue loading and this is a function of the steady loads (which are not shown here) and the oscillatory loads, which in this case, are largely dominated by the first and second harmonics. In terms of vibratory loading, what is of most interest is the 3, 4, and 5/rev shears at the hub for this four-bladed rotor. The size of the steady component and first two harmonics of the rotor loads is such that it generally masks the behavior of the vibratory loads. Unfortunately, the vibratory loads are rarely shown by themselves and this has acted as an impediment to improved understanding.

Status of Technology in 1970s

The status of rotor loads prediction methodology in the early 1970s is best evaluated through two significant events. In March 1973 a "Specialists Meeting on Helicopter Rotor Loads Prediction Methods" was held in Milan under AGARD sponsorship (AGARD CP 122) and was attended by most of the major helicopter manufacturers who presented examples of correlation between their flight test data and their analytical methods. These same prediction methods were used again in February 1974 to predict the loads of a hypothetical helicopter rotor at the Specialists' Meeting on Rotorcraft Dynamics sponsored by NASA Ames Research Center and the American Helicopter Society (ref. 2).

Examples of correlation with flight test data from the Milan AGARD meeting are shown in figures 2 to 4 (refs. 3, 4, and 5, respectively). The predictions of the Boeing Vertol C-60 analysis (ref. 3) show quite good agreement for the pitch link waveform for the aft rotor of a CH-47C aircraft under stall conditions. The agreement for the oscillatory flap bending moment is not as good and it is not clear that the nonuniform downwash model is better than the uniform downwash model. Calculations using the Sikorsky Normal Modes Analysis, Y200, for an articulated single rotor show that a constant inflow model gives nearly the same results for oscillatory loads as the variable inflow model. However, when compared on a time-history basis, the variable inflow model shows better agreement with higher harmonics. On the basis of oscillatory loads, correlation of C81 with data from UH-1D flight test is quite good.

In his assessment of the prediction technology shown at the Milan meeting, Piziali expressed his belief that advances in the previous decade had been primarily in the scope of predictive capability and not accuracy (ref. 6). He felt that the structural problem was in hand, but that the analyses were limited by the

aerodynamic model. This view was not shared by other observers at the Milan meeting. Loewy, in his meeting summary (ref. 7), said that the major development problems of the previous decade had been in the area of structural dynamics. He also felt that major progress had been made in the predictive analyses, particularly in reducing the potential for surprises in new designs.

The importance of the 1974 hypothetical rotor comparison of Ormiston (ref. 2) was that it provided a test of the various comprehensive models for one hypothetical rotor configuration. Figure 5 shows that even for identical blade properties, the rotating natural frequencies calculated in a vacuum with the different math models showed significant differences. The range of variation for the oscillatory blade moments is shown in figure 6 (taken from ref. 8) and shows that the various analyses disagreed widely, especially for the torsional behavior. As a result of the comparison, it was apparent that there were significant problems in one or more of the competing analyses, but as there was no experimental data with which to compare, there was no obvious "right" or "wrong" answer. Ormiston's recommendations for future research were:

1. Continue to make standardized comparisons.

2. Assess in detail the assumptions and semi-empirical factors used in the analyses.

3. Perform fundamental experimental research in the areas of dynamic stall, blade/vortex interaction, and three-dimensional flow effects.

4. Compare the prediction methods (after some progress with items 2 and 3 above) with experimental data from the test of a full-scale rotor in a wind tunnel.

Survey Articles

In the years since the Milan AGARD meeting and the hypothetical rotor comparison of Ormiston, there have been a number of assessments of rotor loads prediction methodology. Arcidiacono and Sopher examined the United States progress in rotor loads predictive capabilities at the AGARD conference on the "Prediction of Aerodynamic Loads on Rotorcraft" held in London in 1982 (ref. 8). They concluded that a good deal of fundamental work had been done with regard to dynamic stall, blade/vortex interaction, and three-dimensional flow effects. In addition, they felt that the modeling of the structure had improved, both in terms of the physics of representing the rotor blade and in the design of structured computer programs. However, it was unclear at what point these analytical advances would be integrated into analyses. They noted that the older analyses were not easily modifiable without a substantial investment of time and money. They expressed optimism that with the development of the Second Generation Comprehensive Helicopter Analysis System (2GCHAS), these advances could be introduced in a controlled and efficient manner.

Johnson assessed the state of rotor loads prediction in a survey paper that covered the entire area of rotorcraft dynamics (ref. 9). He compared predictions

made at the 1973 Milan meeting with more recent calculations shown in the literature, and pointed out that, in general, the analyses are able to calculate the mean and oscillatory loads; but, that an examination of the time histories reveals that the fundamental phenomena are not being modeled correctly.

Friedmann addressed advances in rotorcraft aeroelasticity in a number of survey articles (refs. 10 and 11) and, although these do not deal with the predictive capabilties of the rotor loads analyses, they do provide useful summaries of advances in structural modeling and dynamic stall.

Johnson also provides a detailed survey of recent developments in rotary-wing aerodynamic theory (ref. 12). The survey pays particular attention to efforts in lifting surface theory, panel methods, transonic theory, and transonic blade-vortex interaction analyses. In his treatment, he makes a number of useful comparisons to the equivalent fixed-wing formulations. He concludes that lifting-line theory will remain the basis for rotor-aerodynamic calculations as long as it is the only theory that can accurately include viscous effects. He feels that work should continue toward the goal of turbulent Navier-Stokes calculations for the entire aircraft although there is no immediate expectation of success in this area.

A restricted class of survey articles (nonetheless very useful), are papers that summarize the application of rotor loads technology within a company. Gabel (ref. 3) has provided a useful discussion of how the rotor loads analyses are used at Boeing Vertol, and Yen and Glass (ref. 13) have done the same for Bell Helicopter Textron and included a historical perspective as well. Dadone (ref. 14) has discussed the application of the aerodynamics technology to the rotor design and has shown how it has evolved over the years at Boeing Vertol. Landgrebe (ref. 15) has discussed the evolution of the rotor-wake geometry representation at the United Technologies Research Center (UTRC) and at Sikorsky.

Organization of Paper

This review of rotor loads research is divided into two main sections: research into understanding and improving the capability to predict rotor loads, and research into means of reducing rotor loads. Within the first section, the discussion is organized by breaking the loads problem into the aerodynamics model, the structural model, and solution methods. Within the section on rotor loads reduction, the major topics are investigations into effects of blade tailoring, control of blade loads through kinematic coupling or control system design, and aerodynamic tuning devices. Following these main sections, rotor loads in the presence of gusts and maneuvers is discussed. In the concluding part of the paper, an assessment is made of the progress that has occurred in the rotor loads area in the last 15 years. The role of the U.S. Army and NASA in this process is discussed and some conclusions and recommendations are made as to the major emphasis that should be taken in the years to come.

Two Themes

Two themes will appear and reappear in this paper. The first of these themes deals with the balance between analysis and synthesis, and the second deals with the question of whether progress in controlling rotor loads can be made without understanding the basic mechanisms. The place of analysis in rotor loads research is well established, especially in the goverment laboratories and academia. This process of analysis, the breaking down of a problem into its constituent parts, examining each part in detail, and performing theoretical work and experiment to obtain improved understanding, has often been repeated. But, the process of putting the various pieces together again (which is referred to here as synthesis), is not so easy. To take the improved understanding, and to put the constituent parts back together again and understand their interrelationships, is not done well nor is it done often. When it is done, it is usually within the industry where the need is imperative. The balance between analysis and synthesis is the first of these themes.

The ultimate objective of research in rotor loads is not just the understanding of the fundamental mechanisms involved, but rather to be able to design improved rotor systems. The problem of rotor loads prediction is so intractable that to progress in this area, it is necessary to pursue not just the basic research into rotor loads, but to also pursue research in loads reduction even if the mechanisms to be used are only guessed at. A great deal of effort has been placed on experimentation in recent years--to parametrically vary major rotor properties and to measure the resulting improvement. This research has often been guided by a substantial amount of careful thought and the results have provided insight into the rotor loads mechanisms. The reduction of rotor loads through feedback control is the ultimate extension of this approach. But it must be recognized that the control of rotor loads, either through empiricism or feedback, is a complementary approach; it is not a substitute for research into the mechanisms of rotor loads. This is the second theme, the balance between reducing the rotor loads and understanding the physics.

ROTOR LOADS PREDICTION

> "For a good prediction of loads it is necessary to do everything right, all of the time. With current technology it is possible to do some of the things right, some of the time." - Johnson, 1985

Comparisons of measured rotor loads and prediction methods normally show both areas of agreement and places where things are not right. A number of approaches are made to understand the sources of disagreement and these can be generally categorized as: (1) fundamental investigations of the physics, (2) theoretical and experimental tests of simplified models, and (3) theoretical and experimental tests of the complete model, that is, of the rotor itself. Examples of all three of these approaches will be shown in this section.

For the purposes of this review, research into rotor loads prediction will be broken down into the aerodynamics model, the structural model, and solution methods. The aerodynamics model will be further broken down into dynamic stall, the wake-induced flow, blade-tip effects, and fuselage effects. The structural model discussion will include topics involving the blade structural properties and the influence of the fuselage impedance.

Dynamic Stall

The work of McCroskey and Fisher (ref. 16) with a model rotor that had pressure transducers installed at $r/R = 0.75$ and skin friction gages to characterize the boundary layer behavior, provided a clear description of the sequence of events involved in the dynamic stall of a rotor over the inboard section of the blade. To properly model the dynamic stall process, it is necessary to account for the lift overshoot and the large pitching moment changes that are related to the vortex that is shed from the blade leading edge. Johnson (ref. 17) used the Sikorsky Y200 analysis to test three of the early empirical models: the α, A, B Method developed at UTRC (refs. 18 and 19); the MIT Method (refs. 20 and 21), and the Boeing Vertol Method (ref. 22). The elastic torsion angle for a highly loaded rotor at $\mu = 0.333$ calculated with these models is shown in figure 7. As only one torsion mode was used, the blade-torsion moment is directly proportional to the elastic deflection. Even though the blade dynamics are identical for the three models, the predicted torsion behavior shows significant differences, particularly in the third and fourth quadrants of the rotor.

Sikorsky derived a simplified dynamic-stall model based on a universal nondimensional time constant, $\tau = U_o \Delta t/c$, where Δt describes the start of a stall event determined from two-dimensional (2-D) measurements, U_o is the free-stream velocity, and c the chord length (ref. 23). They tested the predictive capability of this time delay model and the α, A, B Method by comparing first with a simplified experiment, and second with flight-test data (refs. 23 and 24). The simplified

experiment was a test of a 2-D airfoil mounted on a torsion spring and oscillated in and out of stall at 1/rev. The torsion spring was sized to provide an appropriate torsional natural frequency with respect to the 1/rev of the primary oscillation and in this way to simulate stall flutter. These 2-D model tests were representative of full-scale, 3-D tests in ways that were not anticipated, including considerable cycle-to-cycle variation and unresolved ambiguities when the measurements were compared to theory. The time delay method tended to overpredict the 2-D test results and underpredict the 3-D, full-scale test results. Pitch-link loads predicted with the Y200 analysis using the two methods are compared with flight-test data in figure 8. The test data show that the blade stalls at an azimuth of about 190°, and this is not shown by the calculation. The α, A, B Method predicts some stall on the second stall cycle at about 250° while both methods show substantial stall on the third stall cycle. The α, A, B Method shows better agreement in terms of amplitude of the pitch link oscillation.

All of the dynamic stall models are empirically derived from experimental data, normally 2-D wind tunnel tests of oscillating airfoils. McCroskey (ref. 25) used data from an NACA 0012 airfoil tested in the U.S. Army's 7- by 10-Foot Wind Tunnel at Ames (ref. 26) to test the predictions of five empirical dynamic stall models. In addition to the three models that had been examined previously by Johnson, he also included two time delay methods (refs. 23 and 27) and a method derived by Lockheed (ref. 28). The methods were evaluated for their ability to predict the phase angles of lift and moment stall, and maximum values of the normal force and pitching moment coefficients. No single method was notably better than the others, and each was deficient in some area of prediction.

A new empirical model for dynamic stall that has been developed and integrated into the Sikorsky analyses is reported by Gangwani (refs. 29-31). As in the α, A, B Method, this model uses the angle of attack and pitch rate as major parameters, but the angle of attack acceleration term, B, is replaced with a parameter that accounts for the time-history effects of changes in angle of attack and is based on the Wagner function. Lift, pitching moment, and drag are all determined as functions of these parameters where the functional behavior is determined from a least squares fit of 2-D oscillating airfoil data. The comparison of this empirical model and available 2-D oscillating airfoil data (ref. 30) is more extensive than for any of the other dynamic stall models. However, only limited comparisons with flight test data are shown. Gangwani (ref. 32) has also integrated this empirical model into a rotor loads analysis based on a model developed at Rochester Applied Science Associates (RASA) and described in reference 33, and has compared the results with data obtained from flight test of an AH-1G (ref. 34). The use of the synthesized-stall data does not improve the flap or chord bending moment correlation, but does show an improvement in the modeling of the torsion moment.

There have been no direct comparisons of the various dynamic stall models since Johnson (ref. 17), nor are there any extensive comparisons between any of these models and flight test data published in the literature. Future comparisons should include the ONERA dynamic stall model (ref. 35) with the extensions recommended by Peters (ref. 36). Any extensive correlation with flight test data may have to model

the fuselage induced flow as well. As shown by Wilby et al. (ref. 37) the upwash from the fuselage may increase the blade angle of attack sufficiently to cause stall over the nose of the aircraft. The stall-induced pitch-link load that is seen in figure 8 at a blade azimuth of about 190° for the CH-53A may be a result of this phenomenon.

The dynamic stall models in use today are empirically based on 2-D airfoil data. Near the blade tip, the blade stalling process will be 3-D and in some situations, the interaction of a previous blade's vortex will also induce a 3-D form of stall. Brotherhood and Riley (ref. 38) show the rotor blade of a Wessex helicopter in two different kinds of stall as visualized by pressure transducers mounted in the blade's leading edge. The pressure time histories are shown in figure 9 as a function of the blade azimuth. The first stall event appears at $r/R = 0.90$ and is seen to move outboard. This event corresponds to the passage of the previous blade's vortex across the tip of the blade. The flow reattaches after the passage of the vortex, and then a second stall event is seen on the three outer blade stations, but this time the stall is simultaneous. How such complicated events can be modeled (or even if they need to be) is unclear. One useful approach has been taken by Costes (ref. 39) who has made experimental measurements on an oscillating half-span airfoil and compared the unsteady pressure measurements to calculations which were based on an extension of the ONERA dynamic stall model to three-dimensions. It appears that the blade lift can be estimated satisfactorily with this model, but the pitching moment cannot. This problem will become more important as variation in tip planform is used more frequently in the design of new rotors.

Wake-Induced Flow

In his seminal paper (ref. 40) Hooper has examined seven sets of airload measurements made on full-scale rotors using Cartesian, 3-D plots to visualize the data obtained in flight or wind tunnel tests. He has demonstrated that the low-speed (or transition) flight regime vibratory airloading is dominated by the interaction of the blade and the preceding blade's tip vortex first on the advancing side of the disk and then on the retreating side. This behavior is seen regardless of rotor type or blade number. At higher speeds, it appears that the greatest part of the vibratory airloads is caused by events on the advancing side of the disk, but in this case, there appear to be substantial differences which are due to rotor type or blade number. The low-speed or transition case will be discussed first as this has drawn the most attention of investigators in the past. The high-speed vibratory loading will be discussed at the end of this section on wake-induced flow.

An example of the low-speed vibratory loading is shown in figure 10 in the manner of Hooper using the data of reference 41. On the advancing side of the disk, there is a down-up pulse in the airload as the blade passes first through the downwash, and then the upwash, of the preceding blade's tip vortex as that vortex moves inward on the blade. On the retreating side, there is an up-down pulse as that same vortex moves radially outward on the blade. To properly calculate the wake induced

airload, it is necessary to correctly model the wake geometry, the vortex strength, and the blade-vortex interaction.

The advent of the digital computer has made feasible the calculation of the induced flow including the effects of a realistic wake representation. By the start of the time period covered in this paper, the use of a prescribed wake, that is, a wake where the tip and root vortices are assumed to follow a prescribed helical pattern, was well established. In addition, calculations using a free wake, where the wake geometry is modified by self-induced effects, had been developed and applied to a number of problems (refs. 15 and 42).

The free-wake calculations have shown that distortions of the wake geometry are primarily in the vertical or axial direction. In the plane of the rotor disk, the wake geometry lies very close to the cycloidal pattern of the prescribed wake. This has been shown from flight testing of pressure-instrumented rotors where the vortex passage can be identified from the characteristic up-down or down-up pulse in the measured pressure. Measurements obtained using a Puma helicopter (ref. 43) are compared with the cycloidal geometry in figure 11 and show little distortion in the disk plane from advance ratios of 0.11 to 0.35. Landgrebe and Bellinger (ref. 44) have compared their free-wake calculation to the measured axial geometries obtained by Lehman in a water tunnel (ref. 45) and have achieved good results. Johnson (ref. 46) has compared a free-wake analysis to the laser-velocimeter measurements of the wake geometry of a two-bladed rotor in a wind tunnel which were obtained by Biggers et al. (ref. 47) and has also demonstrated good agreement. However, he notes that in this case, the tip-path plane angle of attack was sufficiently large so that the difference in axial-wake position predicted with either the prescribed or free wake had no effect on the blade loading.

The predictions of wake geometry using free-wake analyses appear good in those cases where data are available, but the predictions of the airloads and blade bending moments have not been done as well. Egolf and Landgrebe (ref. 48, summarized in ref. 49) and Yamauchi et al. (ref. 50) have compared the analytical predictions of a rotor loads analysis that includes a free-wake model with measurements of blade airloads and structural loads obtained in flight. Figure 12 compares the blade airloads measured on the CH-34 rotor at the 0.90R radial station (the same case as was shown in fig. 10) with predictions using both prescribed and free-wake analyses (ref. 48). The data show the influence of the blade-vortex intersections on the advancing and retreating sides of the disk. The prescribed-wake calculation shows similar behavior, but the load is much reduced in strength. The free-wake calculation shows multiple tip-vortex intersections (that is, intersections with two or more tip vortices from the preceding blades), but these are not apparent in the test data. The analysis predicts very high blade airloads due to the initial intersection, much higher than those measured in the test, as these calculations show a direct intersection of the tip vortex and the blade. The resulting blade flap bending moments using the free-wake analysis, coupled to the Sikorsky Y200 rotor loads program, are shown in figure 13. The airload peak seen in figure 12 is highly localized so its impact on blade loading is not severe. Both the theoretical prediction and the measured loads are rich in higher harmonics, but except for the

loading at about 270° azimuth, the agreement in amplitude and phase is not particularly good.

Yamauchi et al. (ref. 50) compare predictions using the prescribed and free-wake analyses of CAMRAD with flight-test data for the Aerospatiale SA 349-2. Airloads data for this test program were obtained at r/R = 0.75, 0.88, and 0.97. The CAMRAD predictions for lift coefficient are compared in figure 14 with the measurements made at 0.88R and an advance ratio of 0.14. As with the CH-34 results, the data show loads caused by the blade vortex interaction on both the advancing and retreating sides of the disk and the free wake provides a better prediction of the loading induced by the vortex wake. Again, as with the CH-34 case, the theoretical predictions show multiple vortex intersections that are not apparent in the data. The core size used in the CAMRAD free-wake prediction shown here has been determined after an a posteriori fitting of the data. Calculation of the flap bending moments for the SA 349-2 using the free-wake analysis show mixed results with good agreement at the blade midspan, but poor agreement elsewhere.

The influence of blade vortices at high speed is not as clear as for the low-speed transition case. Figure 15 shows the vibratory loading measured on the CH-34 rotor in the 40- by 80-Foot Wind Tunnel at an advance ratio of 0.39 (refs. 1 and 51). A strong, impulsive loading is seen on the advancing side of the disk, but unlike the low-speed case, the load is an up-down pulse, suggesting that the blade is encountering first an upwash and then a downwash. Miller (ref. 52) has proposed that, because the outer portion of the blade is negatively loaded for this case, that two vortices of opposite sign are trailed from the blade as shown in figure 16. An analysis of this case made using a number of simplifying assumptions, including fixing the position of the midspan or inboard vortex, shows good agreement with the measurements as shown in figure 17. This progress is encouraging, as Hooper has shown in reference 40 that neither the Boeing Vertol C-60 analysis nor CAMRAD show satisfactory agreement for this case. (However, note that Phelan and Tarzanin, ref. 53, have reported correcting a programming error in C-60 and now show much better agreement for the airloads in this case.)

The importance of the blade-vortex interaction studied in the CH-34 high-speed case is not entirely clear since it appears to be strongly related to the amount of negative lift on the advancing side of the disk. The CH-34 which was studied in the 40- by 80-Foot Wind Tunnel was operated at reduced lift (about 60-70% of the lift for normal flight), and data on the XH-51A and NH-3A compound aircraft studied by Hooper were obtained with some of the lift provided by the aircraft wing. Unfortunately, there are few high-speed data available for conventional rotors. The maximum speed case studied for the CH-53A aircraft was an advance ratio of 0.32 and the vibratory loading is quite different from that seen in figure 15. Measurements made on the outer blade stations of the SA 349-2 at an advance ratio of 0.38 do not show any clear evidence of vortex-induced loads (ref. 54). However, model-scale data acquired on the Boeing Vertol Model 360 rotor (ref. 55), show airloads that are remarkably similar to the CH-34 airloads as shown in figure 18.

Application of free-wake calculation techniques to rotor loads requires first, that the physics of the phenomena be correctly modeled and second, that the wake

calculations be efficiently integrated into the rotor loads calculation. It seems evident from the research with the free-wake models that the first step has not yet been achieved. It is not possible at this time to accurately model the free wake. However, some progress has been made in making the calculation more efficient. Egolf and Landgrebe (ref. 48) have approached this problem for their free-wake calculations by constructing an approximate or generalized model of the wake, and in this fashion, reduced the computational time by a factor of a thousand.

Young (ref. 56) has taken a different approach to the problem of an efficient wake calculation by starting with a simplified wake model that is very efficient and then modifying it step-by-step to see how much improvement is obtained and at what cost in computation time. Young models the near wake with rigid semicircles of constant vorticity whose radius varies as the blade moves around the azimuth, and the far wake as a series of vortex rings. As vortex rings will not give the same blade vortex intersection as a cycloidal path, the actual intersection geometry is used to fix the outer position of the wake vortex rings. Figure 19 compares the flap bending moments measured on a Puma with the original vortex ring model, and the vortex ring model with the improvements discussed by Young in reference 56. The representation of the higher harmonic loads appears reasonably accurate in both amplitude and phase.

Alternative approaches to the calculation of aerodynamic loading have been devised using the acceleration potential. Costes has demonstrated the feasibility of this method and compared his results to rotor measurements obtained in a wind tunnel (ref. 57). Runyan and Tai (ref. 58) have developed a similar approach and made limited comparisons with model rotor loads measurements. Pierce and Vaidyanathan (ref. 59) have applied the method of Van Holten (ref. 60) to the prediction of the airloads measured on the CH-34 in flight and in the wind tunnel. In general, the prediction of the oscillatory loads is good, but the prediction of harmonics beyond two is difficult to judge as they are masked by the first and second harmonics.

Blade-Tip Effects

The calculation of rotor loads based on lifting-line theory normally accounts for the reduction of lift at the blade tip by introducing a tip-loss factor for the blade normal force, but the chordwise force is assumed to extend to the blade tip. When the wake-induced flow is calculated by a prescribed or free wake then the radial distribution of bound vorticity is determined as part of the solution. Johnson (ref. 46) has compared the calculated bound vorticity using a free-wake analysis to measurements obtained with a laser velocimeter on a model rotor in a wind tunnel (ref. 47) and these show fairly good agreement, particularly near the tip. This comparison was made at an advance ratio of 0.18 and it is expected that the calculation problem will become more difficult at higher speeds as transonic effects begin to dominate the loading.

A great deal of progress has been made in recent years in developing finite difference codes to analyse the flow over an advancing blade including the effects

of shocks and unsteadiness. Caradonna and Tung (ref. 61) have provided a comprehensive discussion of the present status of these codes and have compared a number of the code predictions with surface pressures measured in nonlifting and lifting rotor experiments. At the present time, the codes are being integrated into comprehensive analyses either in a partially coupled manner (ref. 62) or as a post-processor (ref. 55). In the former case, the comprehensive analysis (CAMRAD in ref. 62) is used to obtain the trim solution and then to provide the finite-difference code with a partial inflow distribution along the blade. The calculated inflow from the comprehensive analysis excludes the influence of the trailing vortex sheet that is calculated as a part of the finite difference grid. The finite difference program, in turn, provides the comprehensive analysis with an improved estimate of the blade lift. The solutions are matched when there is no change in lift from one iteration to the next. The blade pitching moment and drag are not coupled in this manner, and spanwise discontinuities in calculated properties are allowed at the grid inner boundary. There is great optimism as to the utility of these new methods, but the applications are in their infancy.

Fuselage Flow Effects

The U.S. Army developed four prototype aircraft in the early 1970s to meet the needs of their utility and attack helicopter missions. All of these prototypes encountered severe vibration problems, and in each case, the rotor shaft was extended; as a consequence, the vibration was reduced. There was a great deal of intense activity at that time to understand the problem, but because of the competitive aspects of the developments little information was published. (An account of some of these problems was given by Gabel in a panel at the 2nd Decennial Specialists' Meeting on Rotorcraft Dynamics held at Ames in 1984, ref. 63.)

The effect of a fuselage on the air flow during flight will be to cause an upwash on the forward side of the disk and a downwash on the rearward side. This will cause a 1/rev variation in the induced flow at the rotor disk and will affect the rotor loads. The rotor wake may also impinge on the fuselage and cause vibratory excitations. Wilby et al. (ref. 37) have presented results from model tests with and without a fuselage. The flap bending moments measured at an advance ratio of 0.3 are shown in figure 20 for this model. Although the fuselage causes a 1/rev variation in the induced flow, the effect on the blade is to cause an increase in the 5/rev moments at 400 rpm and 4/rev moments at 600 rpm. In both cases, the increased loading corresponds to the second flap mode frequency. Similar effects are seen in experimental measurements reported by Freeman and Wilson (ref. 64).

Huber and Polz (ref. 65) have used an analytical model to examine the effect of the fuselage aerodynamics on the blade loads. Figure 21 shows that the calculated effect of the fuselage is to cause an upwash over the nose of the aircraft and a downwash over the tail. The greatest effect is seen in the 2 and 3/rev loads. Huber and Polz note that the upwash is a maximum at about 0.4R and that this corresponds to the antinode of the second flapping mode and explains why the second flap mode responds so strongly to the fuselage induced flow.

The effect of the fuselage on full-scale rotor loads has been studied by Jepson et al. (ref. 66) using flight test data, wind tunnel data, and calculation. Figure 22(a) shows flap bending moments measured at 0.70R on an S-76 rotor in flight and in the Ames 40- by 80-Foot Wind Tunnel (ref. 67). Figure 22(b) shows calculations using Y201 for the S-76 rotor alone and for the rotor with the aircraft fuselage. The calculations show that the effect of the fuselage is to cause a significant increase in the 3/rev flap bending moments. This same sort of increase is seen in comparing the flight-test results with the wind tunnel measurements. In the wind tunnel, the rotor was mounted on the Ames Rotor Test Apparatus (RTA). Calculations in reference 66 show that the S-76 fuselage increases the angle of attack about 1° over the fuselage nose compared to the predicted effect of the RTA.

The theoretical calculations discussed above have all represented the fuselage using potential flow-panel methods. Johnson and Yamauchi (ref. 68) have used a modification to slender body theory to represent the fuselage and have shown that this approach gives the same results as did a panel method for axisymmetric bodies at zero angle of attack, but at a much lower computational cost. Typically, the use of the modified slender body theory increases the computational run time (including a prescribed wake) by only 10-20% with respect to an isolated rotor calculation. Using this approach, the influence of the RTA on rotor loads has been estimated (ref. 69) and it was shown that the flap bending moments increase by 5-10% and the chord bending by 10-15%. The effect on pitch-link loads is negligible. The measurement of rotor loads on the RTA, therefore, is a reasonable approximation of isolated rotor conditions.

The measurements and calculations made in the last decade examining the effects of the flow induced by the fuselage have all shown a significant effect on higher harmonic loads. It seems clear from this perspective that testing future improvements to rotor loads prediction methods will be fruitless unless the effect of the fuselage induced flow is accounted for.

Blade Response

A substantial amount of research has been performed in the last 10-15 years to understand the influence of the blade structural, inertial, and kinematic properties of the rotor loads. A great deal of this research has been directed toward loads reduction and this will be discussed in more detail below in the Rotor Loads Reduction section. The emphasis of the material covered here under the Blade Response heading is the improved understanding of how the rotor responds to the aerodynamic loading.

The understanding of rotor loads is greatly enhanced when the source of the blade loads can be identified by harmonic and blade mode. In the 1973 Milan AGARD meeting, McKenzie and Howell (ref. 70) compared the Westland rotor loads analysis with flight-test data from the Lynx; examples are shown in figures 23 and 24. In figure 23, the 4/rev rotor hub pitch and rolling moments are broken out by the proportion of the moment that occurs in the first three flapping modes. As the 4/rev hub moments are the primary source of vibratory loads on the Lynx, this

technique is valuable; first, in identifying which blade modes are most important for vibration reduction, and second, to judge how well these loads can be predicted. (Note that the modal contributions cannot be directly measured from flight test, but are obtained by using the blade-bending moment data to estimate the amplitudes of the modes as generalized coordinates. This technique has been used by other investigators (refs. 71 and 72), but none of these references discuss the technique or its limitations in any detail. It appears that the method is similar to the formalism of the Strain Pattern Analysis Method (refs. 73 and 74).) Figure 23 shows that the second-flap mode contribution is most important for the Lynx as determined from flight measurement, but that the theory predicts approximately equal effects from both the second- and third-flap modes. Figure 24 compares the theory and flight-test estimates for the second mode deflection for three harmonics of blade loading. The 1/rev deflection is overpredicted, while the 2 and 3/rev deflections are underpredicted. This approach to comparing measurement and prediction provides a better assessment of the rotor behavior and the validity of the prediction model than more typical approaches that are based on the comparison of oscillatory loads or azimuthal waveforms.

Blackwell and Commerford (ref. 24, summarized in ref. 75) have made an extensive theoretical investigation of the means of reducing stall-induced loads. One of the advantages of the theoretical approach is that it is relatively straightforward to break down the various components of a load to understand what is the primary cause and what can be done to reduce its influence. In that study they calculated that a reduction in torsion frequency would reduce the stall-induced pitch link loads. Figure 25 shows the torsion moment at the root caused by the aerodynamic pitch moment; the moment caused by the inertial loads; the moment caused by deflection and shear of the blade, and their sum. The plot shows one rotor revolution starting at 180° to better illustrate the stall-flutter behavior. For this articulated rotor, the effect of blade deflections in combination with shears has only a small effect; the largest effect is caused by the aerodynamic pitching moment and the inertial moment which are of opposite phase. The change in torsional frequency does not change the aerodynamic pitching moment very much, but does reduce the inertial load and this accounts for the calculated reduction in the root moment. It is expected that shear/deflection loading will be much more important for hingeless and bearingless rotor designs.

Extensive data have been obtained in the Langley Transonic Dynamics Tunnel (TDT) on the conformable model rotors and the data show that the tip design, blade camber, and torsional stiffness all have a substantial influence on the rotor loads (refs. 76 and 77). These data are discussed in detail in the Rotor Loads Reduction section, but mention is made here because the data have stimulated additional work by Blackwell and Kottapalli to understand the reasons for the observed changes in rotor loads.

Blackwell (ref. 72) has re-examined the data obtained in the TDT and has fitted the measured blade bending moments with calculated modal moments to identify the generalized coordinates. He states that the hub shears calculated in this fashion "trended directly" with the loads measured on the rotor balance, although no results

are shown. The major differences seen in comparing the rectangular- and swept-tip configurations are the reductions in the 3/rev vertical shears at the hinge, and the 3 and 5/rev inplane shears at the hinge for the swept tip. The generalized coordinate amplitudes show that most of this reduction is in the second flap mode.

Kottapalli (ref. 78) has taken a purely theoretical approach to better understand the changes in rotor loads that were seen as the model blade-tab deflection was changed in the TDT tests. Using the Sikorsky Y201/F389 family of programs he shows that the reduction in 4/rev vertical root shears is related to reductions in the blades' 4/rev angle of attack distribution. The angle of attack reduction is calculated to be due to reductions in elastic torsion (42%), elastic flapping (39%), and inflow (19%).

The complementary approaches of Blackwell and Kottapalli are useful in providing an improved understanding of rotor loads behavior, but both approaches have substantial limitations. The experimental approach of Blackwell can break the problem down to a certain level, but not to the individual terms of the equations of motion. Relationships between different properties can be demonstrated experimentally, but the cause and effect cannot necessarily be derived. The theoretical approach, however, can break the problem down to the level of the individual terms of the equations of motion and, in some cases, clearly demonstrate cause and effect. However, the inability of the analysis to predict rotor loads as measured in flight test makes the analysis untrustworthy.

Blackwell has also looked at the effects of spanwise mass distribution on vibratory loads in reference 72. Based on a simple analytical representation, he suggests that the distribution of spanwise mass should modify the blade-root shears which depend upon the product of the airload distribution and the mode shape. Taylor (ref. 79) has pursued this approach and examined the sum of the modal root shear contributions for all blades and derived a Modal Shaping Parameter which is defined as

$$\text{MSP} = \frac{(\text{Modal Shear Integral}) \times (\text{Generalized Force})}{(\text{Generalized Mass})}$$

Taylor assumes the airload can be represented as a polynomial in the radial coordinate and, once the loading is defined, that the modal shaping parameter provides a design method to seek a reduced vibratory load. Taylor extends this approach in reference 80. In this study he uses the G400 analysis to calculate the rotor loads and breaks down each component into essentially the terms of the equations of motion. Figure 26 shows an example of the calculation of 3/rev lateral shears where each component of shear is identified in terms of amplitude and phase. As changes are made to the blade design based on the modal shaping parameter, then the behavior of each component of the vibratory shear can be observed, and insight into the loads behavior obtained. This approach holds great promise once more reliable analyses are developed as the reduction in rotor loads will be accompanied by an understanding of the system behavior. This must be contrasted with the formal optimization

approach where an understanding of the physics is not necessary to the achievement of loads reduction.

Another approach to understanding the blade response problem has been taken by Esculier and Bousman (ref. 81) who have calculated the blade response for the CH-34 using measured airloads. This approach avoids the question of the adequacy of the aerodynamic model by substituting measurements, and in this way, the adequacy of the structural model can be evaluated. Figure 27 compares the measured moments from reference 1 with calculations for the first harmonic of blade loads. Two calculations are shown for the flap and chord bending moments: an uncoupled calculation and a coupled calculation assuming the flap and chord motions are coupled through the local pitch angle. The comparison of the flap bending moments show very good agreement between the measurements and the calculations based on measured airloads. This good agreement is, in general, obtained through the ninth harmonic. This means that for relatively simple rotors such as the CH-34, the flap bending loads can be calculated quite precisely if the aerodynamic model is correct.

This is not the case for the chord loads as neither the coupled or uncoupled calculations accurately predict the blade chord bending moments. Two reasons for this were identified in reference 81. First, the chord airloads are not measured directly, but are obtained from the flap airloads, and second, the CH-34 hydraulic damper is represented as a linear viscous damper, but the data suggest that it also acts as a relatively strong spring. The blade torsional moments appear fairly well predicted using the measured pitching moments, especially in phase, but as pointed out in reference 81 the calculation of torsional moments is sensitive to the control system stiffness and that was not measured in reference 1.

The adequacy of blade structural modeling has also been assessed by testing of rotors in a vacuum. Lee (ref. 82) measured modal frequencies and displacements of a rotating, cantilevered UH-1D blade in a vacuum chamber and obtained good agreement with prediction for the lower frequency modes as long as they were not strongly coupled. The mode shape prediction was not as good for the higher frequency and more strongly coupled modes. Srinivasan et al. (ref. 83) have made frequency and modal strain measurements of a torsionally soft model rotor spinning in a vacuum chamber. These measurements may become useful for validating the prediction of structural models because of the extensive model properties documentation that have been obtained for these blades (ref. 84).

Fuselage Impedance

Rotor loads predictions are normally made assuming the rotor is mounted to an infinitely stiff structure. One exception to this is that Bell Helicopter Textron models the pylon flexibility in calculating the rotor natural frequencies and mode shapes used by the C81 analysis for their two-bladed rotor designs. Yen and McLarty (ref. 85) have shown the importance of modeling the pylon impedance for the calculation of rotor loads, and an example for the OH-58A is shown in figure 28. The effect of the pylon impedance on the oscillatory loads is clearly shown here and it has also been shown by measurements in wind tunnel tests (ref. 86).

Sopher et al. (refs. 87 and 88) have reported on the development of an analysis that couples the Sikorsky G400 rotor loads analysis to a fuselage model and allows the calculation of rotor loads and vibration. These calculations showed that the hub impedance has a large effect on the rotor loads when a rotor frequency is close to an N/rev. However, the predicted effect was very sensitive to the fuselage representation used and the reasons for this were not determined.

Gabel and Sankewitsch (ref. 89) have reported the development of a method to couple the Boeing Vertol C-60 rotor loads analysis to a fuselage representation through an impedance-matching technique. The fuselage impedance is shown to have a significant effect on the hub vibratory loads, but the effect on blade loads is not discussed.

Solution Methods

The modal blade representation used for the solution of the rotor equations is usually based on a set of uncoupled or coupled rotating modes (ref. 2). In the case of coupled modes, the calculation is made for a representative blade pitch angle and the effects of variation in the geometric pitch angle around the azimuth are assumed negligible. Harvey (ref. 90) has examined this assumption using a rotor model that represents the actual pitch angle of each blade. He applied this analysis to a simplified model of a two-bladed rotor and compared the results of calculations with and without the cyclic variation. The effect on the blade harmonic loads is small when the pitch bearing is at 0.25R, but large when it is located at the rotor centerline.

Hansford (ref. 91) has also addressed this problem and has derived correction terms for the coupled modes that depend upon the cyclic pitch. Comparison with model and flight-test data show that the correction terms are not important for the calculation of the flap bending moments, but are important in some cases for the chord bending moments. Figure 29 compares flight-test measurements from the Lynx to rotor load predictions using the conventional modal representation and a modified theory that uses the cyclic correction terms. The modification does not appear important at the inboard station, but does have a significant effect outboard. For this case, it appears that the modified theory provides a better representation of the blade loads than does the conventional modal representation.

Once the modal solution is obtained, there are alternative approaches to the calculation of the rotor-bending moments. The normal approach is to sum the contribution of all of the modes. However, where there is a discontinuity in the loading, such as a load path split on a bearingless rotor design, then the modal-summation approach will not accurately model the load distribution at the discontinuity. Bielawa has examined this problem in reference 92 by comparing the modal-summation method with a force-integration technique where the bending moment at any location is obtained by calculating the balance of forces out to the blade tip. He shows that the force-integration method can properly represent the rotor loading at discontinuities, but the method is computationally more expensive. Hansford (ref. 93) has devised a method of unifying the two approaches by deriving correction terms to

the modal-summation method based on the force-integration expression. This unified method is applied to the Sea King where the lag damper causes a discontinuity in the load at the inboard end of the blade. The modal-summation method and the unified method are compared to Sea King flight-test data in figure 30. The unified formulation shows much better agreement with the data.

A related problem in obtaining a modal solution for rotor loads prediction is knowing how many modes are needed for accurate prediction. Yamauchi et al. (ref. 50) have examined the effect of the number of modes used in comparing CAMRAD with the SA 349-2 flight-test data. The analysis uses up to eight coupled flap and chord modes, and up to four torsion modes. A comparison with the flight-test data shows there is little effect on the flap bending moment correlation beyond the use of five coupled modes, and for the chord bending moment correlation little change is seen after seven coupled modes. For the blade torsional moment, it appears that two torsion modes are sufficient.

ROTOR LOADS REDUCTION

> "Compared to the volume of literature available concerning various devices which can reduce unacceptable vibration (absorbers, isolators, higher harmonic control systems, etc.) there appears to be a decided lack of information describing the origin of the vibratory loading and how the loads may be affected (reduced) through blade design. There may well be design procedures which will substantially reduce or eliminate the need for other vibration control treatment." - Blackwell, 1981

The aeroelastic environment of the rotor blade has several natural divisions used by researchers to modify blade loads. First, one may define a series of loads reduction concepts where the blade is aeroelastically tuned to avoid critical driving mechanisms such as severe aerodynamic loadings or frequency coalescence. A second classification of research reduces the loads through blade and control system coupling. Third, a substantial effort has been made to modify the blade's aerodynamics to provide less excitation to the aeroelastic response of the rotor. The following sections will address these three research areas through examples of research and design concepts.

Blade Tailoring

Tuning the rotor blade to avoid critical driving mechanisms, both elastic and aerodynamic, has involved several different approaches. These have included nonstructural mass placement, stiffness and mass distributions, and aeroelastic coupling parameters. An example of the latter is the aeroelastically conformable rotor (ACR) concept.

Conformable Rotor Research- Studies of conformable rotors at the beginning of the review period examined the effects of blade properties on stall-induced control loads. Blackwell and Commerford (ref. 24, summarized in ref. 75) examined the effects of a number of blade parameters on control loads and concluded that torsional frequency and inertia had a major influence on the loads (see fig. 25 and discussion in Rotor Loads Prediction section). A similar effort by Tarzanin and Ranieri (ref. 94, summarized in ref. 95) based on limited model test data and theoretical studies using C-60, also concluded that the torsion degree of freedom had a significant influence on control loads, showing substantial reductions on the retreating side as torsional frequency was reduced. However, they predicted that further reductions in torsional frequency would show increased loads on the advancing side.

Later studies suggested that careful attention to the blade design could reduce all blade vibratory loads and this has become known as the conformable rotor concept. Reference 96 included a study of airload and vibratory loads from flight

data. According to that reference, for three different rotor types ". . . the phase angles and spanwise distributions of the principal harmonics of airloads were remarkably similar . . . and the bending load distributions and phases were predictably related to the hub configurations and to the modal natural frequencies." This revealed a constancy in character for the forcing function and some hope of tailoring the blade to redistribute the loads. It was suggested that vibratory flap bending and lift deficiency be attacked using elastic twist distribution with such design parameters as camber, chordwise c.g. position, and blade sweep. Test results from a Mach-scaled hingeless rotor indicated that for a representative high speed cruise condition, introducing a nose-up pitching moment reduced mid-span flap bending (1 and 2/rev) by 40%. Furthermore, a 10° sweepback of the outer 35% of the rotor radius reduced midspan flap loads by 10% in 1/rev and by 30% in 2/rev. It was noted, however, that phasing of flap loading harmonics with blade sweep prevented unloading of the retreating blade and further inertial tuning would be required.

Studies such as the above encouraged a series of NASA/Army sponsored analyses and tests of the ACR concept. Blackwell and Merkley (ref. 97) analytically investigated time-varying elastic twist to improve performance and reduce loads, and then provided design guidelines for elastic twist by qualifying the potential of several blade parameters for producing favorable elastic twist. The impetus for this study was a maximum rotor efficiency for a given rotor class. The Y200 analysis with two inflow models was used to define the improvements possible with airload redistribution as shown in figure 31 using the elastic twist distribution shown in figure 32. Parametric sensitivity to rotor-design variables was investigated for a torsionally soft rotor during the study with encouraging results (figure 33). Recommendations for model designs were made which emphasized the predicted tradeoff between performance and blade loads for the ranges of conformable rotor design variables employed.

Testing of candidate ACR designs has included work in the Langley Transonic Dynamics Tunnel (TDT). Weller (ref. 98) tested a four-bladed articulated rotor with four different tip shapes. The blades had a high torsional stiffness ($\omega_\theta \simeq 11$/rev). It was found that aft sweep of the blade tip by itself decreased flap and chord oscillatory loads with respect to a rectangular tip as shown in figures 34(a) and 34(b). The addition of tip anhedral, however, increased these loads. Both sweep and anhedral in the tip region reduced torsional and control loads as shown in figure 34(c).

The above analytical and experimental results encouraged more comprehensive model testing of conformable concepts including that reported by Blackwell et al. (refs. 76 and 77). In that research effort two blade sets of different torsional stiffness were tested in the Langley TDT at four advance ratios and several hover tip Mach numbers. Three tip shapes were used as well as trailing-edge tab deflection variations. It is noted that in the search for load alleviation, several design parameters were incorporated for each model configuration. The elastic twist differences caused by configuration changes shown in figure 35 were significant, and an analysis of the resulting loads and blade response yielded several useful design guides. For example, for the configurations tested that reduced advancing blade

twist, blade loads were generally reduced as is shown in figure 36. It is of interest to note that the torsionally soft configurations provided both the best and the worst vibration environments with the highest vibratory loads on the rectangular ACR and the lowest on the ACR with sweep and camber change. The camber changes also generated the highest torsion moments at high blade loading.

Performance and rotor control sensitivity were evaluated for several configurations. A correlation study using the Y200 code resulted in good trend agreement for the elastic twist resulting from camber changes. However, the effects of sweep on steady and 1/rev elastic twist were overpredicted by the analysis. Wave form correlation was poor as is shown in figure 37, but the trend of oscillatory loads with rotor task was described as fairly good. The effect of configuration changes on performance and loads for the rotor tasks shown was predicted fairly well as is shown in figure 38. It should be noted that performance "rankings" changed significantly with rotor task. Several conclusions from this study are useful to loads reduction tailoring. The paper cites that a pitching moment coefficient change of +0.03 effected a much larger dynamic twist than did 20° of tip sweep, and that both sweep and camber reduced vibratory loads for the torsionally soft blade. However, the torsionally soft blade generated loads as high or higher than the baseline rotor.

The extensive work of reference 77 showed the potential of several design variables for loads reduction when used in several combinations, but the isolated sensitivity of each parameter and the effectiveness of each when used in combinations remained elusive.

In an effort to understand and explore the relationship between torsional loading and rotor performance, Yeager and Mantay (ref. 99) did an expanded test and analysis of the configurations tested by Weller (ref. 98) including additional tip configurations. For the baseline torsionally stiff ($\omega_\theta \sim$ 11/rev) model rotor used in that test, the parametric variations of tip sweep, taper, and anhedral measurably changed the elastic twist and integrated performance, but there did not appear to be a strong connection between the two phenomena. The oscillatory and mean torsional moment data of references 98 and 99 agreed with respect to configuration trends.

Yeager and Mantay (ref. 100) reported additional tests of the rotor originally used in references 76 and 77, but with extended tips. This reference presents data in tabular and graphic formats. Performance, harmonic blade and fixed system loads, and torsional deflection data were offered to the analyst for correlation purposes.

The Army contractual effort which initiated much of the above ACR analysis and testing also provided the impetus for the work described by Sutton et al. (ref. 101). In that study, a selection of primary ACR parameters was made. A series of codes providing predictions for performance, forced response, and stability were used to parametrically vary key aeroelastic parameters for a four-bladed rotor. The relative performance benefits of each parameter combination were assessed, with torsional stiffness and tip sweep being found to be the most effective. A model rotor was constructed and tested in the Langley TDT for four configurations. Figure 39 shows the measured variation in the flap bending moment for the

three four-bladed rotor models that were tested. A conclusion to this effort cited the potential of the ACR concept if the cause and effect relationships of the design variables could be well understood.

The ACR research effort reported on in references 76 and 77 was expanded in order to understand the effects of aeroelastic couplings on loads and performance. Mantay and Yeager have reported the results of a first stage of testing in reference 102 and the complete results in reference 103. Although the earlier work had demonstrated the importance of tab deflection on vibratory loads, the primary research emphasis of the new experiments was on the blade tip. Seven tips, incorporating single and combined sweep, taper, and anhedral, were tested for two different blade torsional stiffnesses at several advance ratios in the TDT. Twist and inertial properties were held to known values. Rotor loads were correlated with elastic twist magnitude and azimuthal activity while explanations were offered for the resulting rotor-control phenomena and substantial performance variations effected by the simple and controlled combinations of ACR tip parameters. The practical aspects of ACR track sensitivity were also addressed with significant differences in torsional loads and response characteristics for the ACR maverick blade. The conclusions offered in these references included the existence of a strong correlation between azimuthal variation of elastic twist and rotor performance and loads. The oscillatory flap bending moments are shown relative to performance rank in figure 40. The elastic twist variation with azimuth is shown in figure 41 for three configurations as the performance rank decreases from 1 to 5 to 13. In addition, there did not exist a strong correlation of elastic twist magnitude with performance as is shown in figure 42. Finally, fixed system and blade loads as well as rotor track for potential ACR candidates appeared very sensitive to parametric rotor changes as shown in figure 43.

A similar parametric effort was analytically accomplished by Tarzanin and Vlaminck (ref. 104). The goal of that study was to evaluate the effect of sweep parameters on vibratory hub, blade, and control system loads. Furthermore, the relative importance of flapwise and torsional stiffness was evaluated along with the aeroelastic mechanism which produces the reductions in loads. An analytical investigation was performed on a reference blade for which aft sweep was generally beneficial to oscillatory loading. The C-60 was used, which included coupled torsion and flap, planform sweep variations, shear center, neutral axis, chordwise c.g. and pitch axis location variations. Airloads were modeled using compressibility, stall, 3-D flow, unsteady aerodynamics, and nonuniform downwash. The reference rotor in this study was predicted to have its 4/rev loads significantly reduced by tip sweep over a wide range of airspeeds. It was found that although the blade torsional stiffness must not be too high and, thus, obviate the tip sweep effectiveness, specific blade frequency placement and flap/pitch coupling were not necessary for hub load reductions with sweep for the reference rotor. Reductions in 4/rev hub loads were predicted for forward mass and aft aerodynamic center configurations with respect to the blade's elastic axis. Elastic twist via c.g./ac distributions was quantified and the correlation between 4/rev elastic twist and vibratory loads strengthened. Several nonreferenced blade designs exhibited detrimental qualities with aft tip sweep, but could be further altered with the predicted parameter

sensitivities acquired in this study. The understanding of the hub load reduction method is illustrated in figure 44.

Modal Tailoring- The review of rotorcraft applications for design optimization by Miura (ref. 105) included an overview of government and industry research in loads reduction using new design methodologies. Several studies in loads tailoring have been undertaken using empirical modal techniques and automated design analyses. During these studies requirements to understand rotor loading mechanisms and design parameter sensitivity were addressed.

Peters et al. (ref. 106) have presented the results of a grant effort to investigate the potential of tailoring blade properties to achieve weight, inertia, and dynamic goals. A finite element model was used with the CONMIN code to solve 21 design problems. Simple beams as well as teetering and articulated rotor blades were tailored for frequency placement. Reference 106 states that the frequency placement formulation is a useful approach to vibration reduction for a prescribed airload distribution. Numerical procedures and preferred operation of the design method were defined. The achievement possible in the modal optimization process was defined in large part by the rotor's rotational speed.

Prescribed airloads were also used by Pritchard et al. (ref. 107) for a sensitivity analysis and optimization of nodal point locations for reduced vibratory loads. Lumped masses were chosen as the design variables to move a node where either low response is required, or to a point which makes a mode shape orthogonal to the force distribution while minimizing the total amount of added mass. Direct comparison with an optimization scheme that minimizes the generalized force indicated that nodal placement has essentially the same success.

Friedmann and Shanthakumaran (ref. 108) have used optimization techniques to directly minimize oscillatory vertical shears or roll moments at a specified advance ratio. Frequency placements and hover stability margins were used as constraints. Instead of prescribed airloads, a fully coupled flap-lag-torsion analysis was used. The example chosen was a soft inplane hingeless rotor which, when optimized, exhibited a 15-40% reduction in vibration, and was 20% lighter than the initial design (though mass was not an objective function). At a cruise condition ($\mu = 0.30$) use of linear hub shears as an objective function produced both shear reductions at all advance ratios below 0.30 and hub rolling moment reductions. Nonstructural mass, used for blade tailoring, was best placed along the elastic axis for the outboard blade sections, since its impact on hub rolling moments and stability was not detrimental. The use of roll moment as the objective function with vibratory shear as the constraint proved less efficient and the optimization technique of this work offered little for a stiff inplane design in the proximity of an aeroelastic stability margin.

Empirical methods for modal tailoring have been advocated by several research organizations. Taylor (ref. 79) has presented a theoretical formulation which shows that consideration of blade mode shapes can be as important as frequency placement for vibration control. A modal shaping parameter (MSP) is derived that is a measure of blade modal vibration severity (as was discussed in the Rotor Loads Prediction

section above). When blade variables such as stiffness, mass, and mass distribution are changed to drive MSPs to low values for a prescribed loading, Taylor predicts that a lower vibration blade design will result. The Sikorsky analysis G400 was used to predict the effects of modifications to a baseline blade and calculated reductions in the root shears and the blade loads as shown in figures 45 and 46, respectively.

During a recent test of a Growth Black Hawk Rotor candidate in the Langley TDT, modal-shaping techniques were attempted on the model blade. This was done with nonstructural mass placement in an attempt to control the blade's second and third flap modes. Two independent analyses were used to alter the modal properties based on the predicted airload distributions and the predicted shears are shown in figure 47. The two analyses predict different locations for optimal mass placement and each analysis indicates that the other's prediction will be nonoptimal. An experimental program has been initiated at the U.S. Army Aerostructures Directorate and NASA Langley which will provide for parametric modal shaping tests to evaluate this passive technique further and provide a means for analysis verification.

A more complex approach to modal tailoring is presented by Yen (ref. 109) that stresses that the interaction of structural properties of a rotor with airloads distribution is a powerful tool for vibration reduction. In this approach, blade stiffnesses, as well as radial and chordwise mass distributions, are design variables. For a four-bladed hingeless rotor, for example, the primary blade modes for tailoring are cited as the second cyclic flap bending mode, which dominates the 3/rev blade root flap bending moment; the third collective flap bending mode, which drives the 4/rev blade root vertical shear; and the second cyclic chord bending mode, which influences the 5/rev blade root flap bending moment. Several design methodologies are advocated. One uses assumed airload harmonic distributions and a modal participation factor to lower the vibration contributions of offending modes. An optimum design approach is also offered with constraints on blade weight, rotational inertia, and bounds on stiffness and weight distribution. The objective function includes 4/rev shears and moments. A comparison of the reduction in root shear and moment obtained from prediction and a model test in a wind tunnel is shown in figure 48.

The feasibility of using this tailoring technique for advanced blade geometries, especially with unknown airload harmonics, provided the impetus for the Tailored Bearingless Rotor Program. This program provides for the design and fabrication of aeroelastically tailored model rotor blades for testing in the Langley TDT. The five sets of blades include two baseline rotors, one with government-designed advanced aerodynamic characteristics in terms of planform, airfoil selection, and twist. The three remaining rotors will have improved blade dynamics using the Bell "nodalization" method. One of the three "nodalized" blade sets will also have Bell-designed advanced aerodynamics characteristics. The primary purpose of this effort is to determine what effects, if any, the "nodalization" method has on rotor blades with advanced aerodynamic design. All five blade sets will be tested on the ARES model in the TDT using a Bell model bearingless rotor hub. Rotor

performance, as well as rotor and fixed-system loads, will be measured for all rotors over a wide range of test conditions.

Taylor (ref. 80) has conducted an analytical investigation to understand the importance of certain blade-design parameters on rotor response. Blade modal shaping, frequency placement, aerodynamic, structural, and intermodal couplings were examined systematically to identify vibratory sensitivity to these techniques. An example of how the various components of vibration combine has already been shown in figure 26. Taylor states several "obvious" and "nonobvious" results from his study. For example, the role of the lag mode in the 3/rev inplane shears and the canceling of the applied forcing by the inertial response is listed as an obvious result. The role of the flapping motion in forcing the example rotor's 3/rev edgewise mode is cited as a "nonobvious" result of the research effort. In looking for a consistent method to predict vibratory loads in rotor blades, Taylor concludes that nonuniform inflow is not needed in cruise to produce vibration; the rotor operating in uniform inflow is sufficient to induce vibratory loads.

Blade/Control Coupling for Loads Modification

Several research activities in the rotorcraft community have explored concepts which modify blade loads through direct couplings in the rotor system or decoupling devices in the rotating system. These concepts rely on prescribed blade motions effected by control designs or load alleviation attained by rotor load non-transmittal along the blade. An example of the first system, strongly supported by Army/NASA rotorcraft research, is higher harmonic control (HHC).

HHC Blade Loading- The results of wind tunnel testing of an HHC concept are described by Hammond (ref. 110). A dynamically scaled four-bladed model, incorporating harmonic pitch control, used an adaptive control system in a test in the Langley TDT. Reduced vibratory loads in the fixed system were sought by altering the loads at their source (the blade's aeroelastic environment). The vibratory forces and moments to be minimized provided inputs to the HHC algorithms being evaluated. The particular series of tests described by Hammond used the fixed-system model strain gage balance as the vibratory load sensor. The model was tested at advance ratios above 0.2, simulating 1g level flight, with the rotor trimmed to the shaft. Blade loads data obtained for $\mu = 0.3$ were fairly consistent with previous open-loop testing in the TDT. Figure 49 shows a small reduction in the flap bending moment, a large increase in the oscillatory chord bending, and a moderate increase in the torsional moment. A possible explanation of the increase in the chord-bending moment was the close proximity of the chord-elastic mode to 6/rev which may have been aggravated by impurities in the 3/rev control inputs. Pitch link loads increased with HHC because of the 3, 4, and 5/rev input requirements as is shown in figure 50.

The goals of the wind tunnel program (reduced fixed-system vibratory loads) were largely met. This provided impetus for an HHC flight program on an OH-6A (ref. 111). In this test series, the HHC system was flown open and closed loop. In addition to the flight proof-of-concept program goals, the test scrutinized the

rotating system loads. An example is shown in figure 51 for a 70-knot level flight condition with ±0.33° lateral blade pitch in the open-loop HHC mode. The flapwise harmonics follow the same trend with controller phase as the fixed-system vibratory loads. The chord 3 and 4/rev do also, but the 5/rev harmonic is above the baseline value, independent of controller phase.

Controllable Twist Rotor Loads- The controllable twist rotor (CTR) concept has been studied for multicyclic operation by McCloud (ref. 112). The required torsional deflections of the blade were driven by a servo flap as shown in figure 52. This theoretical work used a transfer-matrix technique with a general rotor-control code to explore the potential for altering loads. McCloud predicted that substantial reductions in fixed-system vibration could be achieved with four harmonics of servo flap control, with 2/rev controls providing most of the advantage. Adding 4/rev (instead of 3/rev excitation) reduced vibration at the expense of blade oscillatory bending loads.

Decoupler Concepts- Blade designs which prevent transmission of vibratory loads across blade stations have provided loads data for unconventional boundary conditions. An example of such a concept was tested in the Langley TDT by Hammond and Weller (ref. 113) as part of a teetering rotor, scale model investigation of stall flutter phenomena. Two sets of wide chord, 1/5 scale, teetering rotors were tested; one set had a midspan flapping hinge. As shown in figure 53 the hinge was effective in reducing the flapwise loads. This was accomplished without the blades exhibiting instability or excessive motion.

Aerodynamic Tuning Devices

Modifying the relationship between blade aerodynamics and blade motion has been suggested as a means of altering loading mechanisms on the rotor. Several concepts have been advocated such as blade-tip shapes, vortex alleviation devices, prescribed tip motion, and blade/wake geometry variations. The vibratory loads which are impacted by such concepts are of research interest because of the (usually) controlled manner in which aerodynamic-design parameters are used.

Variable Geometry Rotor- A systematic design program was undertaken (as reported by Mantay and Rorke, ref. 114) to study the phenomena associated with blade/wake geometry, and to design a rotor which takes advantage of common aerodynamic and geometric relationships. The resulting design was the variable geometry rotor (VGR). Maneuver flight loads observed during vortex/blade interaction provided the motivation for a rotor-system design which could effect changes in the geometric relationship between a rotor and its wake. The test plan for the VGR included theoretical studies with a free wake (ref. 115), flow visualization, and model scale hover, and forward-flight wind tunnel tests (ref. 116). Further analyses simulating maneuvers (ref. 117) and a full-scale hover program (ref. 118) contributed to the design's ability to alter blade loads and performance. Parameters of interest in the above investigations are shown in figure 54.

Initial studies (ref. 115) on the VGR indicated that changes in azimuthal geometry and vertical spacing caused less excursions in harmonic loading between rotors than did other key aerodynamic parameters. Radii and collective pitch changes between rotors resulted in larger harmonic changes in certain rotor loads. These initial efforts provided the impetus for a model rotor experiment, though the driver was rotor performance, not the loads. Figure 55 shows a photograph of the VGR model in the UTRC wind tunnel. Inertial scaling for the model configurations was not matched to a representative full-scale rotor. In addition, forward-flight configurations were chosen based on hover-performance results. The measured vibration for the VGR configurations tested did not vary with $\Delta\psi$, Δz, or with differences in blade pitch angle, and hence, provided no conclusive load-tailoring information to support the predictions made in reference 115.

When full-scale VGR hover tests (ref. 118) were conducted, no vibration or loads conclusions were drawn because of the hover mode. However, blade-tracking phenomena were observed for the configurations tested. Loads information for the VGR needed to be obtained while in forward flight on a dynamically scaled model. To prepare for this, a comprehensive analysis was conducted (ref. 117) at several advance ratios and for a symmetrical pullup condition. Blade shears, bending moments, and pitching moments were calculated using analytical tools similar to the reference 113 work.

An example of the predicted effect of VGR configuration on upper rotor-flap shear harmonics is shown in figure 56. The loading harmonics on the lower rotor were affected mainly by $\Delta\psi$ variations. Reference 117 provided numerous examples of harmonic loadings for geometric parameter variations between the rotors and their wakes. In general, for a six-bladed VGR in a cruise condition, the lowest harmonic loads occurred for two rotors vertically separated by Δz = 1 chord and azimuthally symmetric. In a pullup maneuver, the lowest flap shears were predicted to occur for $\Delta\psi = 90°$ for the same six-bladed rotor system.

Tip Planform- The rotor-tip region has long been recognized as critical for performance and acoustics phenomena. Many researchers have explored the effect of the blade tip's elastic, inertial, and aerodynamic characteristics on blade loads. The effects of four different tips on the performance and loads of a full-scale rotor have been studied in the Ames 40- by 80-Foot Wind Tunnel (refs. 67 and 119). The tip geometries used are shown in figure 57, and the blade layout and instrumentation are shown in figure 58. Performance and the first 10 harmonics of loads data are tabulated in reference 67. In studying the effects of the different blade tips, Rabbott and Niebanck (ref. 119) have concentrated on the control-loads information and observed that significant variations in the loads were caused by tip-planform changes. Major reductions in control-load harmonics were seen for one of the configurations (swept-tapered). In figure 59, the data show high-frequency content that was not predicted by the pretest aeroelastic analysis. Time histories of control and flap-bending moments are given in figure 60 and show that tip shape alters the advancing blade pitch-down moment and its effects on vibratory loads.

Prescribed Aerodynamic Devices- Imposing an aerodynamic loading at critical blade stations has been the impetus for several rotor designs. The free-tip rotor

is described in reference 120 and uses a tip-moment controller that applies a prescribed moment, driving the tip to a nearly constant lift. (A schematic is shown in fig. 61.) The concept was tested small scale (5.1 m diam) with interesting power and loads results. An example of inboard flap-bending moment is shown in figure 62. Harmonic analysis of these data cite 1 and 2/rev load reductions as the main cause for oscillatory load reductions, at the values of advance ratio where reductions occur. Figure 63, however, shows a substantial increase in inboard oscillatory chord moment. The free-tip concept prescribes a weathervane effect, which seems to generate lower control loads than does a fixed tip of the same (swept) planform as shown in figure 64.

Another prescribed aerodynamic concept tested for loads alleviation is the multicyclic jet-flap rotor (ref. 121). This 12 m diam, two-bladed teetering jet-flap rotor was subjected to experimental transfer functions in forward flight in the Ames 40- by 80-Foot Wind Tunnel. This was done to minimize either specific harmonic bending stresses, rms levels of those stresses, or to lower fixed-system vertical vibratory loads. It was shown that three harmonic controls could greatly reduce specific components of loads.

GUST LOADING

Dave Brandt: ". . . to the best of your knowlege, has this analysis [for gust loading] or any analysis that's similar to this, ever designed so much as one rivet on any piece of flightworthy hardware in the helicopter industry?"

Peter Arcidiacono: "To the best of my knowledge, I think the answer is no."

- NASA SP-352, 1974

For design purposes, the effects of gusts are modeled by calculating an incremental load factor using a simplified quasi-steady theory and multiplying this incremental load factor by a gust-alleviation factor. For military aircraft, this gust-alleviation factor is specified in the helicopter structural-design specification, MIL-S-8698. The adequacy of this gust alleviation factor has been examined by comparing the predictions of the Bell Helicopter Textron analysis C81 (ref. 122) and the Sikorsky analysis Y200 (refs. 123 and 124) to simplified theory. Both the Bell and Sikorsky studies concluded that the structural specification was too conservative and that the gust-alleviation factor should be reduced. The Sikorsky study did note, however, that if blade stall was encountered, the appropriate gust-alleviation factor was increased, but the requirements of MIL-S-8698 were still considered unrealistic.

Arcidiacono et al. (ref. 124) have also summarized extensive measurements obtained on aircraft during military operations. These measurements included load factor and control positions. From the measurements it was possible to determine load factors induced by maneuvers, and load factors induced by turbulence. A comparison showed that incremental load factors caused by gusts were much less than those induced by maneuver, and the gust-induced loads represented only a small percentage of the flight experience. This is summarized in figure 65 which shows the frequency of occurence for both gusts and maneuvers. This figure clearly shows that the rotor-design problem for military aircraft is one of specifying the maneuver loading, not the gust loading.

The emphasis of the research in gust loading over the period covered by this paper has been towards the development of calculation methods. Gaonkar (ref. 125) provides an extensive review of the gust response of helicopters and relates this to parallel work with fixed-wing models. Bir and Chopra (refs. 126 and 127) have developed a math model to represent the response of a helicopter to a deterministic gust field, and in their analysis, have included blade flap, chord, and torsional flexibility; fuselage degrees of freedom; and a dynamic inflow representation of the wake. They show that the rotor and fuselage response is sensitive to all of these parameters as well as the assumed gust field. Prussing, Lin, and their colleagues

have used a simplified rotor representation to examine the blade response to a gust where the equations are derived in stochastic form (refs. 128 and 129). This formulation, which is a more accurate representation of the physics, does not change the blade-gust response significantly.

Recent experimental research on gust loading has been limited to examining the response of a teetering helicopter to the vortex wake trailed from a fixed-wing aircraft (refs. 130 and 131). Limited correlation with the Bell C81 analysis shows fair agreement with the measurements. The analysis of Bir and Chopra (ref. 127) has been extended to treat this case as well in reference 132. The methods of extending rotor loads analyses to treat gust loads appear to be well in hand. However, the significant problems that remain in calculating rotor loads accurately under trimmed-flight conditions have prevented their extension to the problems of predicting loads or ride quality in the forward flight gust environment. It does not appear that gust loading is important in defining the vehicle load capacity. However, gust-induced loads may be important for some rotor components, especially when the rotor is stalled. Tarzanin (ref. 133) has pointed out that flight-test data used to compare with predictions are normally selected from smooth air tests and carefully checked for repeatability. If, however, data are used from flights which include turbulence, substantial load variations can be encountered. Figure 66 shows the scatter band of measured CH-47C pitch-link loads for five test flights. This is a case where the pitch-link loads are rising rapidly because of blade stall and represent a critical loading condition. Although there is no information on the actual flight conditions, the wide variation in loading suggests that the pitch link load is very sensitive to gust loading under stalled conditions.

MANEUVER LOADING

"In the future, it may be possible to predict envelope loads completely by analytical means." - Gabel, 1973

The structural envelope for a new aircraft in terms of load factor and airspeed will look something like the sketch in figure 67. The problem of loads prediction discussed in this paper so far deals only with the loads on the rotor in trimmed, 1 g flight. In the figure, this is represented by the long dash line that extends from the maximum rearward flight speed to the forward speed at the 30-min rating of the engine, V_H. If a maneuver requirement is imposed, it might be something like maintaining a specified load factor for a specified number of seconds without losing too much airspeed. This is shown schematically in figure 67 by the heavy bar. The periphery of the envelope represents structural limits. There are other limits as well such as the engine power limit, and rotor aerodynamic limits. The power limit, which is not shown here, may be thought of as the additional load factor that could be obtained from excess power. For the case shown here, there is no excess power available at either V_H or hover; but in between, there is excess power, and the peak in excess power will correspond to the speed for minimum power. The rotor aerodynamic limit can be estimated from model tests reported by McHugh (refs. 134 and 135) where the blade lift was increased until it reversed sign and thus represents an aerodynamic limit, not a structural or actuator limit. Scaled to the V-n diagram of figure 67 the rotor lift limit is represented by the short dashed line. Operation of the rotor at any point outside these performance limits can only occur for short periods of time. For some aircraft, it may be possible to demonstrate compliance with the structural boundary only with the most extreme maneuvers. To calculate the loads for these conditions requires not only solving all the rotor load prediction problems that have been discussed previously in this paper, but also solving the transient problem, as opposed to the trimmed problem.

A number of the comprehensive analysis programs solve the equations of motions by time integration (ref. 2). Using these analyses, it is relatively straightforward to perform a transient-maneuver calculation starting from a trimmed steady state condition. Van Gaasbeek (ref. 136) has compared the C81 analysis with measurements made on an AH-1G during flight maneuvers. An example for a 2 g pull-up from autorotation is shown in figure 68. The C81 calculation shows good agreement in terms of the maximum level reached; however, there is some oscillatory behavior that is not seen in the flight-test data.

Despite the capability that exists in a number of the comprehensive analyses for calculation of maneuver loads, the normal procedure in the industry is to scale maneuver loads on the basis of previous flight-test experience (refs. 3 and 12). Gabel describes this process in considerable detail in reference 3.

The critical steps in rotor-blade design are the calculation of loads in trimmed, unaccelerated flight to insure that all loads are within material allowables for infinite fatigue life, and the assumed operational fatigue spectrum to

define what the fatigue life will be. Considering the uncertainty that remains in both of these critical areas, it is understandable that that the calculation of maneuver and gust loads has not received a great deal of attention.

ASSESSMENT

> "In fact, it can be argued that government and the helicopter industry have not optimized the basic helicopter blade design before resorting to exotic and sophisticated approaches and devices. The fundamentals of vibration have not been understood, and before radical planform changes, elastic couplings, and active control are implemented, there must be a basis of fundamental understanding based on analysis and experiment." - Taylor, 1984

This paper has reviewed the research performed in the last 13 to 14 years in the areas of rotor loads prediction and reduction. The assessment in this section seeks to put this research into perspective by addressing three topics: (1) how good are the present analyses in predicting rotor loads, (2) to what extent can rotor loads be reduced through design practice, and (3) what has the government contribution been in these areas. Inherent in this assessment is the identification of areas that require new or increased research effort.

The question of how good the present analyses are for predicting rotor loads is addressed below by examining the present predictive capability of the major rotor loads analyses as reported in the literature. In addition, the analyses are examined to identify where advances from rotor loads research have been incorporated or synthesized in the analyses. The question of the extent to which advances in rotor loads reduction have been transferred to design practice is addressed by summarizing the most productive research areas and discussing a limited number of applications that have been reviewed in the literature. Lastly, the contribution of the government is assessed indirectly in two ways. First, government support of research is estimated by tracing the number of papers and reports published. Secondly, the government development of public data bases is assessed by examining the use of these data bases.

Rotor Loads Prediction

The 1973 AGARD meeting in Milan and the hypothetical rotor comparison of 1974 (ref. 2) provided a basis for assessing the capabilities of the rotor loads analyses of the early 1970s. The present assessment is made substantially more difficult as there has been no equivalent demonstration of the industry methods since that time. For that reason, the present judgments are based upon incidental results that have been published in the open literature. In some cases, there have been no calculations published since either the Milan meeting or the hypothetical rotor comparison.

The characteristics of present rotor loads analyses are shown in Table 1 (refs. 137-142) and this provides a useful framework for subsequent discussion. The format for the table is similar to that used in reference 2 although some of the

analyses shown in that reference are no longer in use and are not included here. The table is believed to be current as of 1986.

The history of the development of the Bell Helicopter Textron analysis C81 is covered by Bennett (ref. 5). Subsequent modification and documentation as of 1974 have been provided by Davis (ref. 143). The Army evaluated the capability of C81 to predict rotor loads for aircraft other than teetering rotors by contracting correlation studies for a hingeless rotor (ref. 144) and for articulated rotors (ref. 145). These studies revealed a number of significant limitations with C81, some of which were addressed by McLarty in the 1977 version of the analysis (ref. 146). Further modifications were made by Van Gaasbeek et al. (ref. 147) in 1979 including an option to provide the inflow distribution from a free-wake calculation as an input table. The inflow distribution is based on the free-wake analysis of Crimi (ref. 139). In reference 148 Van Gaasbeek has updated the analysis to provide an interface with DATAMAP.

Extensive comparisons have been made between the OLS measurements obtained on the AH-1G helicopter (ref. 34) and C81 (refs. 34, 149-153). In general, these show good prediction of the oscillatory loads; but the blade higher harmonics are not well-predicted, even using the free-wake analysis. Correlation with flight-test data for a prototype Model 222 with a teetering rotor (ref. 13) is shown in figures 69 and 70. The prediction of the distribution of the oscillatory flap-bending moments is good, but the oscillatory chord-bending moments are overpredicted. Figure 70 shows that the waveform behavior is not well predicted either with or without unsteady aerodynamics. This lack of C81 waveform correlation is typical for the OLS data for all blade loads (ref. 151).

The predictive capability of the C81 analysis for the four-bladed Model 412 rotor is shown in figures 71 and 72 (ref. 154). The comparison includes a configuration where a tab on the outer portion of the blade is used to provide a nose-up pitching moment. The prediction of the oscillatory blade bending moments is fairly good, although the flap-bending moments are over predicted over the middle of the span. Figure 72 shows that, although the analysis shows similar peak-to-peak levels in the pitch link load, the waveforms are different, especially in terms of higher harmonic content.

The Boeing Vertol analysis C-60 is not documented in the literature as the government has directly funded only a small part of its development. A good description of the program as it was used through the mid-1980s is given in reference 104. Recently the program has undergone two significant changes. First, it has been restructured to take advantage of current programming techniques and to make it more flexible for future use (ref. 53). Second, the blade representation is now fully coupled in flap, lag, and pitch where previously the lag degree of freedom was treated as uncoupled.

Correlation using the modified C-60 has not been published. Correlation using the older version is shown in reference 155 using data obtained during lift-limit tests of an articulated model rotor (refs. 134 and 135). Midspan flap bending and torsion moment data are compared with C-60 in figure 73. The oscillatory loads are

reasonably well predicted for both flap bending and torsion. For flap bending there is good agreement in the first harmonic, but surprisingly, the theory shows higher harmonic content that is not seen in the measurements. The torsion moment data show reasonable agreement on the advancing side of the disk in terms of amplitude and phase, but not on the retreating side.

The Kaman Aircraft Corporation presently uses three analyses: 6F, which was developed to model torsionally soft rotors with servo flaps; DYSCO, which has been designed using current structured software methods; and a version of C81 that has been modified to incorporate a servo flap (without a degree of freedom). The 6F analysis is described in reference 156. (There is no recent correlation published.) The DYSCO analysis (ref. 157) is designed as a general method to couple and analyse the dynamic behavior of individual components. No rotor loads correlation has been published.

McDonnell Douglas Helicopter Company has used three analyses in recent years: DART, which has evolved from the SADSAM analysis; RAVIB, which has evolved from analyses developed at Rochester Applied Science Associates (RASA) in the mid-1970s; and RACAP, which is an entirely new development. The DART analysis is not described in the literature, nor are there any recent published comparisons of DART predictions and measured rotor loads. RACAP is expected to become the primary loads analysis for McDonnell Douglas, but as of yet details of its development and comparisons with rotor loads measurements have not been published.

The RAVIB analysis has been described by Gangwani in reference 32 and correlation with the AH-1G OLS data (ref. 34) is shown in figure 74. For the correlation shown here the model uses a free-wake analysis based on Sadler (ref. 115). In the figure, the flight-test data are compared with a conventional aerodynamics model without dynamic stall and Gangwani's synthesized stall model (ref. 30). The flap-bending moment comparison shows good agreement with the 1/rev load, but does not show good agreement at the higher harmonics. The strong 3/rev loading seen in the chord bending is fairly well predicted regardless of the aerodynamic model used. The blade-torsion moments are only poorly predicted with the conventional aerodynamic model, but the dynamic stall results show much better agreement. Calculations with C81 for similar flight cases (ref. 151) show chord bending and torsion moment waveforms that bear little relationship to the measurements shown here.

Sikorsky Aircraft currently uses three analyses for rotor loads: the Normal Modes Analysis, Y201; G400 as part of the SIMVIB package; and RDYNE, which is a recent development. The Y201 analysis was used for the calculations at the 1973 Milan meeting and for the hypothetical rotor comparison. Modifications have since been made to the aerodynamic model to correct for yawed flow and swept tips. A panel method can be used to represent the fuselage and calculate inflow at the rotor disk which is induced by the fuselage. A new analysis, G400, was developed at the United Technology Research Center in the mid-1970s under government funding. This analysis was designed to model bearingless rotors and is described in references 158-160. It is now incorporated in the SIMVIB executive and can be used for the prediction of vibration as well as rotor loads (ref. 88). Although G400 uses numerical integration to solve the equations of motion, only the harmonic response

is used in the SIMVIB computations. The newest analysis at Sikorsky is RDYNE (ref. 161). It uses a component coupling structure that is the same as SIMVIB, but uses numerical integration to solve the equations. It appears that RDYNE will soon become the primary-loads analysis tool at Sikorsky, and Y201 and G400 will no longer be supported.

The Y201 analysis has been compared with flight-test data and wind tunnel data by Jepson et al. (ref. 66). The wind tunnel data are reported in reference 67. The flight-test and wind tunnel data are quite similar, although the higher harmonic loads are greater for the flight vehicle as was shown in figure 22. Figure 75 compares the radial distribution of the oscillatory flap and chord bending moments as measured in flight and as calculated with the Y201 analysis. The prediction using constant inflow is quite close to the measurements outboard of 0.30R for the flap-bending moment, but neither inflow model gives good results for the chord-bending moments. The variable inflow model is based on a prescribed wake and predicts the oscillatory bending moments quite poorly. It is both surprising and disappointing that increasing sophistication in the inflow model causes the correlation to degrade. The azimuthal time history for these moments, plus the pitch link load, is shown in figure 76. Even if the amplitude were to increase to match the flight test data, the harmonic character would not be matched.

The analysis G400 has been compared with model bearingless rotor data in reference 158. Limited comparisons of oscillatory bending moments have been made in reference 88 using G400 as a part of SIMVIB. However, there is no recent correlation that allows the azimuthal behavior of the analysis to be judged. No correlation has been published for rotor loads using RDYNE.

Johnson has described the development of a comprehensive rotorcraft analysis in references 162-164. The predictions of this analysis, now referred to as CAMRAD, are compared with flight test data obtained on the SA 349-2 in reference 50. Figure 77 compares the lift coefficient obtained from pressure measurements at 0.75R with the prediction of CAMRAD for a high-speed case. The predictions show good agreement with the measurements, except for some high frequency oscillations that are seen on the retreating side of the disk where the velocity is low. The calculations shown here were made with a prescribed wake. Calculation with a free wake showed little difference, but both gave better results than calculation using uniform inflow. The correlation for rotor loads is shown in figure 78 for this case. The predicted flap bending shows good agreement with the measurements for this station, but the chord bending shows a great deal of 5/rev response that is not seen in the data. The oscillatory pitch-link loads are overpredicted by CAMRAD, and the agreement in waveform is not particularly good.

The results presented in the 1973 Milan AGARD meeting and in the 1974 hypothetical rotor comparison indicated that the available rotor loads analyses could make reasonable predictions of oscillatory rotor-blade loads. These loads are important for the fatigue design of the rotor blade and control system. It seems to be generally accepted that the scatter in predictions that was calculated for the hypothetical rotor and is shown in figure 6 represents a worst case (or outer bound) on the prediction methods. Within each company, it is felt that the oscillatory loads can

be predicted with better accuracy if a new design does not differ too much from previous designs. However, the results shown here suggest that even for the prediction of oscillatory loads significant differences do occur and are not understood. It does not appear that oscillatory loads can be predicted with any more confidence now than in 1973.

An examination of the correlation for rotor load waveforms or time histories suggests that the basic physics of the problem are not accurately modeled by any of the rotor loads analyses. Even when the amplitude of the first harmonic load is reasonably well-predicted, the phase is not. The correlation for higher harmonics appears worse, but here it is difficult to make judgments as the waveform behavior is normally dominated by the first and second harmonics, and this obscures the higher harmonic behavior. There appears to have been some progress in the analysis of separate parts of the problem; a great deal has been learned about dynamic stall and wake induced velocities. But the various pieces of the problem have not gone back together correctly; there has been no improvement in the synthesis.

The major features of the present rotor loads analyses came into place in the early 1970s with the incorporation of dynamic stall and unsteady aerodynamics in most of the analyses. Since then, there have been minor improvements and upgrades to most of these analyses, but with the exception of the addition of the calculation of fuselage induced inflow to Y201 and CAMRAD, there has been no change to these analyses to improve their ability to represent the physics of the rotor loads problem.

Computation speed has increased by at least a factor of 50 over this time period and available computational capability does not appear to have hindered development of improved analyses. What does appear to have limited advances in the prediction of rotor loads is the twofold perception that, first, the prediction of oscillatory loads is adequate, and, second, vibratory loads cannot be predicted by anyone for the foreseeable future. That perception will not change until the accurate prediction of vibratory loads is demonstrated.

Rotor Loads Reduction

The application of the conformable or compliant rotor has, to a degree, preceded the research into the ACR concept. The tip shape of the S-76 which first flew in March 1977, was selected in part to reduce the control loads (ref. 165). The S-76 swept/tapered tip does show a reduction in control loads for most thrust and airspeed conditions when compared to other blade tips, as was shown in tests in the 40- by 80-Foot Wind Tunnel (refs. 119 and 67). The research efforts that followed and that have been reviewed in this paper, examined blades that are, in general, much softer in torsion than the S-76. As yet, the best combination of tip design and torsional stiffness for reduced loads is unclear; what is necessary here are further experimental and theoretical efforts.

The ACR research has demonstrated that pitching-moment changes induced by a tab deflection can have a significant effect on the rotor loads and this approach has

been used during a number of recent development programs after high vibratory loads were encountered in initial flight tests. Yen and Weller (ref. 154) report the application of negative camber to reduce steady and oscillatory rotor loads encountered in the development of the Bell Model 412 rotor. During development flight testing, it was determined that the steady pitch-link loads were higher than predicted and this limited maximum up collective during boost-off operation. In addition, the oscillatory flap bending and torsion moments were higher than predicted. They examined the effects of negative camber on rotor loads using th C81 analysis based on the test experience with conformable rotors reported by Blackwell et al. (ref. 77). This work suggested that the loads could be reduced for the Model 412 rotor, and as a consequence, they added a 1.25 in. tab between 0.80 and 0.87R with the tab set to -12° (trailing edge up). This resulted in approximately a 40% reduction in the steady pitch link loads, a 40% reduction in the oscillatory blade torsion loads, and a 15% reduction in the oscillatory flap-bending loads.

Gupta (ref. 166) has reported on vibration and loads problems that were encountered during the testing of a Composite Main Rotor Blade (CMRB) for the McDonnell Douglas AH-64. Unlike the Model 412 rotor, there was a steady positive torsion moment on the blade, and positive camber was used to reduce the steady torsion load, and this also reduced the vibration. It was also determined that the vibration could be reduced by reducing the tip thickness. Although it is stated that the DART analysis was used during this investigation, no examples of its predictive capability are given.

Yen and Tanner (ref. 167) discussed development tests of a Composite Main Rotor Blade (CMRB) for the UH-1 aircraft. The design goal was to significantly improve the performance of the blade without changing the dynamics. Design calculations using C81 showed that the CMRB 2/rev hub shears were substantially higher than on the metal blade. A number of design changes were examined and two were selected: a chordwise c.g. shift and a reduction in nonlinear twist. Calculation showed that this reduced the hub shears, but they were still higher than for the metal blade. When the CMRB was flight tested, the predictions of C81 were borne out as the cockpit vibration was significantly higher. To reduce the vibratory shears, a tab was added outboard and this was able to reduce the vibratory loads back to the level of the metal blades. It is not clear at this time whether the original performance goals of this rotor can be met following the modifications that have been made necessary by the high vibratory loads.

Research into the potential for loads reduction through mass and stiffness distribution changes has shown great promise. Yen (ref. 109) has described a number of approaches used at Bell including the classical frequency-separation approach, a preliminary design method that calculates root shears based on assumed airloads, and a formal optimization approach. The newer approaches have shown considerable promise for model-scale data (fig. 48) and these techniques will be applied on the next generation of rotors at Bell. Similar techniques have also been applied at Westland for the British Experimental Rotor Program (BERP) rotor as described by Hansford (ref. 168) and have shown a substantial reduction in vibratory loads. These

successes suggest that the design for vibratory load reduction will become more important in the preliminary and detail design process for new rotor developments.

The research into loads reduction using mechanical or electrical feedback has been relatively inconsequential over the last decade with the exception of higher harmonic control (HHC). The demonstration programs to date have shown that HHC is a very powerful means of loads control, but any future applications will be directed toward vibration reduction in the cockpit.

Recent research into new rotor configurations that include loads reductions as a benefit has been done in the period covered by this paper. This includes the jet-flap rotor, the variable geometry rotor, and the free-tip rotor. However, at this time only the latter concept is being pursued.

Government Support of Rotor Loads Research

The government support of rotor loads research is assessed in two ways. First, research funding is examined in terms of its output; that is, published papers and reports. Second, the value of government-supported data bases is assessed by examining their use in research. Neither of these measures is comprehensive nor exact; such a metric does not exist. However, they do provide a useful framework for a discussion of the government role in rotor loads research.

The results of government research funding can be assessed by tracking the number of research reports and papers published each year that were funded under government contract or grant. All papers examined as part of this review are included (not all cited) with the exception of survey or summary papers. The data are filtered using a 3-year running average and are shown in figure 79. The number of papers published tends to be cyclical depending on the technical meetings being held each year. In general, the number of papers or reports being published each year is holding constant and, hence, the funding for rotor loads is assumed to have been holding relatively constant. Research into load-reduction methods appears to use a quarter to a third of the resources applying the measure used here.

The government contribution to rotor loads research appears to have held fairly constant over the last decade. A major transition that has occurred, however, is that the government investment in comprehensive analyses is now largely restricted to programs that have been (or are being) developed internally, that is, CAMRAD and the Second Generation Comprehensive Helicopter Analysis System (2GCHAS). The government has made a major contribution in the past to the development of a number of the comprehensive models used by industry and has attempted to transform some of these analyses into well-documented, general-purpose analyses that could be used by both industry and the government. This effort to develop a public domain, comprehensive model based on an industry code has not been successful. As a consequence, the government is proceeding with the development of 2GCHAS with industry participation. Although CAMRAD was developed more by individual initiative than government plan, its continued development represents an essential part of research in the

rotor loads area at least until 2GCHAS is operational and has demonstrated that it can support future progress in this area.

The second measure that is used to gauge government support of rotor loads research is the development of rotor loads data bases. Research in rotor loads and a means of reducing rotor loads has been continuously guided by experimentation. Data obtained in flight tests or wind tunnel tests have been used to improve the capability to predict rotor loads and to find methods to reduce rotor loads. The effort and expense of obtaining a set of data may be justified by the immediate answers that are provided by the data, or in some cases, the major justification for the data is its long-term value in the form of a data base.

The government makes a major contribution to research in rotor loads either by funding or performing the experiments that lead to the development of data bases. The experimental data and data bases may be used in many ways and this use is sometimes published and sometimes kept proprietary. For this assessment, it is only possible to examine the published uses of data. Although the limitations of this approach are recognized, the approach is still considered useful.

The experimental data obtained over the period covered by this paper were examined, and if the data were provided either in tabulated form or on a formatted tape, then the data were considered to constitute a data base. Nine data bases were found and these are listed in Table 2 (refs. 169-175). Most of these data bases were used by the original investigators, at least to a limited extent, and this use is referred to as a "primary reference." If the data base was subsequently used by another investigator, then that use is referred to as a "secondary reference." Of the nine data bases, only one has been used regularly by subsequent investigators and that is the AH-1G OLS flight-test data base.

All of the data bases in Table 2 were funded by the government except for the SA 349-2 flight-test data base. The use of the AH-1G OLS flight test-data by subsequent users is clearly a success, but the lack of use of the other data bases is discouraging. It is recognized, as noted above, that the published use of a data base is not its only justification. Unpublished use of a data base to guide proprietary design or aircraft development may justify the expense of developing that data base. In addition, a well-documented data base may prove valuable for many years, and the lack of initial use does not mean that the data base may not become very useful. No better example of this facet of data base use can be seen than in Hooper's comparison of data bases many years after they were obtained (ref. 40). However, it is unclear whether the use of the government-developed data bases justifies the expense in creating them. Certainly the development of new data bases should not be undertaken without a substantial expectation of their future use.

Table 2 evaluates only the use of data bases developed during the time frame of this paper. A related question is what has been the use of all data bases during the past 13-14 years, not just the recently developed ones. This question is examined by looking only at a subset of available data bases, those that include both surface-pressure measurements and blade-moment measurements. The nine data bases that fall into this category are shown in Table 3 (refs. 176-180). First, all use

of these data bases in the time frame of the paper are categorized as "references." Secondly, when the data base was used by an organization other than the test aircraft manufacturers, then this is referred to as a "non-self reference." Of the nine major data bases, two have never been used. These are the CH-47A and AH-1G TAAT data bases for which tabulated data were never provided and the data on tape have been too difficult of access to encourage use. The UH-1 and XH-51A aircraft data bases have had only limited use in recent years. The NH-3A and CH-53A data bases have had fairly extensive use, but only by the aircraft manufacturer. Of the nine data bases, only three appear to be in widespread use--the CH-34 flight test, the CH-34 wind tunnel test, and the AH-1G OLS flight test. The development of a major rotor loads data base is clearly expensive, but the use that these data bases will be put to is never so clear.

An alternative approach of assessing the use of data bases is to compare the use of proprietary data bases with those that have been developed and supported by the government. Again, the basis for comparison is imperfect as only the published literature is used to judge comparative use. Sixty-five references to full-scale, flight-test data were noted in preparing this paper. Of these 60% referenced a government-developed data base, while the other 40% referenced company proprietary data bases. The use of proprietary data bases is, of course, much more significant for unpublished work. What governs the choice of a data base is not completely clear. However, it does appear that there are at least three primary factors: (1) ease of access to the data base, (2) test documentation, and (3) validation of the data. These factors are more easily accommodated in the development of a proprietary data base than a public one.

CONCLUSIONS

The present paper has reviewed the research that has been performed in the area of rotor loads in the 13 to 14 year period since the 1973 AGARD Milan meeting and the 1974 hypothetical rotor comparison. The conclusions of this review are:

1. The detailed predictive capability of the present rotor loads analyses is barely satisfactory for the prediction of oscillatory loads. It is not satisfactory for the prediction of vibratory loads.

2. There is a pressing need for an improved rotor loads predictive capability within the government. At the present time, there is no clear evidence of what the major limitations are of the current rotor loads analyses for the prediction of vibratory loads. This information cannot be obtained without a systematic comparison of prediction and measurement using CAMRAD now, and 2GCHAS when it becomes available.

3. There is a significant need for quality data including blade-pressure measurements and extensive and complete structural measurments. Maximum efforts should be made to insure that the data are valid during both the experiment and the data-reduction process. In the case of aircraft flight test, there must be a commitment of open test time for subsequent tests. Development of data bases should proceed only if there is a firm, long-range program to use the data within the government.

4. The research in rotor loads reduction has demonstrated that there is a substantial potential for reduced vibratory loads in new rotor design. However, clear design guidelines have not been developed from research performed to date. Additional theoretical and experimental work is needed to understand the sources and mechanisms of vibration.

RECOMMENDATIONS

As a result of this survey it is recommended that:

1. The government should continue the development of its own comprehensive rotor analyses, specifically CAMRAD, which is operational, and 2GCHAS, which is under development. It is important that this work be done by the government using their best analysts.

2. Systematic comparisons of theory and experiment for rotor loads should be expanded. These comparisons should specifically examine the behavior of the vibratory loads for harmonics three and higher.

3. A program of theoretical model testing should be started using CAMRAD. The objective of this testing should be to compare the relative merits of alternative theoretical models using experimental data where possible to discriminate between approaches.

4. The government should initiate a program of full-scale rotor testing with limited blade surface pressure instrumentation to support the development of rotor loads analyses and theoretical-model testing. This program should be considered complementary to the fully-instrumented rotor tests that are presently being planned.

REFERENCES

1. Rabbott, J. P., Jr.; Lizak, A. A.; and Paglino, V. M.: A Presentation of Measured and Calculated Full-Scale Rotor Blade Aerodynamic and Structural Loads. USAAVLABS TR 66-31, 1966.

2. Ormiston, Robert A.: Comparison of Several Methods for Predicting Loads on a Hypothetical Helicopter Rotor. NASA SP-352, 1974.

3. Gabel, Richard: Current Loads Technology for Helicopter Rotors. AGARD Conf. Proc. No. 122, Mar. 1973.

4. Arcidiacono, Peter J.; and Carlson, Raymond G.: Helicopter Rotor Loads Prediction. AGARD Conf. Proc. No. 122, Mar. 1973.

5. Bennett, Richard L.: Rotor System Design and Evaluation Using a General Purpose Helicopter Flight Simulation Program. AGARD Conf. Proc. No. 122, Mar. 1973.

6. Piziali, R. A.: Rotor Aeroelastic Simulation--A Review. AGARD Conf. Proc. No. 122, Mar. 1973.

7. Loewy, Robert G.: Summary Analysis. AGARD Conf. Proc. No. 122, Mar. 1973.

8. Arcidiacono, Peter J.; and Sopher, Robert: Review of Rotor Loads Prediction Methods. AGARD Conf. Proc. No. 334, May 1982.

9. Johnson, Wayne: Recent Developments in the Dynamics of Advanced Rotor Systems. NASA TM 86669, 1985.

10. Friedmann, P. P.: Formulation and Solutions of Rotary-wing Aeroelastic Stability and Response Problems. Vertica, vol. 7, 1983, pp. 101-104.

11. Friedmann, P. P.: Recent Trends in Rotary-Wing Aeroelasticity. Paper No. 55, Twelfth Eur. Rotorcraft Forum, Sept. 1986.

12. Johnson, Wayne: Recent Developments in Rotary-Wing Aerodyanmic Theory. AIAA Journal, vol. 24, Aug. 1986, pp. 1219-1244.

13. Yen, Jing G.; and Glass, Max: Helicopter Rotor Load Prediction. Preprint No. 6, Amer. Hel. Soc. Specialists Meeting on Helicopter Fatigue Methodology, Mar. 1980.

14. Dadone, L.: The Role of Analysis in the Aerodynamic Design of Advanced Rotors. AGARD Conf. Proc. No. 334, May 1982.

15. Landgrebe, A. J.: Overview of Helicopter Wake and Airloads Technology. Amer. Hel. Soc./Nanjing Aero. Inst. International Seminar--The Theoretical Basis of Helicopter Technology, Nov. 1985. Also: Paper No. 18, Twelfth Eur. Rotorcraft Forum, Sept. 1986.

16. McCroskey, W. J.; and Fisher, Richard K., Jr.: Detailed Aerodynamic Measurements on a Model Rotor in the Blade Stall Regime. J. Amer. Hel. Soc., vol. 17, no. 1, Jan. 1972, pp. 20-30.

17. Johnson, Wayne: Comparison of Three Methods for Calculation of Helicopter Rotor Blade Loading and Stresses Due to Stall. NASA TN D-7833, 1974.

18. Carta, F. O.; Casellini, L. M.; Arcidiacono, P. J.; and Elman, H. L.: Analytical Study of Helicopter Rotor Stall Flutter. Amer. Hel. Soc. 26th Annual National Forum, May 1970.

19. Arcidiacono, P. J.; Carta, F. O.; Casellini, L. M.; and Elman, H. L.: Investigation of Helicopter Control Loads Induced by Stall Flutter. USAAVLABS TR 70-2, 1970.

20. Johnson, Wayne: The Effect of Dynamic Stall on the Response and Airloading of Helicopter Rotor Blades. J. Amer. Hel. Soc., vol. 14, no. 2, Apr.1969, pp. 68-79.

21. Johnson, Wayne: The Response and Airloading of Helicopter Rotor Blades Due to Dynamic Stall. Massachusetts Institute of Technology, ASRL TR 130-1, May 1970.

22. Gormont, Ronald E.: A Mathematical Model of Unsteady Aerodynamics and Radial Flow for Application to Helicopter Rotors. USAAMRDL TR 72-67, 1973.

23. Carlson, R. G.; Blackwell, R. H.; Commerford, G. L.; and Mirick, P. H.: Dynamic Stall Modeling and Correlation with Experimental Data on Airfoils and Rotors. NASA SP-352, 1974.

24. Blackwell, R. H.; and Commerford, G. L.: Investigation of the Effects of Blade Structural Design Parameters on Helicopter Stall Boundaries. USAAMRDL TR 74-25, 1974.

25. McCroskey, W. J.: Prediction of Unsteady Separated Flows on Oscillating Airfoils. AGARD Lecture Series No. 94, 1978.

26. McAllister, K. W.; Carr, L. W.; and McCroskey, W. J.: Dynamic Stall Experiments on the NACA 0012 Airfoil. NASA TP 1100, 1977.

27. Beddoes, T. S.: A Syntesis of Unsteady Aerodynamics Stall Effects, Including Hysteresis. Paper No. 17, First European Rotorcraft and Powered Lift Aircraft Forum, Sept. 1975.

28. Ericsson, L. E.; and Reding, J. P.: Dynamics Stall Analysis in the Light of Recent Numerical and Experimental Results. J. Aircraft, vol. 13, Apr. 1976, pp. 248-255.

29. Gangwani, Santu T.: Prediction of Dynamic Stall and Unsteady Airloads for Rotor Blades. J. Amer. Hel. Soc., vol. 27, no. 4, Oct. 1982, pp. 57-64.

30. Gangwani, Santu T.: Synthesized Airfoil Data Method for Prediction of Dynamic Stall and Unsteady Airloads. NASA CR 3672, 1983.

31. Gangwani, Santu T.: Synthesized Airfoil Data Method for Prediction of Dynamic Stall and Unsteady Airloads. Vertica, vol. 8, 1984, pp. 93-118. Also: Amer. Hel. Soc. 39th Annual Forum Proceedings, May 1983, pp. 15-33.

32. Gangwani, Santu T.: Development of an Unsteady Aerodynamics Model to Improve Correlation of Computed Blade Stresses With Test Data. Paper No. 8, Amer. Hel. Soc./NASA 2nd Decennial Specialists' Meeting on Rotorcraft Dynamics Proceedings, Nov. 1984. Also: NASA CP 2400, 1985.

33. Sutton, L. R.; and Gangwani, S. T.: The Development and Application of an Analysis for the Determination Coupled Tail Rotor/Helicopter Air Resonance Behavior. USAAMRDL TR 75-35, 1975.

34. Shockey, Gerald A.; Cox, Charles R.; and Williamson, Joe W.: AH-1G Helicopter Aerodynamic and Structural Loads Survey. USAAMRDL TR 76-39, 1977.

35. Tran, C. T.; and Petot, D.: Semi-Empirical Model for the Dynamic Stall of Airfoils in View of the Application to the Calculation of Response of a Helicopter Blade in Forward Flight. Paper No. 48, Sixth Eur. Rotorcraft and Powered Lift Aircraft Forum, Sept. 1980.

36. Peters, David A.: Toward a Unified Aerodynamic Model for Use in Rotor Blade Stability Analyses. Amer. Hel. Soc. 40th Annual Forum Proceedings, May 1984, pp. 525-538.

37. Wilby, P. G.; Young, C.; and Grant, J.: An Investigation of the Influence of Fuselage Flow Field on Rotor Loads and the Effects of Vehicle Configuration. Vertica, vol. 3, 1979, pp. 79-94. Also: Paper No. 8, Fourth European Rotorcraft and Powered Lift Aircraft Forum, Sept. 1978.

38. Brotherhood, P.; and Riley, M. J.: Flight Experiments on Aerodynamic Features Affecting Helicopter Blade Design. Vertica, vol. 2, 1978, pp. 27-42.

39. Costes, J. J.: Unsteady Three-Dimensional Stall on a Rectangular Wing. Paper No. 30, Twelfth Eur. Rotorcraft Forum, Sept. 1986.

40. Hooper, W. E.: The Vibratory Airloading of Helicopter Rotors. Vertica, vol. 8, 1984, pp. 71-92. Also: Paper No. 46, Ninth Eur. Rotorcraft Forum, Sept. 1983.

41. Scheiman, James: A Tabulation of Helicopter Rotor-Blade Differential Pressures, Stresses, and Motions as Measured in Flight. NASA TM X-952, 1964.

42. Johnson, Wayne: Helicopter Theory. Princeton University Press, 1980.

43. Brotherhood, P.: An Appraisal of Rotor Blade-Tip Vortex Interaction and Wake Geometry from Flight Measurements. AGARD Conf. Proc. 134, May 1982.

44. Landgrebe, A. J.; and Bellinger, E. D.: An Investigation of the Quantitative Applicability of Model Helicopter Rotor Wake Patterns Obtained from a Water Tunnel. USAAMRDL TR 71-69, Dec. 1971.

45. Lehman, A. F.: Model Studies of Helicopter Rotor Flow Patterns. USAAVLABS TR 68-17, Apr.1968.

46. Johnson, Wayne: Comparison of Calculated and Measured Model Rotor Loading and Wake Geometry. NASA TM 81189, 1980.

47. Biggers, James C.; Lee, Albert; Orloff, Kenneth L.; and Lemmer, Opal J.: Laser Velocimeter Measurements of Two-Bladed Helicopter Rotor Flow Fields. NASA TM 73238, 1977.

48. Egolf, T. A.; and Landgrebe, A. J.: Helicopter Rotor Wake Geometry and Its Influence in Forward Flight, Volume I - Generalized Wake Geometry and Wake Effect on Rotor Airloads and Performance. NASA CR 3726, 1983.

49. Egolf, T. A.; and Landgrebe, A. J.: Generalized Wake Geometry for a Helicopter Rotor in Forward Flight and Effect of Wake Deformation on Airloads. Amer. Hel. Soc. 40th Annual Forum Proc., May 1984, pp. 359-376.

50. Yamauchi, Gloria K.; Heffernan, Ruth M.; and Gaubert, Michel: Correlation of SA349/2 Helicopter Flight Test Data with a Comprehensive Rotorcraft Model. NASA TM 88351, 1987. Replaces Paper No. 74, Twelfth Eur. Rotorcraft Forum, Sept. 1986.

51. Rabbott, J. P., Jr.; Lizak, A. A.; and Paglino, V. M.: Tabulated CH-34 Blade Surface Pressures Measured at NASA/Ames Full Scale Wind Tunnel. SER-58399, Dec. 1965.

52. Miller, R. H.: Factors Influencing Rotor Aerodynamics in Hover and Forward Flight. Vertica, vol. 9, 1985, pp. 155-164. Also: Paper No. 11, Tenth Eur. Rotorcraft Forum, Aug. 1984.

53. Phelan, P. G.; and Tarzanin, F. J., Jr.: Restructuring the Rotor Analysis Program C-60. Paper No. 12, Amer. Hel. Soc./NASA 2nd Decennial Specialists' Meeting on Rotorcraft Dynamics Proceedings, Nov. 1984. Also: NASA CP 2400, 1985.

54. Heffernan, R.; and Gaubert, M.: Structural and Aerodynamic Loads and Performance Measurements of an SA349/2 Helicopter with an Advanced Geometry Rotor. NASA TM 88370, 1986.

55. Cowan, John; Dadone, Leo; and Gangwani, Santu: Wind Tunnel Test of a Pressure Instrumented Model Scale Advanced Rotor. Amer. Hel. Soc. 42nd Annual Forum Proceedings, June 1986, pp. 217-229.

56. Young, C.: Development of the Vortex Ring Wake Model and Its Influence on the Prediction of Rotor Loads. AGARD Conf. Proc. No. 334, May 1982.

57. Costes, J. J.: Calcul des Forces Aerodynamiques Instationnaires sur les Pales d'un Rotor d'Helicoptere. La Recherche Aerospatiale, No. 1972-2, 1972. Also: NASA TT F-15039, 1973.

58. Runyan, Harry L.; and Tai, Hsiang: Application of a Lifting Surface Theory for a Helicopter in Forward Flight. Paper No. 24, Eleventh Eur. Rotorcraft Forum, Sept. 1985.

59. Pierce, G. Alvin; and Vaidyanathan, Arnand R.: Helicopter Rotor Loads Using Discretized Matched Asymptotic Expansions. NASA CR 166092, May 1983.

60. Van Holten, Th.: On the Validity of Lifting Line Concepts in Rotor Analysis. Vertica, vol. 1, 1977, pp. 239-254.

61. Caradonna, F. X.; and Tung, C.: A Review of Current Finite Difference Rotor Flow Methods. Amer. Hel. Soc. 42nd Annual Forum Proceedings, June 1986, pp. 967-983.

62. Tung, Chee; Caradonna, Francis X.; and Johnson, Wayne R.: The Prediction of Transonic Flows on Advancing Rotors. J. Amer. Hel. Soc., vol. 31, no. 3, July 1986, pp. 4-9. Also: Amer. Hel. Soc. 40th Annual Forum Proceedings, May 1984, pp. 389-399.

63. Gabel, Richard: Rotor Mast Height. NASA CP 2400, 1985.

64. Freeman, Carl E.; and Wilson, John C.: Rotor-Body Interference (ROBIN) - Analysis and Test. Preprint No. 80-5, Amer. Hel. Soc. 36th Annual Forum, May 1980.

65. Huber, H.; and Polz, G.: Studies on Blade-to-Blade and Rotor-Fuselage-Tail Interferences. AGARD Conf. Proc. No. 334, May 1982.

66. Jepson, D.; Moffitt, R.; Hilzinger, K.; and Bissell, J.: Analysis and Correlation of Test Data From an Advanced Technology Rotor System. NASA CR 3714, 1983.

67. Johnson, Wayne: Performance and Loads Data on a Full-Scale Rotor with Four Tip Planforms. NASA TM 81229, 1980.

68. Johnson, Wayne; and Yamauchi, G. K.: Applications of an Analysis of Axisymmetric Body Effects on Rotor Performance and Loads. Paper No. 3, Tenth Eur. Rotorcraft Forum, Aug. 1984.

69. Yamauchi, Gloria; and Johnson, Wayne: Development and Application of an Analysis of Axisymmetric Body Effects on Helicopter Rotor Aerodynamics Using Modified Slender Body Theory. NASA TM 85934, 1984.

70. McKenzie, K. T.; and Howell, D. A. S.: The Prediction of Loading Actions on High Speed Semirigid Rotor Helicopters. AGARD Conf. Proc. No. 122, Mar. 1973.

71. Taylor, Robert B.; and Teare, Paul A.: Helicopter Vibration Reduction with Pendulum Absorbers. J. Amer. Hel. Soc., vol. 20, no. 3, July 1975, pp. 9-17.

72. Blackwell, R H., Jr.: Blade Design for Reduced Helicopter Vibration. J. Amer. Hel. Soc., vol. 28, no. 3, July 1983, pp. 33-41. Also: Preprint No. 8, Amer. Hel. Soc. Specialists' Meeting on Helicopter Vibration, Nov. 1981.

73. Gaukroger, D. R.; and Hassal, C. J. W.: Measurement of Vibratory Displacements of a Rotating Blade. Vertica, vol. 2, 1978, pp. 111-120.

74. Gaukroger, D. R.; Payen, D. B.; and Walker, A. R.: Application of Strain Gauge Pattern Analysis. Paper No. 19, Sixth European Rotorcraft and Powered Lift Aircraft Forum, Sept. 1980.

75. Blackwell, R. H.; and Mirick, P. H.: Effect of Blade Design Parameters on Helicopter Stall Boundaries. Preprint No. 833, Amer. Hel. Soc. 30th Annual National Forum, May 1974.

76. Blackwell, R. H., Jr.; and Fredrickson, K. C.: Wind Tunnel Evaluation of Aeroelastically Conformable Rotors. USAAVRADCOM TR 80-D-32, 1981.

77. Blackwell, R. H.; Murrill, R. J.; Yeager, W. T., Jr.; and Mirick, P. H.: Wind Tunnel Evaluation of Aeroelastically Conformable Rotors. J. Amer. Hel. Soc., vol. 26, no. 2, Apr. 1981, pp. 31-39. Also: Preprint No. 80-23, Amer. Hel. Soc. 36th Annual Forum, May 1980.

78. Kottapalli, S. B. R.: Hub Loads Reduction by Modification of a Blade Torsional Response. Amer. Hel. Soc. 39th Annual Forum Proceedings, May 1983, pp. 173-179.

79. Taylor, Robert B.: Helicopter Vibration Reduction by Rotor Blade Modal Shaping. Amer. Hel. Soc. 38th Annual Forum Proceedings, May 1982, pp. 90-101.

80. Taylor, Robert B.: Helicopter Rotor Blade Design for Minimum Vibration. NASA CR 3825, 1984.

81. Esculier, Jacques; and Bousman, William G.: Calculated and Measured Blade Structural Response on a Full-Scale Rotor. Amer. Hel. Soc. 42nd Annual Forum Proceedings, June 1986, pp. 81-110.

82. Lee, B. L.: Experimental Measurements of the Rotating Frequencies and Mode Shapes for a Full Scale Helicopter Rotor in a Vacuum and Correlations with Calculated Results. Preprint No. 79-18, Amer. Hel. Soc. 35th Annual National Forum, May 1979.

83. Srinivasan, A. V.; Cutts, D. G.; and Shu, H. T.: An Experimental Investigation of the Structural Dynamics of a Torsionally Soft Rotor in Vacuum. NASA CR 177418, 1986.

84. Sharpe, David L.: An Experimental Investigation of the Flap-Lag-Torsion Aeroelastic Stability of a Small-Scale Hingeless Helicopter Rotor in Hover. NASA TP 2546, 1986.

85. Yen, Jing G.; and McLarty, Tyce T.: Analysis of Rotor-Fuselage Coupling and Its Effect on Rotorcraft Stability and Response. Vertica, vol. 3, 1979, pp. 205-219.

86. Lee, Charles D.; and White, James A.: Investigation of the Effect of Hub Support Parameters on Two-Bladed Rotor Oscillatory Loads. NASA CR-132435, 1974.

87. Sopher, Robert; and Kottapalli, S. B. R.: Correlation of Predicted Vibrations and Test Data for a Wind Tunnel Helicopter Model. Amer. Hel. Soc. 38th Annual Forum Proceedings, May 1982, pp. 102-113.

88. Sopher, Robert; Studwell, R. E.; Cassarino, S.; and Kottapalli, S. B. R.: Coupled Rotor/Airframe Vibration Analysis. NASA CR 3582, 1982.

89. Gabel, Richard; and Sankewitsch, Vladimir: Rotor-Fuselage Coupling by Impedance. Amer. Hel. Soc. 42nd Annual Forum Proceedings, June 1986, pp. 1-11.

90. Harvey, Keith W.: The Effect of Cyclic Feathering Motions on Dynamic Rotor Loads. NASA SP 352, 1974.

91. Hansford, Robert E.: Comparison of Predicted and Experimental Rotor Loads to Evaluate Flap-Lag Coupling with Blade Pitch. J. Amer. Hel. Soc., vol. 24, no. 5, Oct. 1979, pp. 3-11. Also: Preprint No. 78-19, Amer. Hel. Soc. 34th Annual National Forum, May 1978.

92. Bielawa, Richard L.: Blade Stress Calculations - Mode Deflection vs. Force Integration. J. Amer. Hel. Soc., vol. 24, no. 3, July 1978, pp. 10-16. Also: Amer. Hel. Soc. Symposium on Rotor Technology Proceedings, Aug. 1976.

93. Hansford, Robert E.: A Unified Formulation of Rotor Load Prediction Methods. J. Amer. Hel. Soc., vol. 31, no. 2, Apr. 1986, pp. 58-65. Also: Amer. Hel. Soc. 41st Annual Forum Proceedings, May 1985, pp. 73-83.

94. Tarzanin, F. J., Jr.; and Ranieri, J.: Investigation of Torsional Natural Frequency on Stall-Induced Dynamic Loading. USAAVLABS TR 73-94, 1974.

95. Tarzanin, F. J., Jr.; and Mirick, P. H.: Control Load Envelope Shaping by Live Twist. NASA SP-352, 1974.

96. Doman, Glidden S.; Tarzanin, Frank J.; and Shaw, John, Jr.: Investigation of Aeroelastically Adaptive Rotor Systems. Amer. Hel. Soc. Symposium on Rotor Technology Proceedings, Aug. 1976.

97. Blackwell, R. H.; and Merkley, D. J.: The Aeroelastically Conformable Rotor Concept. J. Amer. Hel. Soc., vol. 24, no. 4, July 1979, pp. 37-44. Also: Preprint No. 78-59, Amer. Hel. Soc. 34th Annual Forum, May 1978.

98. Weller, William H.: Experimental Investigation of Effects of Blade Tip Geometry on Loads and Performance for an Articulated Rotor System. NASA TP 1303, 1979.

99. Yeager, William T., Jr.; and Mantay, Wayne R.: Wind-Tunnel Investigation of the Effects of Blade Tip Geometry on the Interaction of Torsional Loads and Performance for an Articulated Helicopter Rotor. NASA TP 1926, 1981.

100. Yeager, William T., Jr.; and Mantay, Wayne R.: Loads and Performance Data from a Wind-Tunnel Test of Model Articulated Helicopter Rotors with Two Different Blade Torsional Stiffnesses. NASA TM 84573, 1983.

101. Sutton, Lawrence R.; White, Richard P., Jr.; and Marker, Robert L.: Wind-Tunnel Evaluation of an Aeroelastically Conformable Rotor. USAAVRADCOM TR 81-D-43, 1982.

102. Mantay, Wayne R.; and Yeager, William T., Jr.: Parametric Tips Effects for Aeroelastically Conformable Rotor Applications. NASA TM 85682, 1983. Also: Paper No. 53, Ninth Eur. Rotorcraft Forum, Sept. 1983.

103. Mantay, Wayne R.; and Yeager, William T., Jr.: Aeroelastic Considerations for Torsionally Soft Rotors. NASA TM 87687, 1986. Paper No. 9, Amer. Hel. Soc./NASA 2nd Decennial Specialists' Meeting on Rotorcraft Dynamics Proceedings, Nov. 1984, and NASA CP 2400, 1985, pp. 117-134.

104. Tarzanin, F. J., Jr.; and Vlaminck, R. R.: Investigation of the Effects of Blade Sweep on Rotor Vibratory Loads. NASA CR-166526, 1983.

105. Miura, H.: Overview: Applications of Numerical Optimization Methods to Helicopter Design Problems. NASA CP 2327, 1984.

106. Peters, David A.; Ko, Timothy; Korn, Alfred; and Rossow, Mark P.: Design of Helicopter Rotor Blades for Desired Placement of Natural Frequencies. Amer. Hel. Soc. 39th Annual Forum Proceedings, May 1983, pp. 674-689.

107. Pritchard, Jocelyn I.; Adelman, Howard M.; and Haftka, Raphael T.: Sensitivity Analysis and Optimization of Nodal Point Placement for Vibration Reduction. NASA TM 87763, 1986.

108. Friedmann, P. P.; and Shanthakumaran, P.: Optimum Design of Rotor Blades for Vibration Reduction in Forward Flight. J. Amer. Hel. Soc., vol. 29, no. 4, Oct. 1984, pp. 70-80.

109. Yen, Jing C.: Coupled Aeroelastic Hub Loads Reduction. Amer. Hel. Soc./ Nanjing Aero. Inst. International Seminar - The Theoretical Basis of Helicopter Technology, Nov. 1985.

110. Hammond, C. E.: Wind Tunnel Results Showing Rotor Vibratory Loads Reduction Using Higher Harmonic Blade Pitch. J. Amer. Hel. Soc., vol. 28, no. 1, Jan. 1983, pp. 10-15. Also: Preprint No. 80-66, Amer. Hel. Soc. 36th Annual Forum, May 1980.

111. Wood, E. Roberts; Powers, Richard W.; Cline, John H.; and Hammond, C. Eugene: On Developing and Flight Testing a Higher Harmonic Control System. J. Amer. Hel. Soc., vol. 30, no. 1, Jan. 1985, pp. 3-20. Also: Amer. Hel. Soc. 39th Annual Forum Proceedings, May 1983, pp. 592-612.

112. McCloud, John L. III: An Analytical Study of a Multicylic Controllable Twist Rotor. Preprint No. 932, Amer. Hel. Soc. 31st Annual National Forum, May 1975.

113. Hammond, C. Eugene; and Weller, William H.: Wind-Tunnel Testing of Aeroelastically Scaled Helicopter Rotor Models. U.S. Army Science Conference, June 1976.

114. Mantay, Wayne R.; and Rorke, James B.: The Evolution of the Variable Geometry Rotor, Amer. Hel. Soc. Symposium on Rotor Technology Proceedings, Aug. 1976.

115. Sadler, S. Gene: Development and Application of a Method for Predicting Rotor Free Wake Positions and Resulting Rotor Blade Air Loads. NASA CR 1911, 1971.

116. Landgrebe, A. J.; and Bellinger, E. D.: Experimental Investigation of Model Variable-Geometry and Ogee Tip Rotors. NASA CR 2275, 1974.

117. Gangwani, Santu T.: The Effect of Helicopter Main Rotor Blade Phasing and Spacing on Performance, Blade Loads, and Acoustics. NASA CR 2737, 1975.

118. Rorke, J. B.: Hover Performance Tests of Full-Scale Variable Geometry Rotors. NASA CR 2713, 1976.

119. Rabbott, John P., Jr.; and Niebanck, Charles F.: Experimental Effects of Tip Shape on Control Loads. Preprint No. 78-61, Amer. Hel. Soc. 34th Annual National Forum, 1978.

120. Stroub, Robert H.; Young, Larry A.; Keys, Charles N.; and Cawthorne, Matthew H.: Free-Tip Rotor Wind Tunnnel Test Results. J. Amer. Hel. Soc., vol. 31, no. 3, July 1986, pp. 19-26. Also: Amer. Hel. Soc. 41st Annual Forum Proceedings, May 1985, pp. 387-411.

121. McCloud, John L.; and Kretz, Marcel: Multicyclic Jet-Flap Control for Alleviation of Helicopter Blade Stresses and Fuselage Vibrtation. NASA SP-352, 1974, pp. 233-238.

122. Harvey, K. W.; Blankenship, B. L.; and Drees, J. M.: Analytical Study of Helicopter Gust Response at High Forward Speeds. USAAVLABS TR 69-1, 1969.

123. Bergquist, Russell R.: Helicopter Gust Response Including Unsteady Aerodynamic Stall Effects. USAAMRDL TR 72-68, 1973.

124. Arcidiacono, Peter J.; Bergquist, Russell R.; and Alexander, W. T., Jr.: Helicopter Gust Response Characteristics Including Unsteady Aerodynamic Stall Effects. J. Amer. Hel. Soc., vol. 19, no. 4, Oct. 1974, pp. 34-43. Also: NASA SP-352, 1974, pp.

125. Gaonkar, G. H.: Gust Response of Rotor and Propeller Systems. J. Aircraft, vol. 18, May 1981, pp. 389-396.

126. Bir, Gunjit Singh; and Chopra, Inderjit: Gust Response of Hingeless Rotors. J. Amer. Hel. Soc., vol. 31, no. 2, Apr. 1986, pp. 33-46. Also: Amer. Hel. Soc. 41th Annual Forum Proceedings, May 1985, pp. 47-72.

127. Bir, Gunjit Singh; and Chopra, Inderjit: Prediction of Blade Stresses Due to Gust Loading. Paper No. 73, Eleventh Eur. Rotorcraft Forum, Sept. 1985.

128. Fuh, J. S.; Hong, C. Y. R.; Lin, Y. K.; and Prussing, J. E.: Coupled Flap-Torsional Response of a Rotor Blade in Forward Flight Due to Atmospheric Turbulence Excitations. J. Amer. Hel. Soc., vol. 28, no. 3, July 1983, pp. 3-12.

129. Prussing, J. E.; Lin, Y. K.; and Shiau, T. N.: Rotor Blade Flap-Lag Stability and Response in Forward Flight in Turbulent Flows. J. Amer. Hel. Soc., vol. 29, no. 4, Oct. 1984, pp. 81-87.

130. Dunham, R. Earl, Jr.; Holbrook, G. Thomas; Mantay, Wayne R.; Campbell, Richard L.; and Van Gunst, Roger W.: Flight-Test Experience of a Helicopter Encountering an Airplane Trailing Vortex. Preprint No. 1063, Amer. Hel. Soc. 32nd Annual National V/STOL Forum, May 1976.

131. Mantay, Wayne R.; Holbrook, G. Thomas; Campbell, Richard L.; and Tomaine, Robert L.: Helicopter Response of an Airplanes's Trailing Vortex. J. Aircraft, vol. 14, Apr. 1977, pp. 357-363.

132. Kim, Ki-Chung; Bir, Gunjit; and Chopra, Inderjit: Helicopter Response to an Airplane's Vortex Wake. Paper No. 43, Twelfth Eur. Rotorcraft Forum, Sept. 1986.

133. Tarzanin, Frank J., Jr.: Panel 1: Prediction of Rotor and Control System Loads. NASA SP-352, 1974.

134. McHugh, Frank J.: What Are the Lift and Propulsive Force Limits At High Speed for the Conventional Rotor? Amer. Hel. Soc. 34th Annual National Forum Proceedings, May 1978, pp. 1-12.

135. McHugh, Frank J.; Clark, Ross; and Solomon, Mary: Wind Tunnel Investigation of Rotor Lift and Propulsive Force at High Speed - Data Analysis. NASA CR 145217-1, 1977.

136. Van Gaasbeek, James R.: An Investigation of High-G Maneuvers of the AH-1G Helicopter. USAAMRDL TR 75-18, Apr. 1975.

137. Tarzanin, F. J., Jr.: Prediction of Control Loads Due to Blade Stall. J. Amer. Hel. Soc., vol. 17, no. 2, Apr. 1972, pp. 33-46. Also: Preprint 513, Amer. Hel. Soc. 27th Annual National Forum, May 1971.

138. Harris, Franklin D.; Tarzanin, Frank J. Jr.; and Fisher, Richard K., Jr.: Rotor High Speed Performance, Theory vs. Test. J. Amer. Hel. Soc., vol. 15, no. 3, July 1970, pp. 35-44.

139. Crimi, P.: Theoretical Prediction of the Flow in the Wake of a Helicopter Rotor. Cornell Aeronautical Laboratory Report No. BB-1994-S-1 and -2, Sept. 1965.

140. Ericsson, L. E.; and Reding, J. P.: Dynamic Stall of Helicopter Blades. J. Amer. Hel. Soc., vol. 17, no. 1, Jan. 1972.

141. Landgrebe, A. J.; and Egolf, T. A.: Rotorcraft Wake Analysis for the Prediction of Induced Velocities. USAAMRDL TR 75-45, 1976.

142. Scully, M. P.: Computation of Helicopter Rotor Wake Geometry and Its Influence on Rotor Harmonic Airloads. Massachusetts Institute of Technology, ASRL TR 178-1, Mar. 1975.

143. Davis, John M.: Rotorcraft Flight Simulation with Aeroelastic Rotor and Improved Aerodynamic Representation, Volume I - Engineer's Manual. USAAMRDL TR 74-10A, 1974.

144. Staley, James A.: Validation of Rotorcraft Flight Simulation Program Through Correlation with Flight Data for Soft-In-Plane Hingeless Rotors. USAAMRDL TR 75-50, 1976.

145. Briczinski, S. J.: Validation of the Rotorcraft Flight Simulation Program (C81) for Articulated Rotor Helicopters Through Correlation With Flight Data. USAAMRDL TR 76-4, 1976.

146. McLarty, Tyce T.: Rotorcraft Flight Simulation With Coupled Rotor Aeroelastic Stability Analysis, Volume I, Engineer's Manual. USAAMRDL TR 76-41A, 1977.

147. Van Gaasbeek, J. R.; McLarty, T. T.; and Sadler, S. G.: Rotorcraft Flight Simulation, Computer Program C81, Volume I - Engineer's Manual. USARTL TR 77-54A, 1979.

148. Van Gaasbeek, James R.: Rotorcraft Flight Simulation Computer Program C81 With DATAMAP Interface, Volume I - User's Manual. USAAVRADCOM TR 80-D-38A, 1981.

149. Shockey, G. A.; Williamson, J. W.; and Cox, C. R.: Helicopter Aerodynamics and Structural Loads Survey. Preprint 1060, Amer. Hel. Soc. 32nd Annual National Forum, May 1976.

150. Van Gaasbeek, James R.; and Austin, Edward E.: Digital Simulation of the Operational Loads Survey Flight Tests. Preprint No. 78-58, Amer. Hel. Soc. 34th Annual National Forum, May 1978.

151. Van Gaasbeek, James R.: Validation of the Rotorcraft Flight Simulation Program (C81) Using Operational Loads Survey Flight Test Data. USAAVRADCOM TR 80-D-4, 1980.

152. Merkley, Donald J.; and Ragosta, Arthur E.: DATAMAP and Its Impact on Prediction Programs. AGARD Conf. Proc. No. 334, May 1982.

153. Dompka, Robert V.; and Corrigan, John J.: AH-1G Flight Vibration Correlation Using NASTRAN and the C81 Rotor/Airframe Coupled Analysis. Amer. Hel. Soc. 42nd Annual Forum Proceedings, June 1986, pp. 45-61.

154. Yen, J. G.; and Weller, W. H.: Analysis and Application of Compliant Rotor Technology. Paper No. 11, Sixth Eur. Rotorcraft and Powered Lift Aircraft Forum, Sept. 1980.

155. Sheffler, Marc: Analysis and Correlation with Theory of Rotor Lift-Limit Test Data. NASA CR 159139, 1979.

156. Lemnios, A. Z.; and Smith, A. F.: An Analytical Evaluation of the Controllable Twist Rotor Performance and Dynamic Behavior. USAAMRDL TR 72-16, 1972.

157. Berman, Alex; Chen, Shyi-Yaung; Gustavson, Bruce; and Hurst, Patricia: Dynamic System Coupler Program (DYSCO 4.0), Volume I - Theoretical Manual. USAAVSCOM TR 85-D-24A, 1986.

158. Bielawa, Richard L.; Cheney, Marvin C., Jr.; and Novak, Richard C.: Investigation of a Bearingless Helicopter Rotor Concept Having A Composite Primary Structure. NASA CR 2637, 1976.

159. Bielawa, Richard L.: Aeroelastic Analysis for Helicopter Rotor Blades With Time-Variable, Nonlinear Structural Twist and Multiple Structural Redundancy - Mathematical Derivation and Program User's Manual. NASA CR 2638, 1976.

160. Bielawa, Richard L.: Aerolastic Analysis for Helicopter Rotors With Blade Appended Pendulum Vibration Absorbers - Mathematical Derivations and Program User's Manual. NASA CR 165896, 1982.

161. Sopher, Robert; and Hallock, Daniel W.: Development and Application of a Time-History Analysis for Rotorcraft Dynamics Based on a Component Approach. Paper No. 11, Amer. Hel. Soc./NASA 2nd Decennial Specialists' Meeting on Rotorcraft Dynamics Proceedings, Nov. 1984. Also: NASA CP 2400, 1985.

162. Johnson, Wayne: A Comprehensive Analytical Model of Rotorcraft Aerodynamics and Dynamics, NASA TM 81182, 1980.

163. Johnson, Wayne: Development of a Comprehensive Analysis for Rotorcraft - I. Rotor Model and Wake Analysis. Vertica, vol. 5, 1981, pp. 99-130.

164. Johnson, Wayne: Development of a Comprehensive Analysis for Rotorcraft - II. Aircraft Model, Solution Procedure and Applications. Vertica, vol. 5, 1981, pp. 185-216.

165. Fradenburgh, Evan A.: Aerodynamic Design of the Sikorsky S-76 SPIRIT Helicopter. J. Amer. Hel. Soc., vol. 24, no. 4, July 1979, pp. 11-19.

166. Gupta, B. P.: Blade Design Parameters Which Affect Helicopter Vibrations. Amer. Hel. Soc. 40th Annual Forum Proceedings, May 1984, pp. 207-217.

167. Yen, Jing C.; and Tanner, Hank: Design of UH-1 CMRB to Minimize Helicopter Vibration. Amer. Hel. Soc. 42nd Annual Forum Proceedings, June 1984, pp. 793-800.

168. Hansford, Robert E.: Rotor Load Correlation with the A. S. P. Blade. Amer. Hel. Soc. 42nd Annual Forum Proceedings, June 1986, pp. 13-26.

169. Charles F. Niebanck, "Model Rotor Test Data for Verification of Blade Response and Rotor Performance Calculations. USAAMRDL TR 74-29, 1974.

170. Morris, Charles E. K., Jr.; Tomaine, Robert L.; and Stevens, Dariene D.: A Flight Investigation of Performance and Loads for a Helicopter With NLR-1T Main-Rotor Blade Sections. NASA TM 80165, 1979.

171. Morris, Charles E. K., Jr.; Stevens, Dariene D.; and Tomaine, Robert L.: A Flight Investigation of Blade-Section Aerodynamics for a Helicopter Main Rotor Having NLR-1T Airfoil Sections. NASA TM 80166, 1980.

172. Morris, Charles E. K., Jr.; Tomaine, Robert L.; and Stevens, Dariene D.: A Flight Investigation of Performance and Loads for a Helicopter With 10-64C Main-Rotor Blade Sections. NASA TM 81871, 1980.

173. Morris, Charles E. K., Jr.: A Flight Investigation of Blade-Section Aerodynamics for a Helicopter Main Rotor Having 10-64C Airfoil Sections. NASA TM 83226, 1982.

174. Morris, Charles E. K., Jr.; Tomaine, Robert L.; and Stevens, Dariene D.: A Flight Investigation of Performance and Loads for a Helicopter With RC-SC2 Main-Rotor Blade Sections. NASA TM 81898, 1980.

175. Charles E. K. Morris, Jr., A Flight Investigation of Blade-Section Aerodynamics for a Helicopter Main Rotor Having RC-SC2 Airfoil Sections, NASA TM 83298, 1982.

176. Burpo, F.: Measurements of Dynamic Airloads on a Full-Scale Semi-Rigid Rotor TCREC TR 62-42, Dec. 1962.

177. Pruyn, R. R.: In-Flight Measurement of Rotor Blade Airloads, Bending Moments, and Motions, Together With Rotor Shaft Loads and Fuselage Vibration, On a Tandem Rotor Helicopter. USAAVLABS TR 67-9A, 1967.

178. Bartsch, E. A.: In-Flight Measurement and Correlation With Theory of Blade Airloads and Responses on the XH-51A Compound Helicopter Rotor, Volume I - Measurement and Data Reduction of Airloads and Structural Loads. USAAVLABS TR 68-22A, 1968.

179. Fenaughty, Ronald; and Beno, Edward: NH-3A Vibratory Airloads and Vibratory Rotor Loads. SER 611493, Jan. 1970.

180. Beno, Edward A.: CH-53A Main Rotor and Stabilizer Vibratory Airloads and Forces. SER 65593, June 1970.

TABLE 1.- CHARACTERISTICS OF ROTOR LOADS ANALYSES

Company	Code	Solution procedure: Method for solving equations of motion	Structural dynamics: Equations of motion	Structural dynamics: Modes included or finite elements	Structural dynamics: Structural and inertial coupling of modes or finite elements	Aerodynamics[a]: Dynamic stall	Aerodynamics[a]: Downwash
Bell Helicopter Textron	C81 •	Numerical integration	Modal	12	Fully coupled normal modes; bending moments determined from modal moment distributions	BUNS option: Lift per Tarzanin, ref. 137 Moment per Carta et al., ref. 18 Drag per Harris et al., ref. 138 UNSAN option: Per Gormont, ref. 22	Modified momentum theory (default), prescribed/free wake by table input, ref. 139
Boeing Vertol	C-60	Harmonic response	Finite element	25 plus flex beam and cuff	Fully coupled	Lift/moment per Tarzanin, ref. 137 Drag per Harris et al., ref. 138	Deformed near wake, prescribed far wake
Kaman	6F	Integrating matrix operator	Modal	Rigid flapping Rigid lead-lag Rigid torsion 1 flap bending 1 torsion Rigid servoflap	Fully coupled. Bending moments determined from uncoupled equations at zero pitch	None	
	DYSCO	Periodic shooting with Newton Raphson Method	Modal	5 flap 3 chord 3 torsion	Fully coupled	Lift per Tarzanin, ref. 137 Moment per Carta et al., ref. 18 Drag per Harris et al., ref. 138	Modified momentum theory
McDonnell-Douglas Helicopter	DART	Numerical integration	Finite element	20	Fully coupled	Lift/moment per Ericsson and Reding, ref. 140. Steady drag	Free wake by table input
	RAVIB	Harmonic response	Finite element	20	Fully coupled	Gangwani, ref. 30	Free wake, ref. 115
	RACAP	Harmonic response	Finite element	30	Fully coupled	Option 1: Per Johnson, ref. 21 Option 2: Per Gangwani, ref. 30	Free wake, refs. 115 and 142
Sikorsky Aircraft	Y201	Numerical integration	Modal	Rigid flapping Rigid lead-lag 3 flap bending 2 chord bending 1 torsion	Uncoupled normal modes obtained for zero pitch and twist. Structural coupling terms included as forcing functions in modal equations	UTRC Method, ref. 18	Prescribed wake, ref. 141
	G400	Numerical integration	Modal	4 flap bending 3 chord bending 3 torsion	Fully coupled	Gangwani, ref. 30	Prescribed wake, ref. 141
	RDYNE	Numerical integration	Modal	30	Fully coupled	Quasi-steady	Influence coefficient, ref. 141
NASA	CAMRAD	Numerical integration	Modal	10 bending 5 torsion	Fully coupled	Option 1: Per Johnson, ref. 21 Option 2: Per Gormont, ref. 22	Free wake, ref. 142

[a]Yawed flow drag and $C_{\ell_{max}}$, ref. 138.

TABLE 2.- USE OF RECENT ROTOR LOADS DATA BASES.

Data base	Source	Type	Primary references	Secondary references
CH-34 model rotor wind tunnel test	Niebanck, 1974 (ref. 169)	Tape	1	1
AH-1G OLS flight test	Shockey et al., 1977 (ref. 36)	Tape	2	8
AH-1G/NLR-1T flight test	Morris et al., 1979 (refs. 170 and 171)	Tabulated	1	0
AH-1G/10-64C flight test	Morris et al., 1980 (refs. 172 and 173)	Tabulated	1	0
AH-1G/RC-SC2 flight test	Morris et al., 1980 (refs. 174 and 175)	Tabulated	1	0
S-76 rotor wind tunnel test	Johnson, 1980 (ref. 67)	Tabulated	2	2
ACR model rotor wind tunnel test	Yeager and Mantay, 1983 (ref. 100)	Tabulated	1	0
AH-1G/tip aeroacoustic test		Tape	0	0
SA 349-2 flight test	Heffernan and Gaubert, 1986 (ref. 54)	Tabulated/ tape	1	0

TABLE 3.- USE OF MAJOR ROTOR LOADS DATA BASES.

Data base	Source	Type	References	Non-self references
UH-1 flight test	Burpo, 1962 (ref. 176)	Tabulated	2	1
CH-34 flight test	Scheiman, 1964 (ref. 41)	Tabulated	10	8
CH-34 wind tunnel test	Rabbott et al., 1966 (refs. 1 and 51)	Tabulated	7	5
CH-47A flight test	Pruyn, 1968 (ref. 177)	Tape	0	0
XH-51A flight test	Bartsch, 1968 (ref. 170)	Tabulated	2	1
NH-3A flight test	Fenaughty and Beno, 1970 (ref. 179)	Tabulated	4	1
CH-53A flight test	Beno, 1970 (ref. 180)	Tabulated	6	1
AH-1G/OLS flight test	Shockey et al., 1977 (ref. 34)	Tape	10	5
AH-1G/TAAT flight test		Tape	0	0

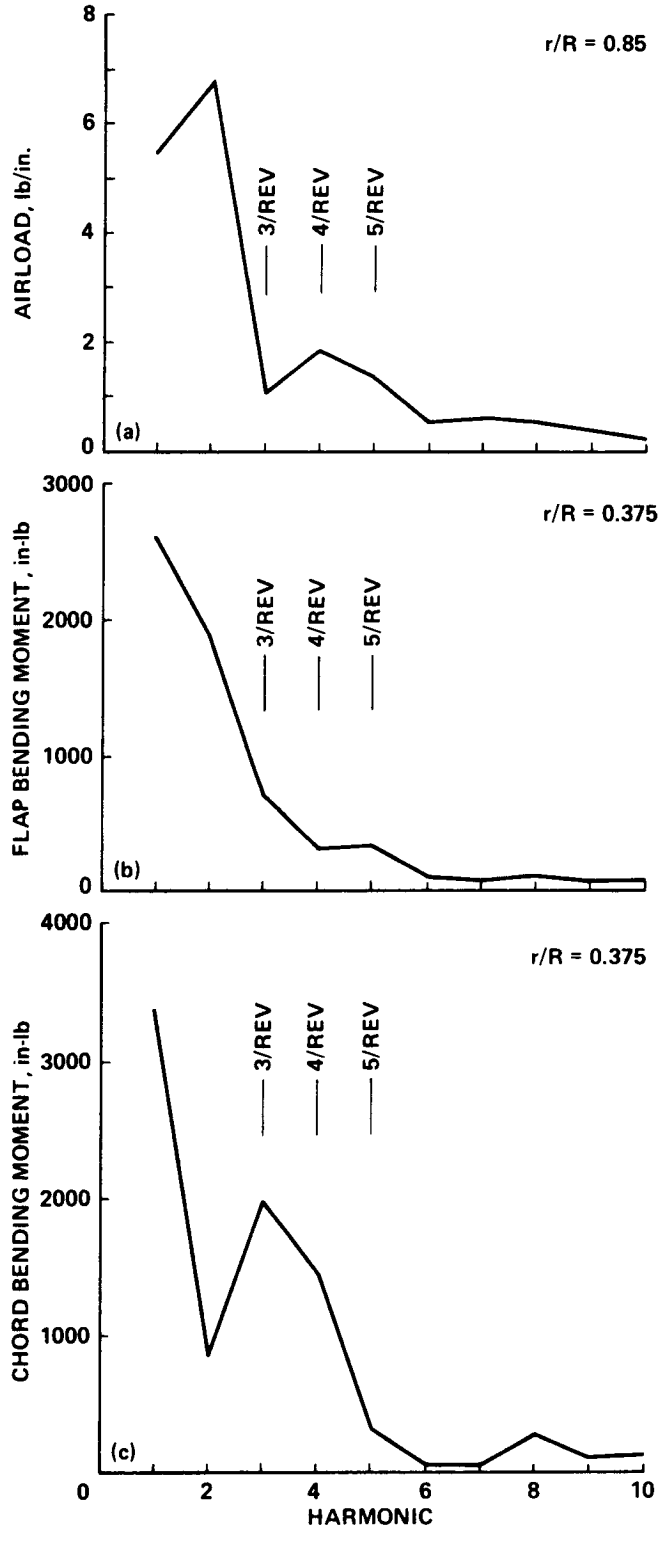

Figure 1.- Airloads and bending moments for CH-34 rotor in 40- by 80-Foot Wind Tunnel; $\mu = 0.39$, $\alpha_s = -5°$ (ref. 1). (a) Airloads. (b) Flap bending moment. (c) Chord bending moment.

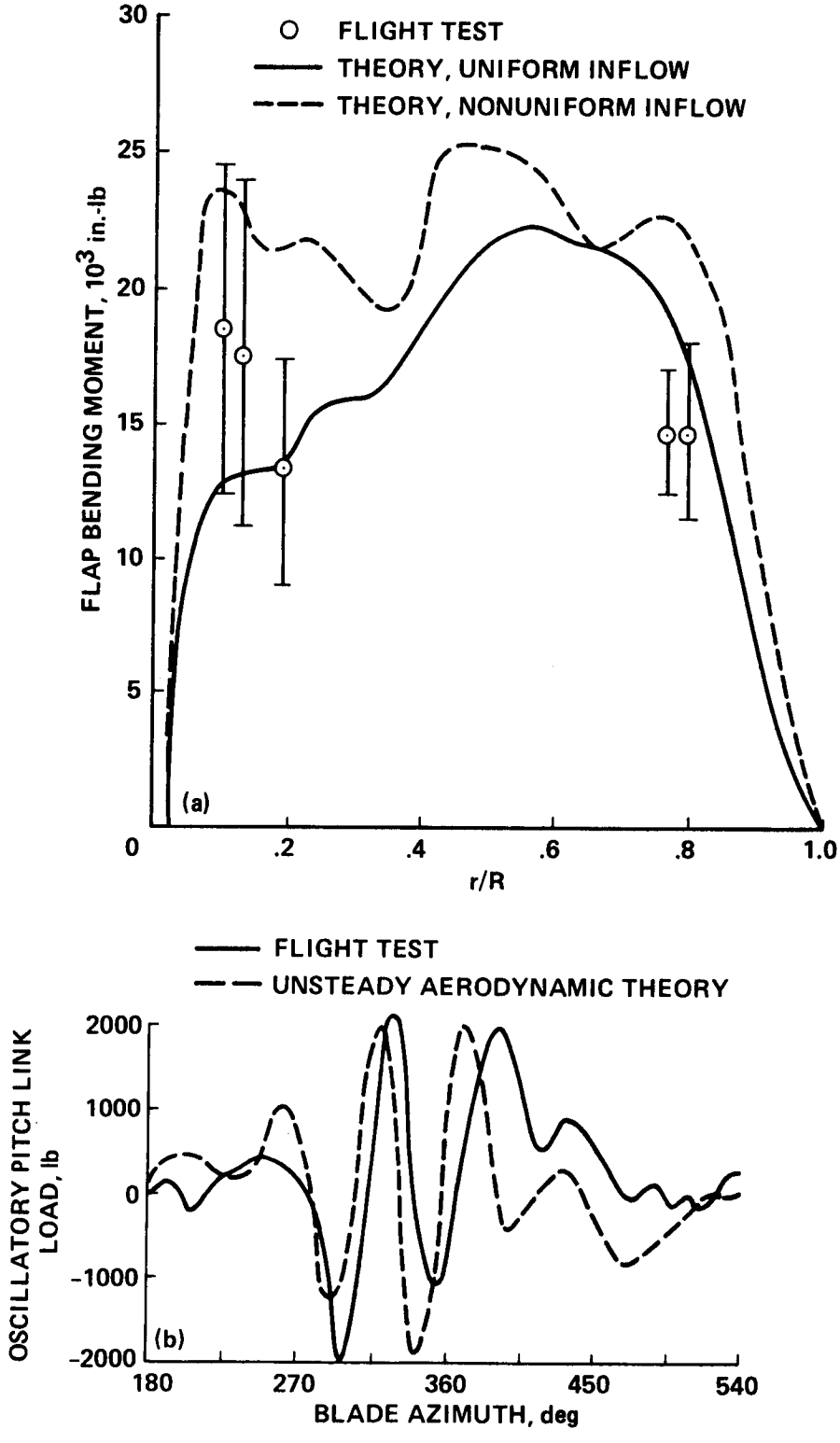

Figure 2.- Comparison of C-60 prediction with flight test data for CH-47C aft rotor; V = 123 knots (ref. 3). (a) Oscillatory flap bending moment; C_T/σ = 0.114. (b) Oscillatory pitch link load; GW = 38,865 lb.

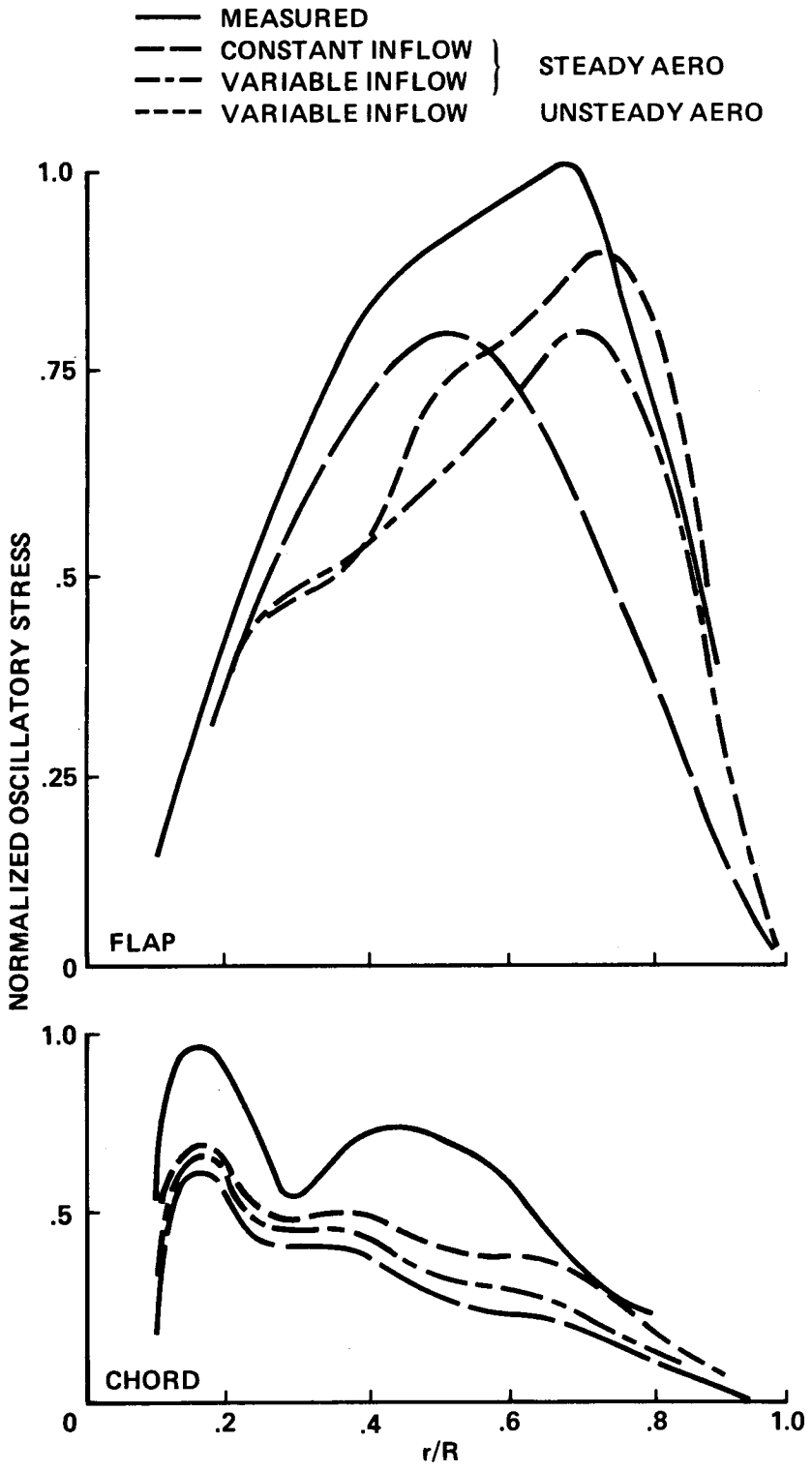

Figure 3.- Comparison of Y200 prediction with normalized oscillatory blade stress for an articulated rotor; $\mu = 0.36$, $C_L/\sigma = 0.0763$ (ref. 4).

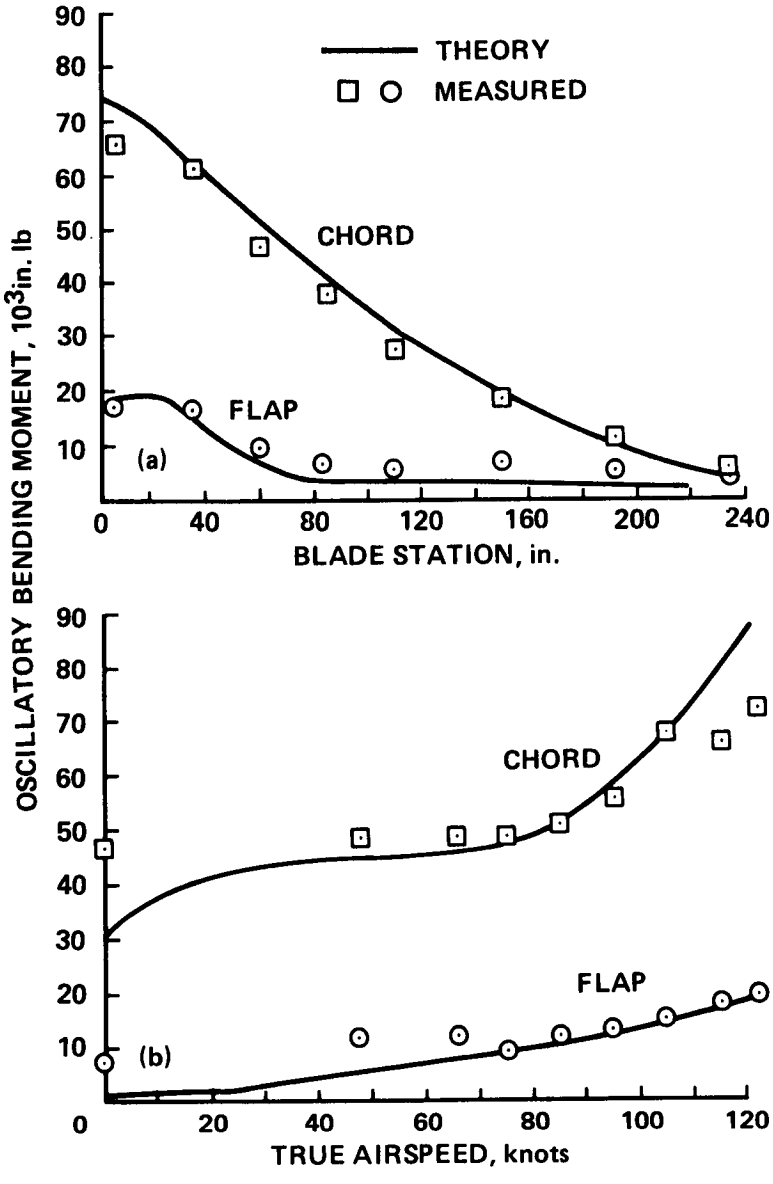

Figure 4.-Comparison of C81 prediction with flight test data for UH-1D; GW = 9,500 lb (ref. 5). (a) Oscillatory bending moment as a function of blade station; V = 115 knots. (b) Oscillatory bending moment as a function of airspeed; blade station 6.0 in.

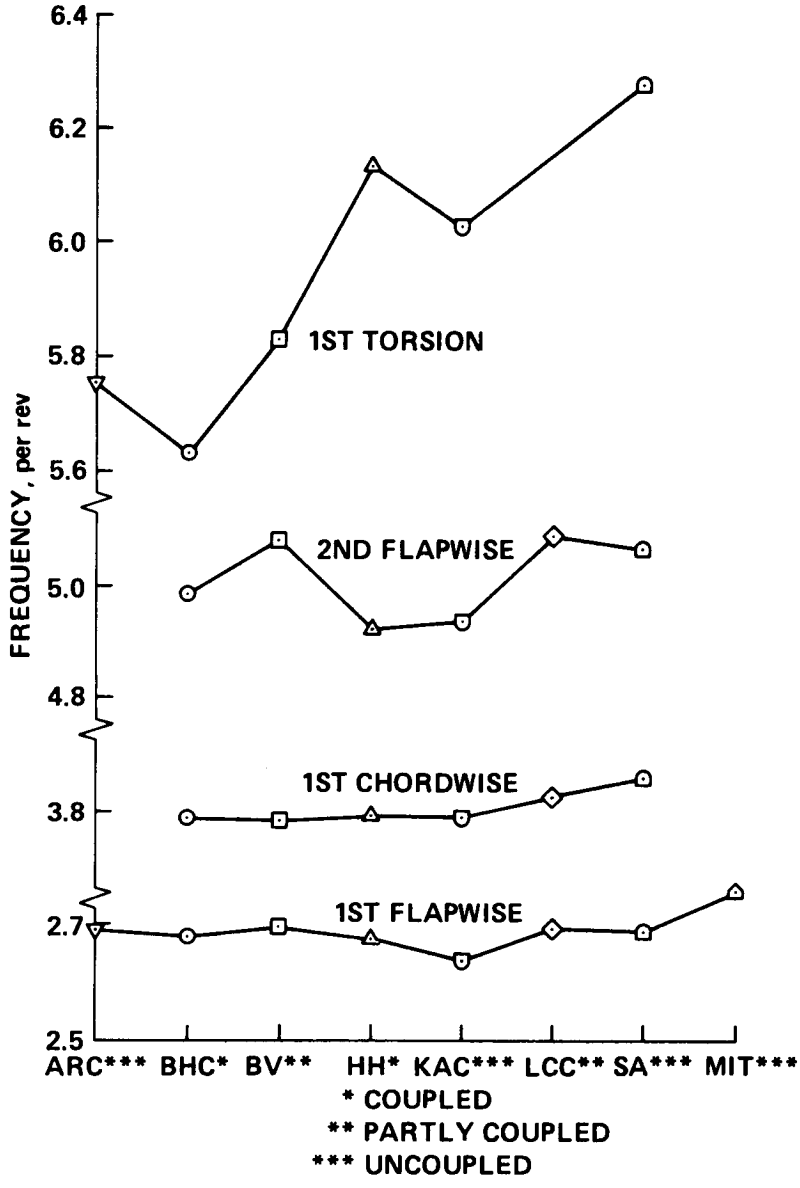

Figure 5.- Rotor blade rotating natural frequencies in vacuo; $\theta_{0.75R} = 0°$ (ref. 2).

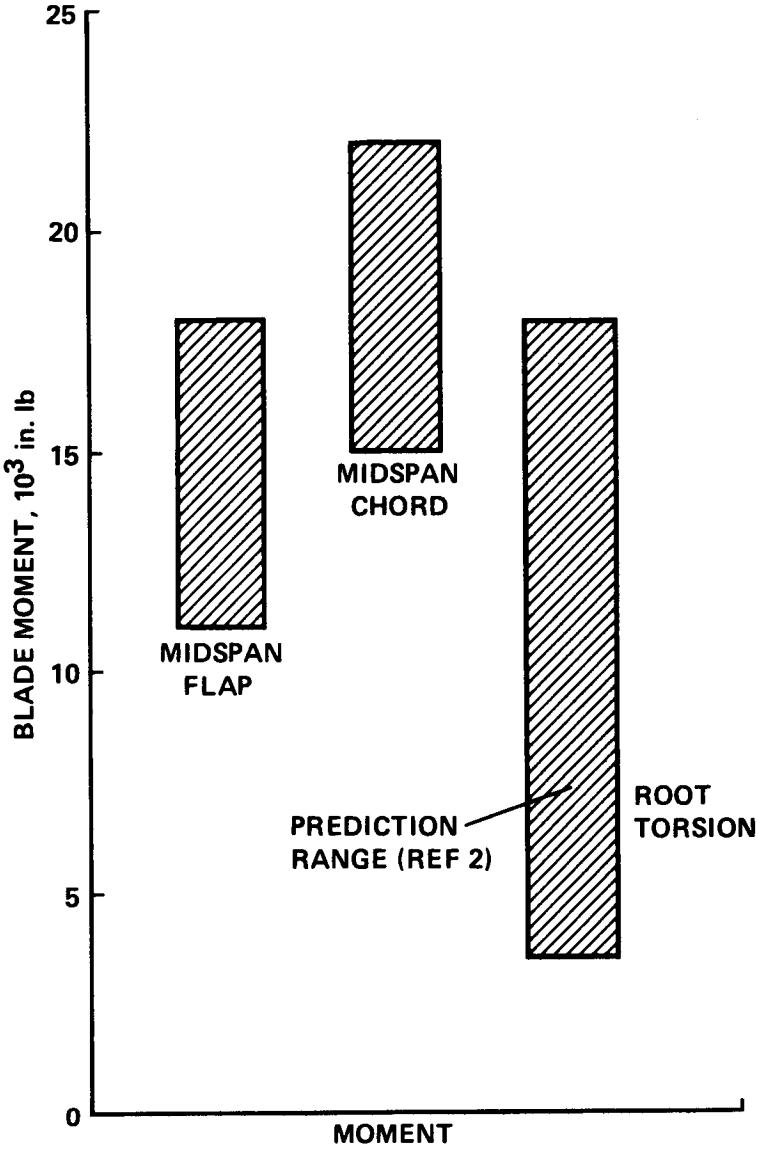

Figure 6.- Range of blade moment predictions for hypothetical rotor; $\mu = 0.33$, unsteady aerodynamics (ref. 8).

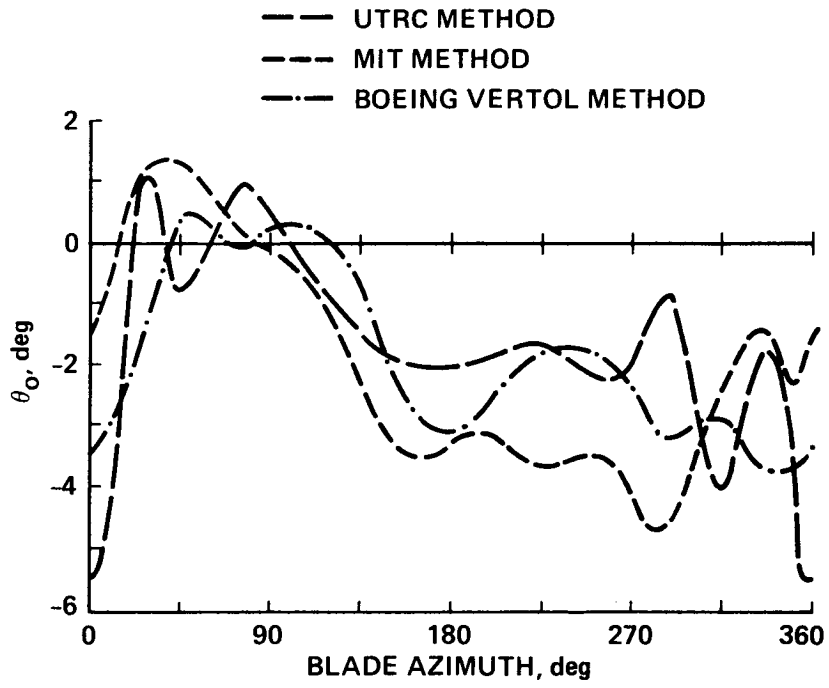

Figure 7.- Elastic torsion angle calculated for a hypothetical rotor using three dynamic stall models; $\mu = 0.333$, $C_T/\sigma = 0.09$ (ref. 17). UTRC Method: refs. 18 and 19; MIT Method: refs. 20 and 21; and Boeing Vertol Method: ref. 22.

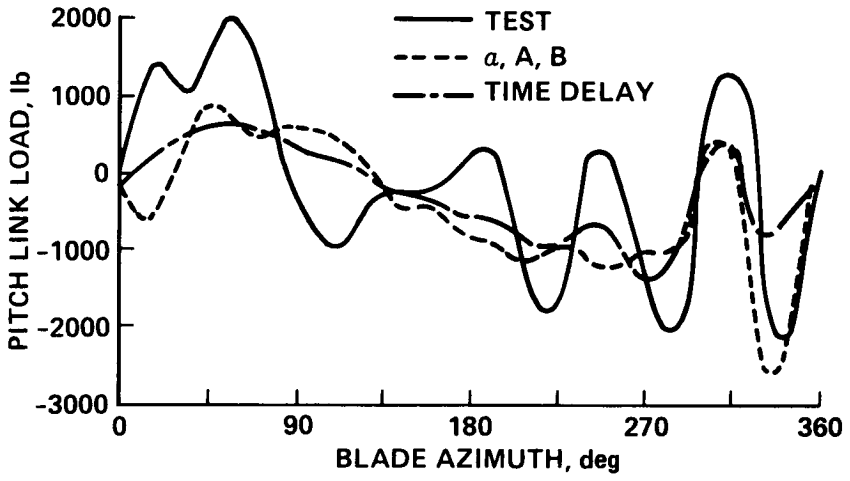

Figure 8.- Comparison of measured and predicted CH-53A pitch link loads using two dynamic stall models; GW = 42,000 lb, V = 155 knots (ref. 24).

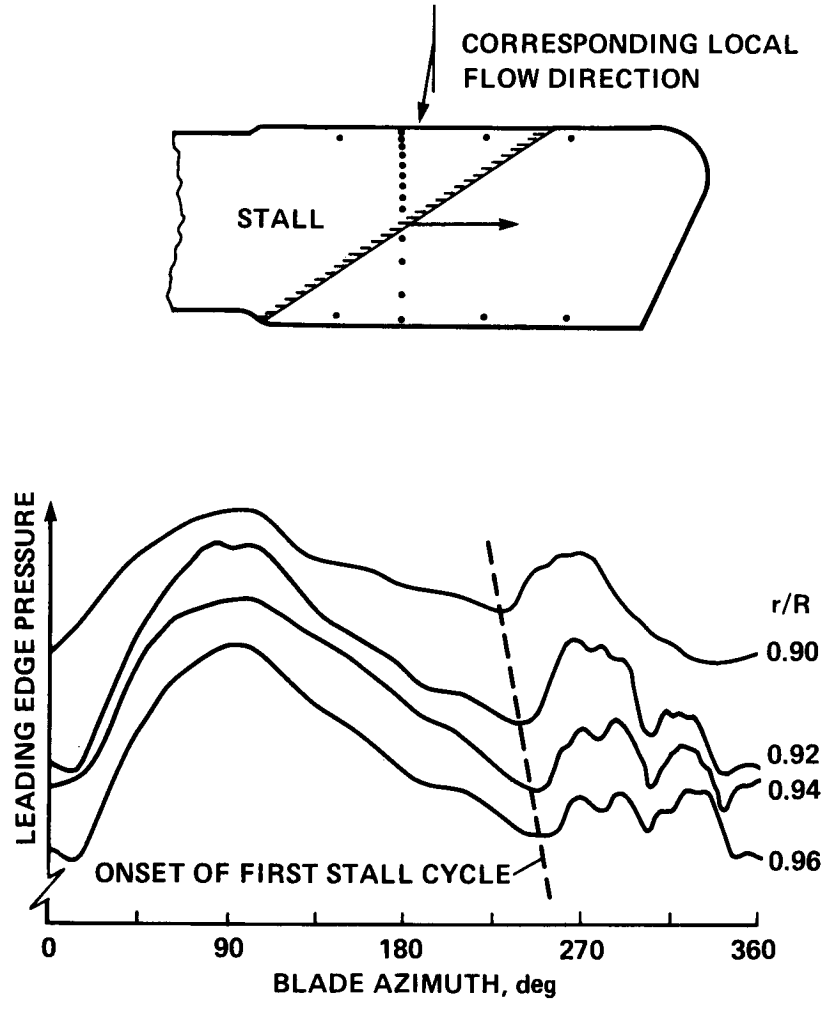

Figure 9.- Pressures measured at the leading edge of a modified blade tip on a Wessex helicopter (ref. 38).

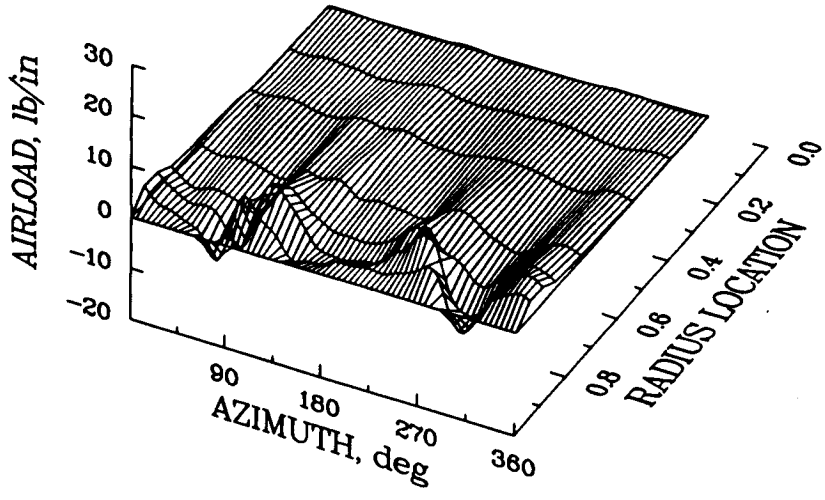

Figure 10.- Vibratory airloads (3-12 harmonics) measured on the CH-34 rotor in flight; $\mu = 0.129$ (ref. 41).

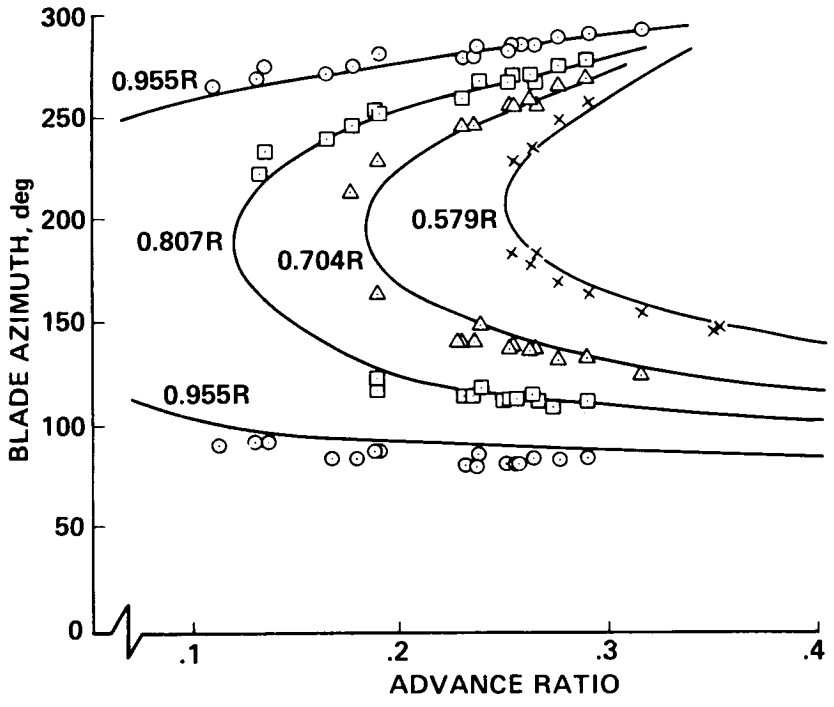

Figure 11.- Flight test measurements of blade-vortex intersections for four blade radial stations (ref. 43).

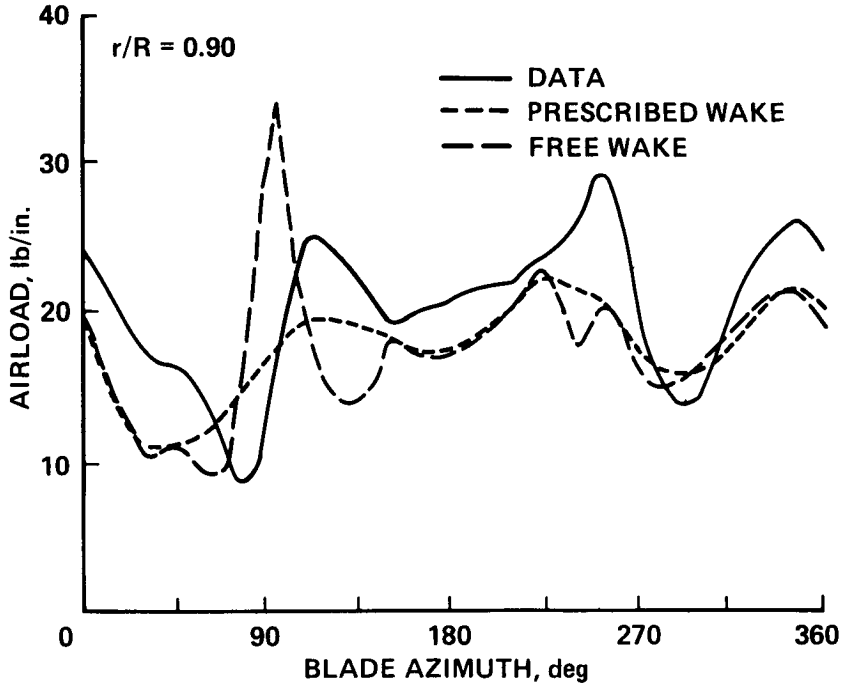

Figure 12.- Comparison of free and prescribed wake calculations with CH-34 flight test data; r/R = 0.90, μ = 0.129 (ref. 48).

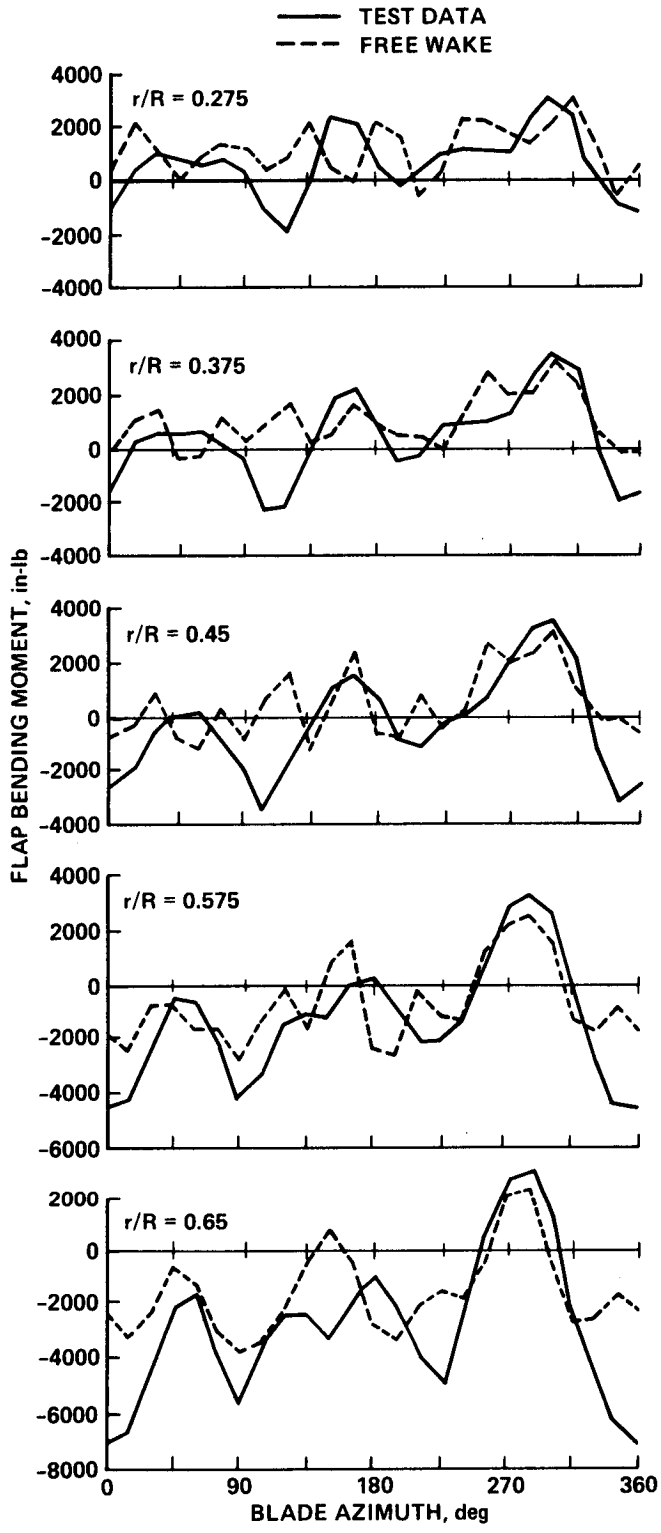

Figure 13.- Comparison of test data with free wake prediction for CH-34 flap bending moment data; $\mu = 0.129$ (ref. 48).

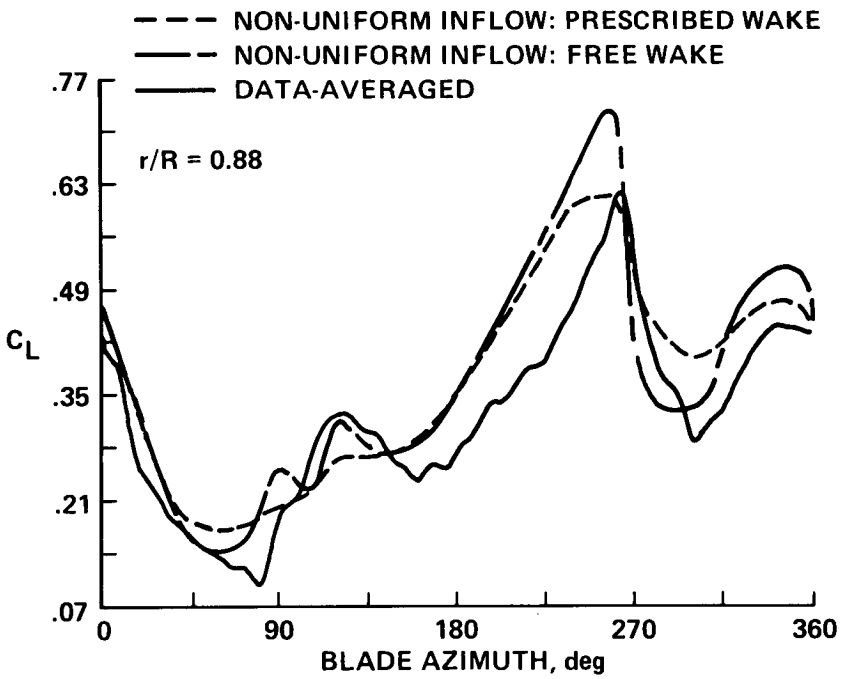

Figure 14.- Comparison of CAMRAD prediction of lift coefficient with SA 349-2 flight test data; μ = 0.14 (ref. 50).

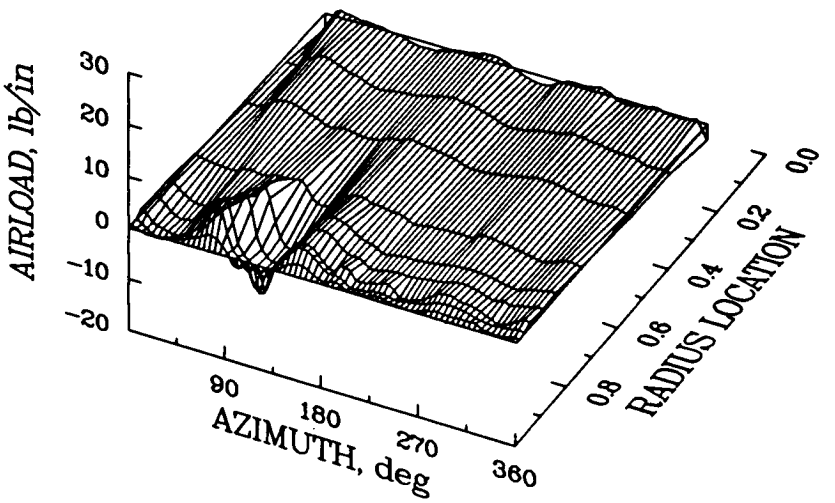

Figure 15.- Vibratory airloads (3-36 harmonics) measured on CH-34 rotor in wind tunnel; μ = 0.39 (refs. 1 and 51).

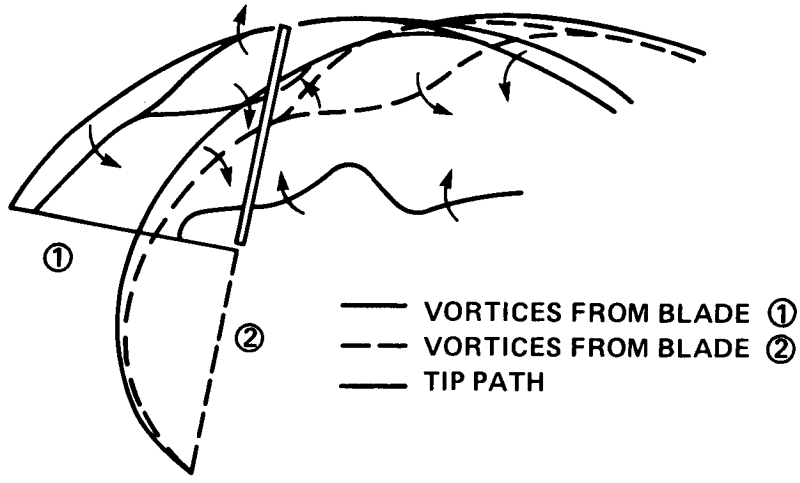

Figure 16.- Sketch of wake geometry for CH-34 high speed case (ref. 52).

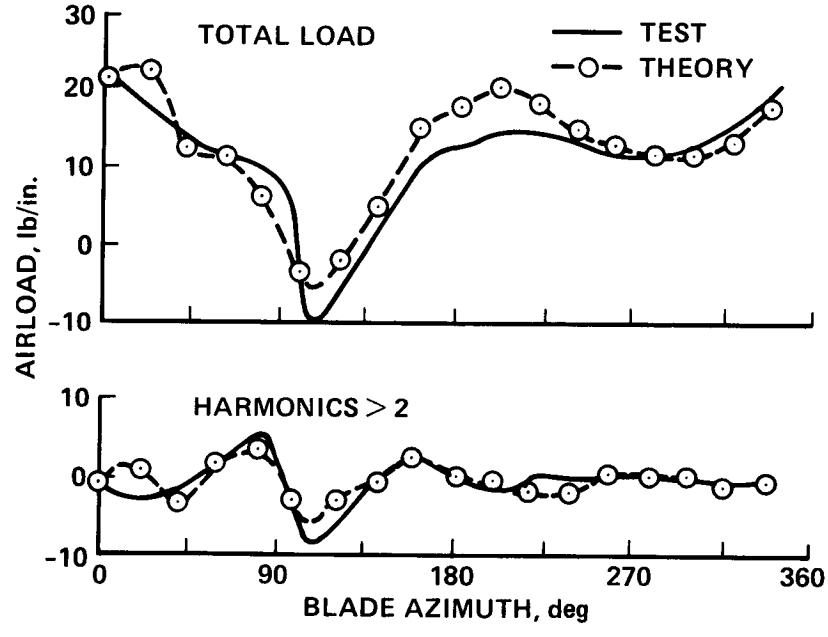

Figure 17.- Blade loading predicted at 0.90R compared to CH-34 wind tunnel measurements; $\mu = 0.39$ (ref. 52).

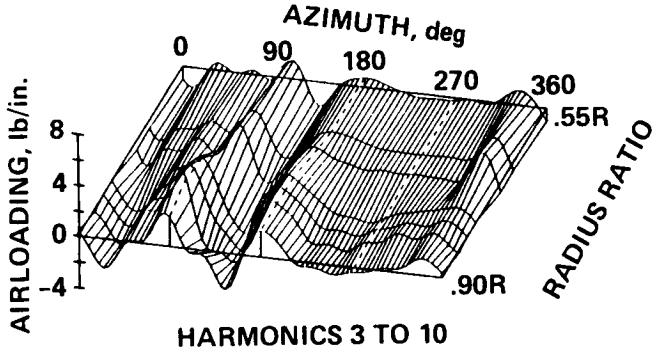

Figure 18.- Model-scale vibratory airloads (3-10 harmonics) for Model 360 rotor; $\mu = 0.405$ (ref. 55).

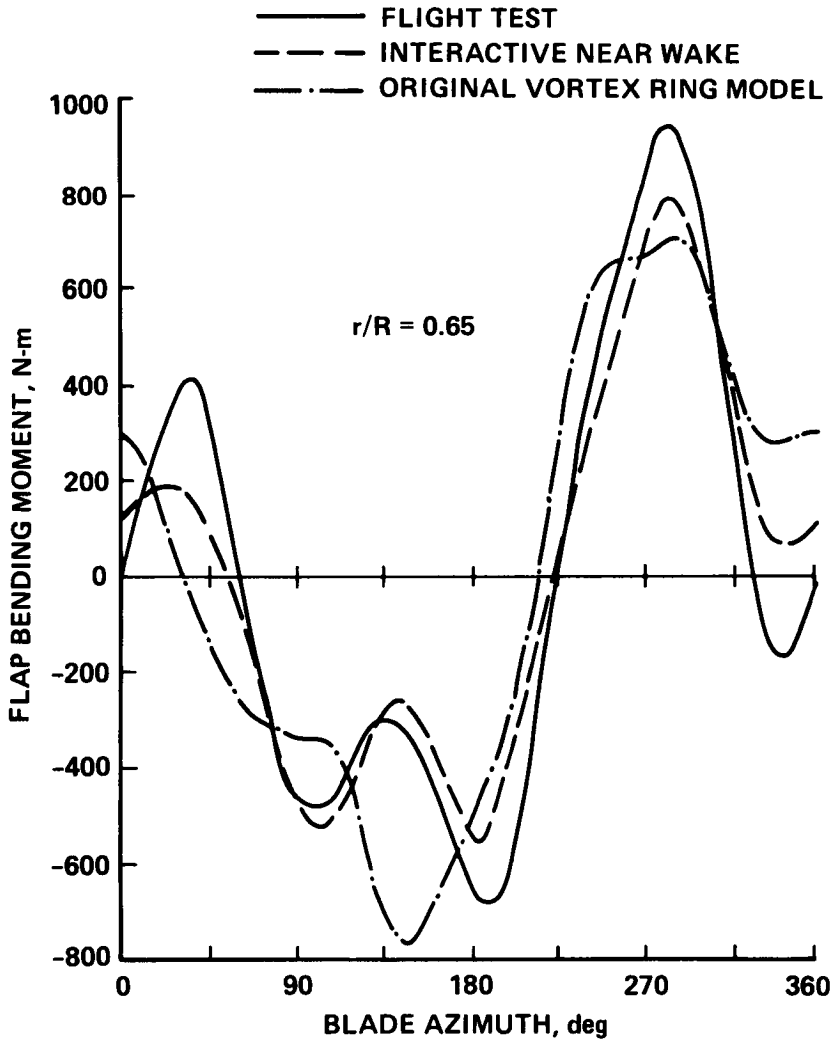

Figure 19.- Comparison of vortex ring wake model with flap bending moments on a Puma; $\mu = 0.32$ (ref. 56).

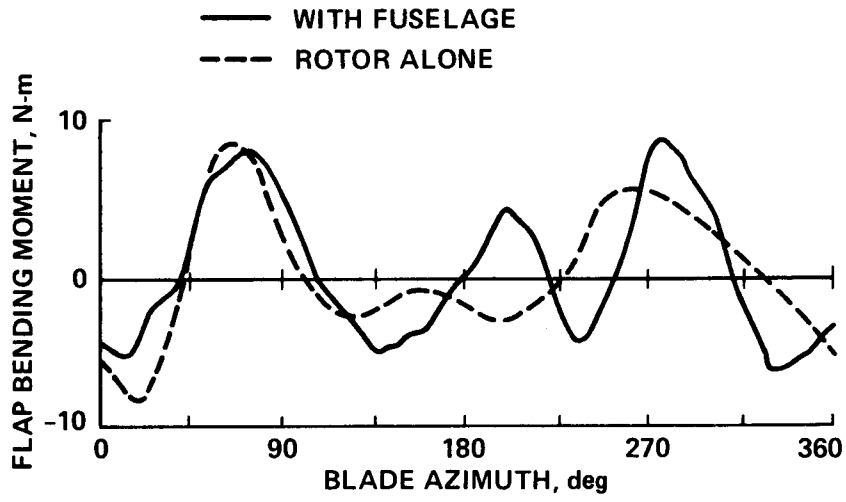

Figure 20.- Model rotor flap bending moments with and without a fuselage; $\mu = 0.3$, $\Omega = 600$ rpm (ref. 37).

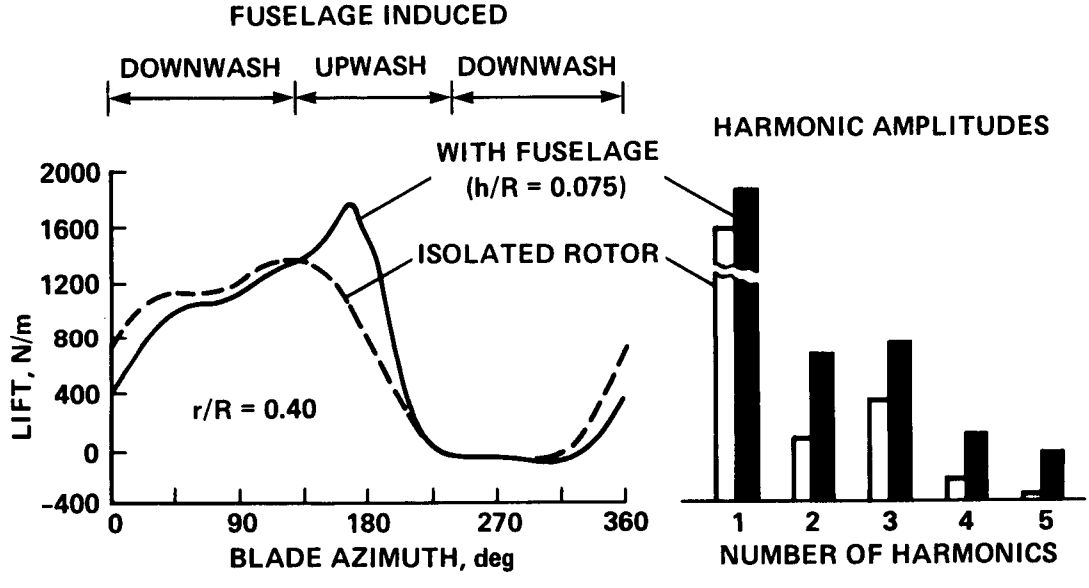

Figure 21.- Calculated effect of fuselage on blade lift and harmonic loads; $V = 150$ knots, $r/R = 0.40$ (ref. 65).

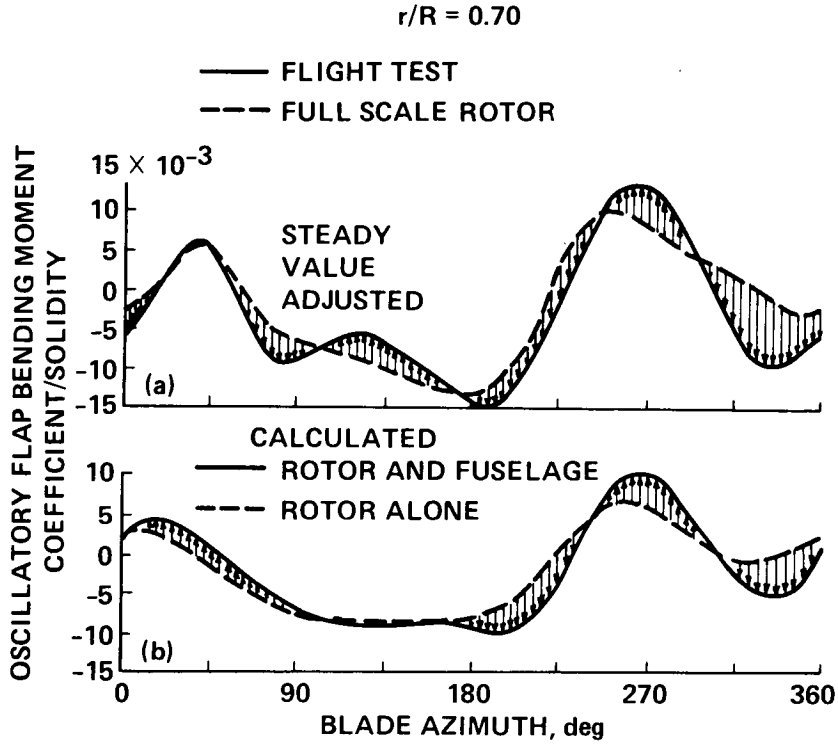

Figure 22.- Influence of fuselage on S-76 flap bending moments; GW = 10,300 lb, μ = 0.375 (ref. 66). (a) Comparison of flight test and wing tunnel test data. (b) Calculation for flight test case with and without fuselage.

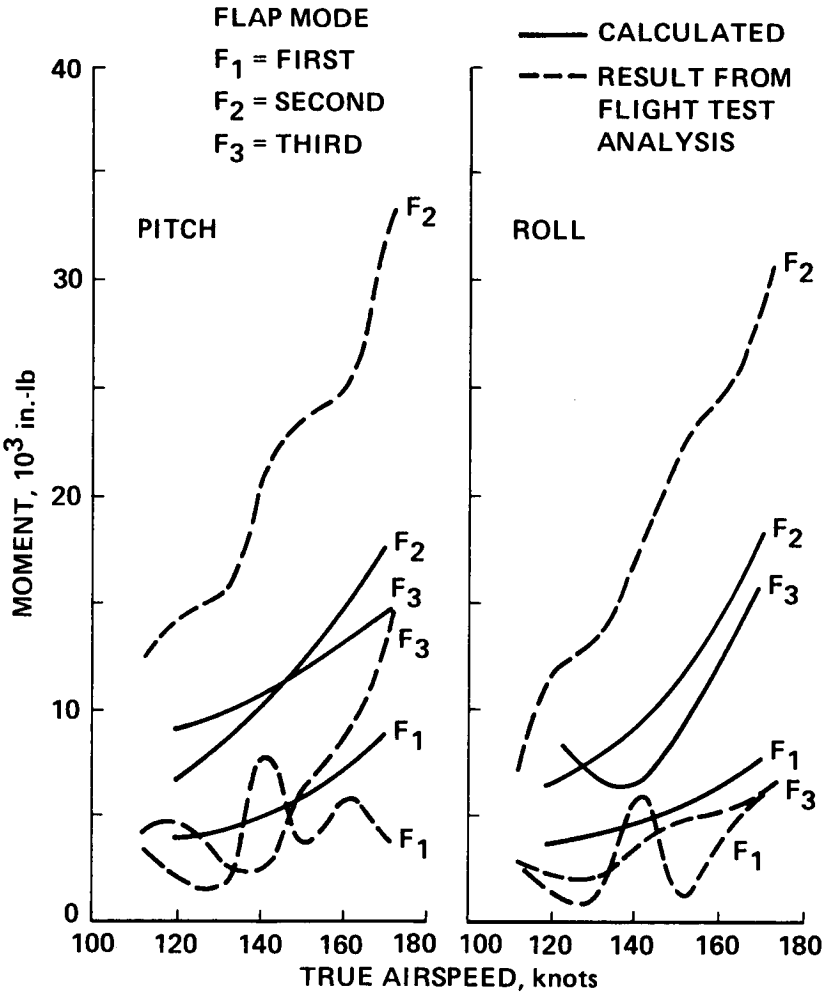

Figure 23.- Modal contributions to 4/rev hub pitch and roll moments for Lynx (ref. 70).

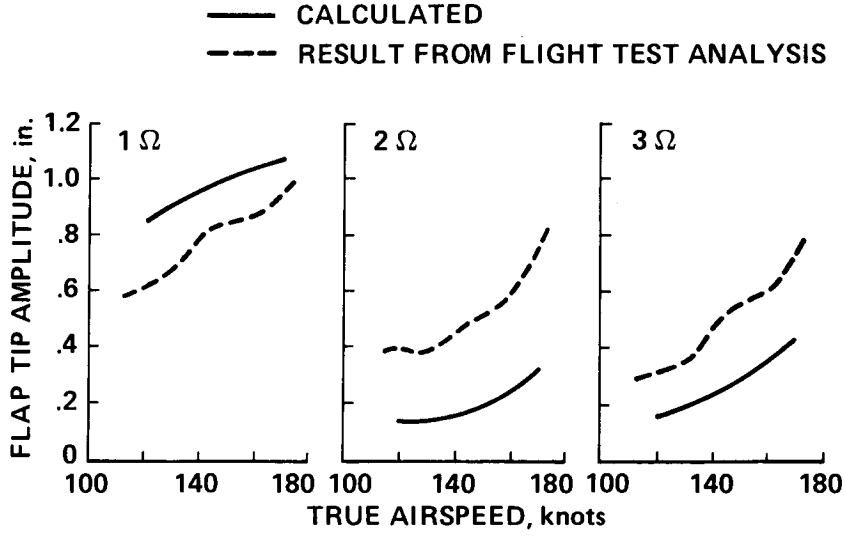

Figure 24.- Second flap mode harmonic amplitudes for Lynx (ref. 70).

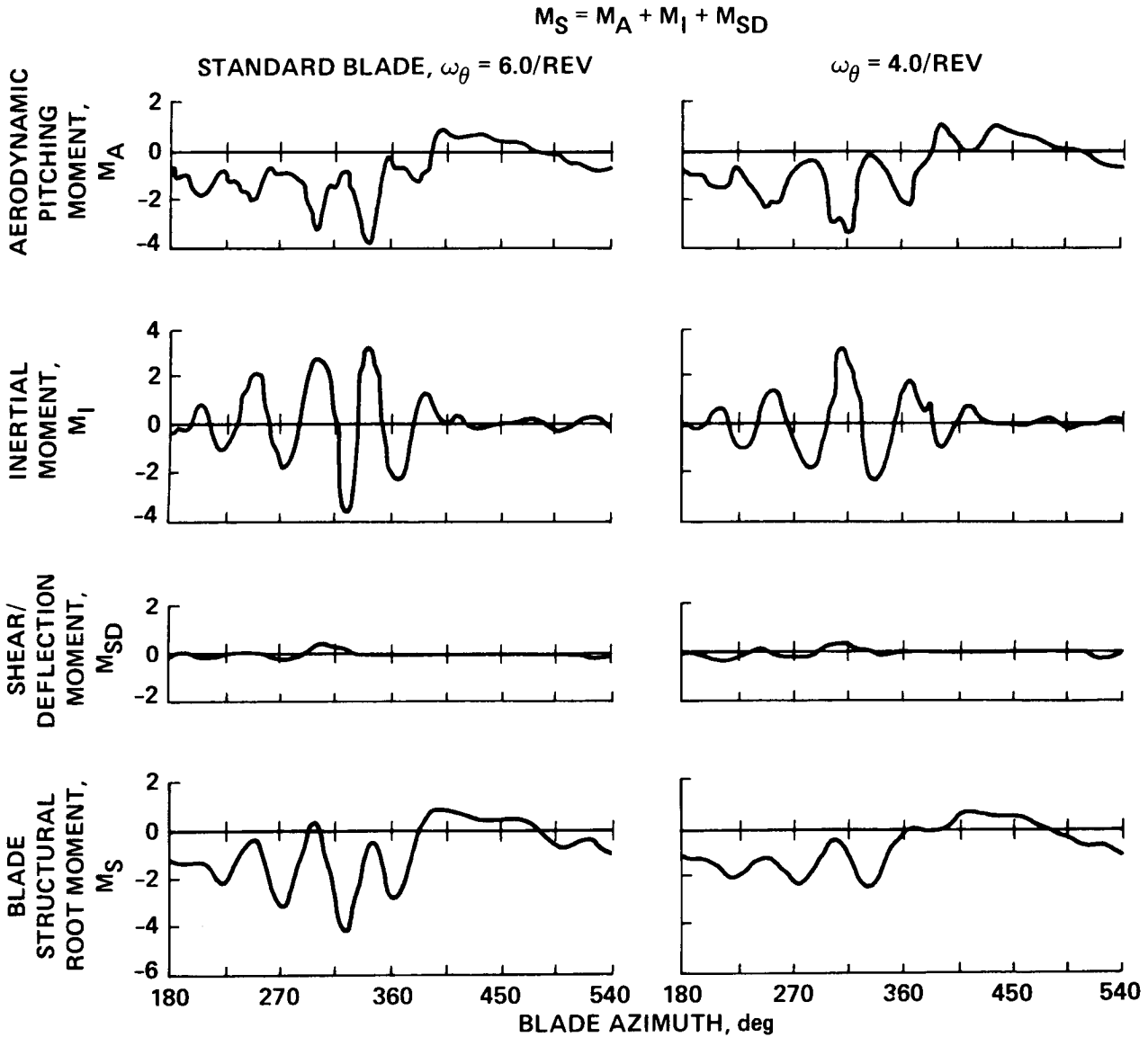

Figure 25.- Calculated effect of torsional frequency for CH-53A; V = 140 knots, GW = 49,000 lb (ref. 24).

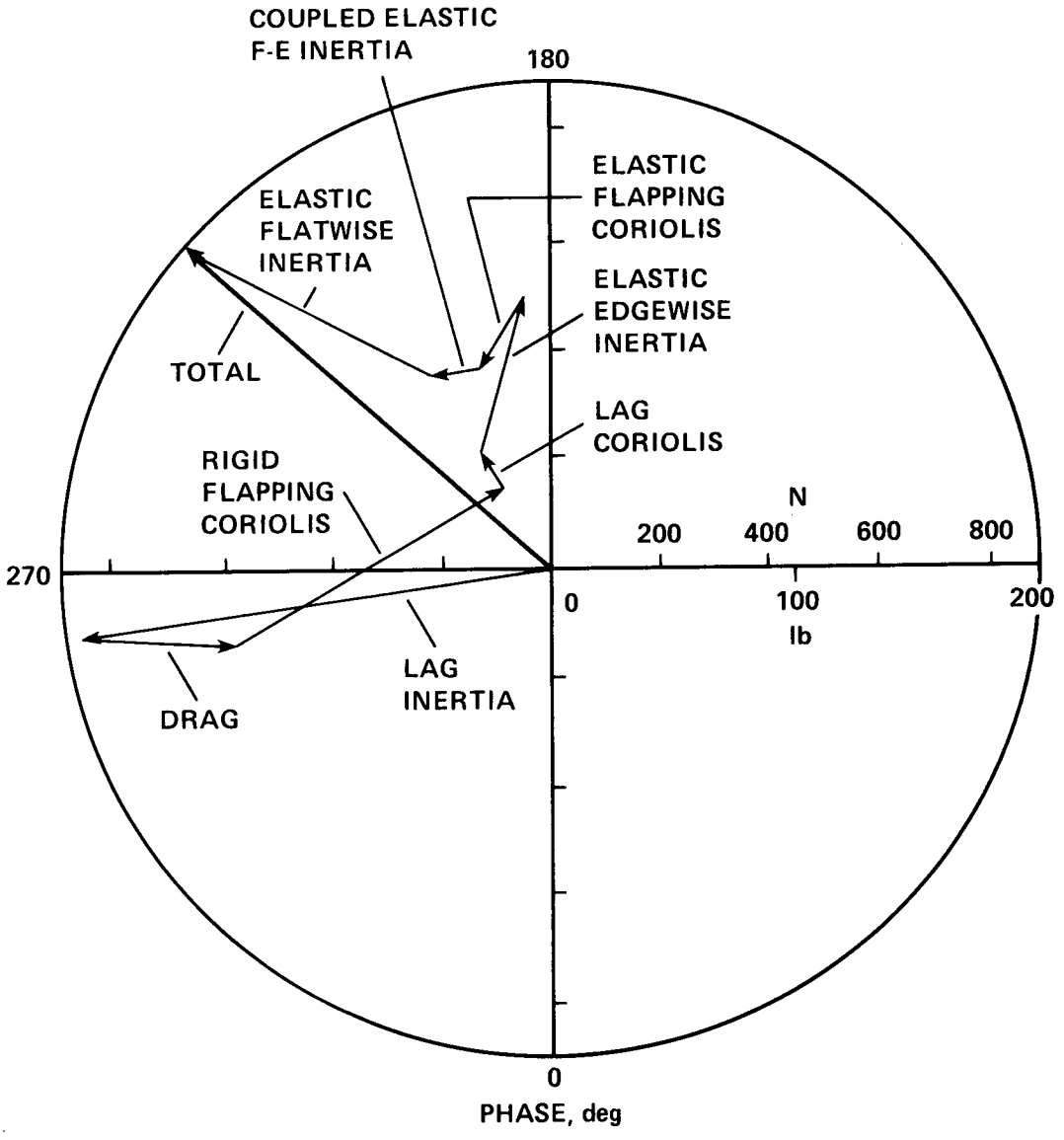

Figure 26.- Calculated 3/rev lateral shear for baseline blade; V = 160 knots (ref. 80).

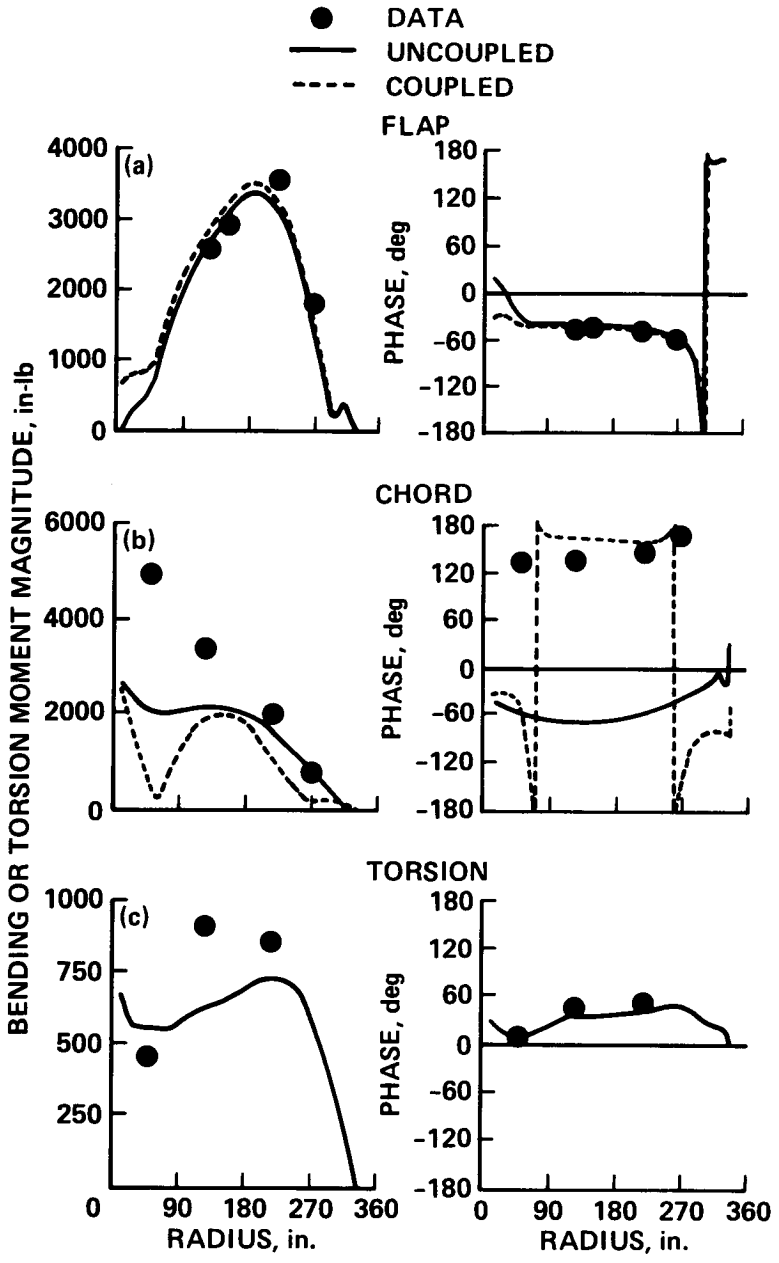

Figure 27.- First harmonic blade moments of CH-34 in wind tunnel obtained from measurement and calculations based on measured pressures; $\mu = 0.39$, $\alpha_s = -5°$ (ref. 81). (a) Flap. (b) Chord. (c) Torsion.

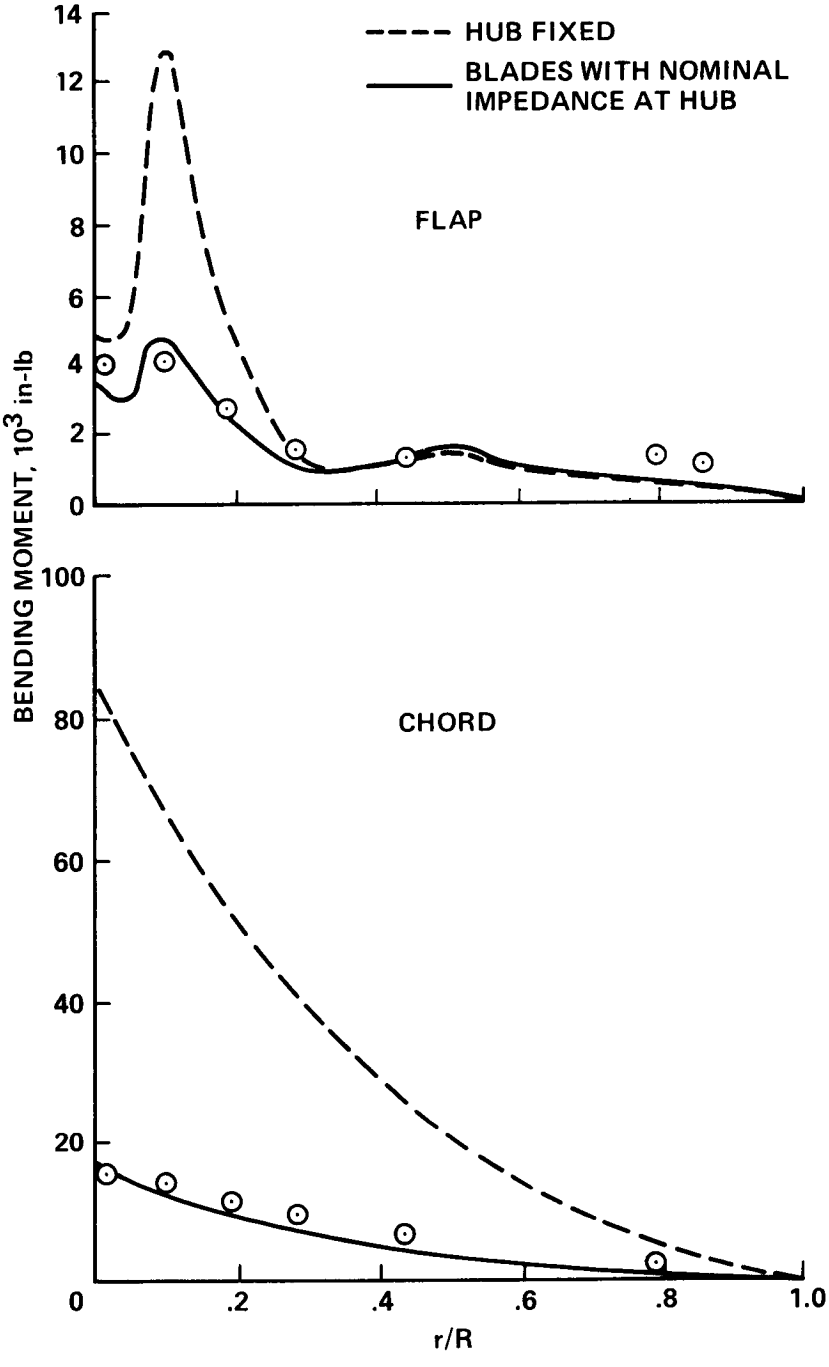

Figure 28.- Comparison of OH-58A blade bending moments with and without modeling of pylon impedance; V = 83 knots (ref. 85).

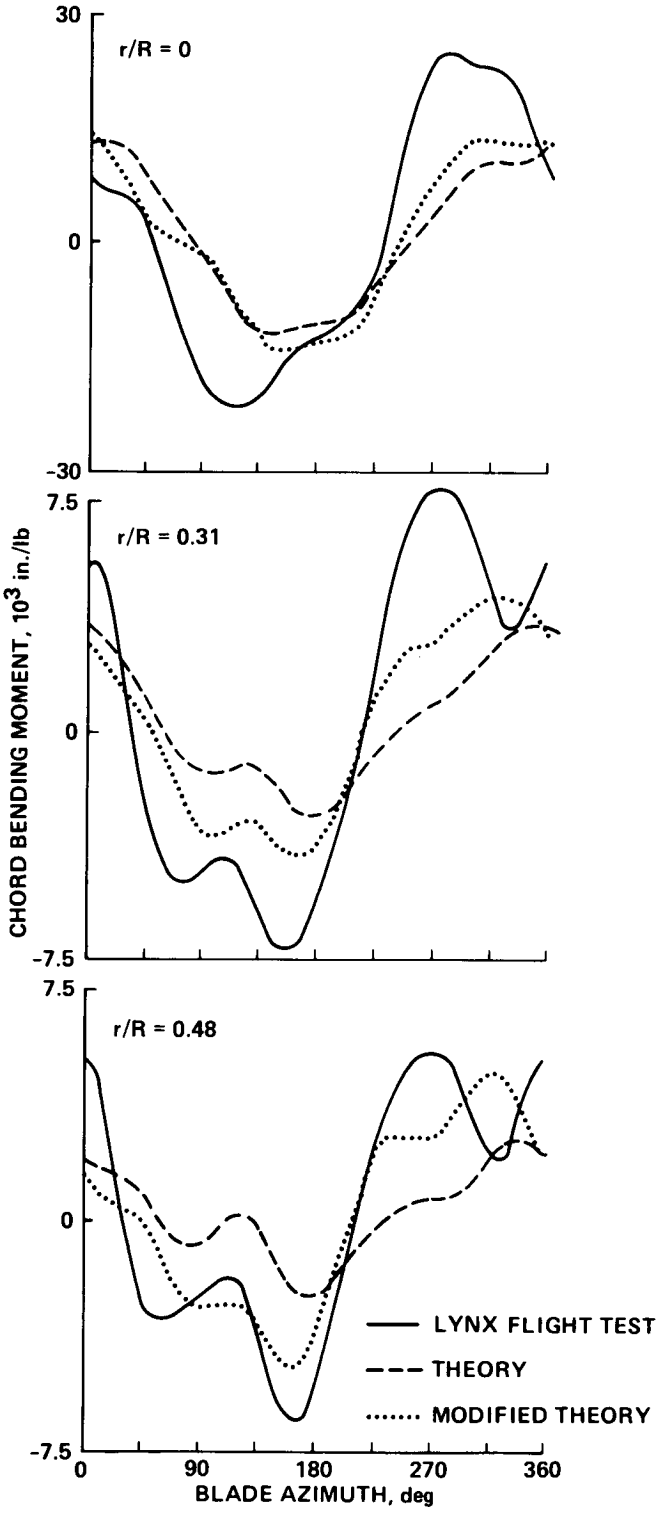

Figure 29.- Comparison of chord bending moments for the Lynx showing effect of modified theory; V = 122 knots (ref. 91).

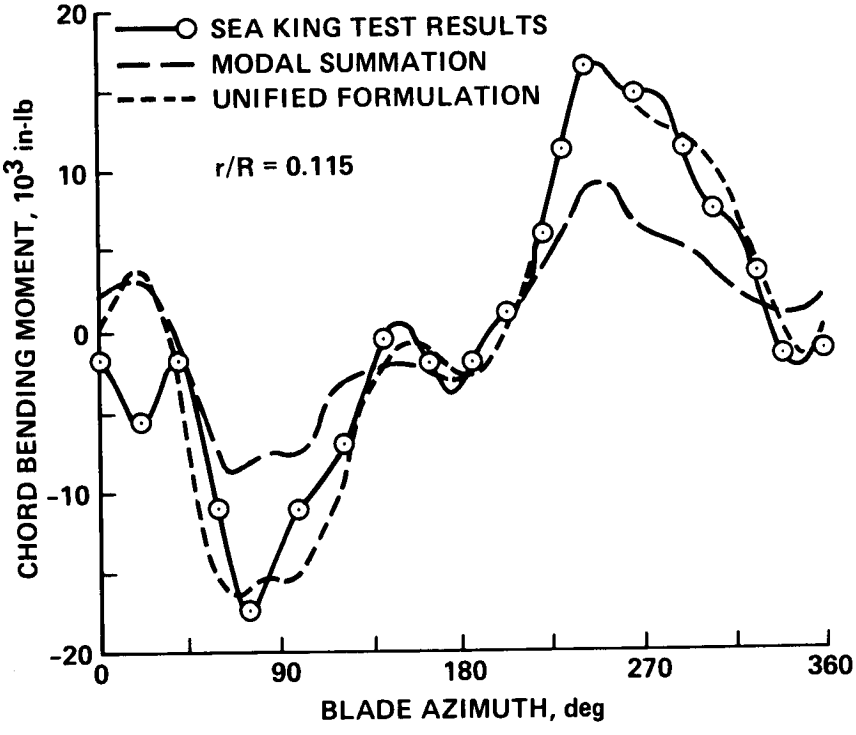

Figure 30.- Comparison of chord bending moment for Sea King with theory using modal summation and unified formulation; V = 120 knots (ref. 90).

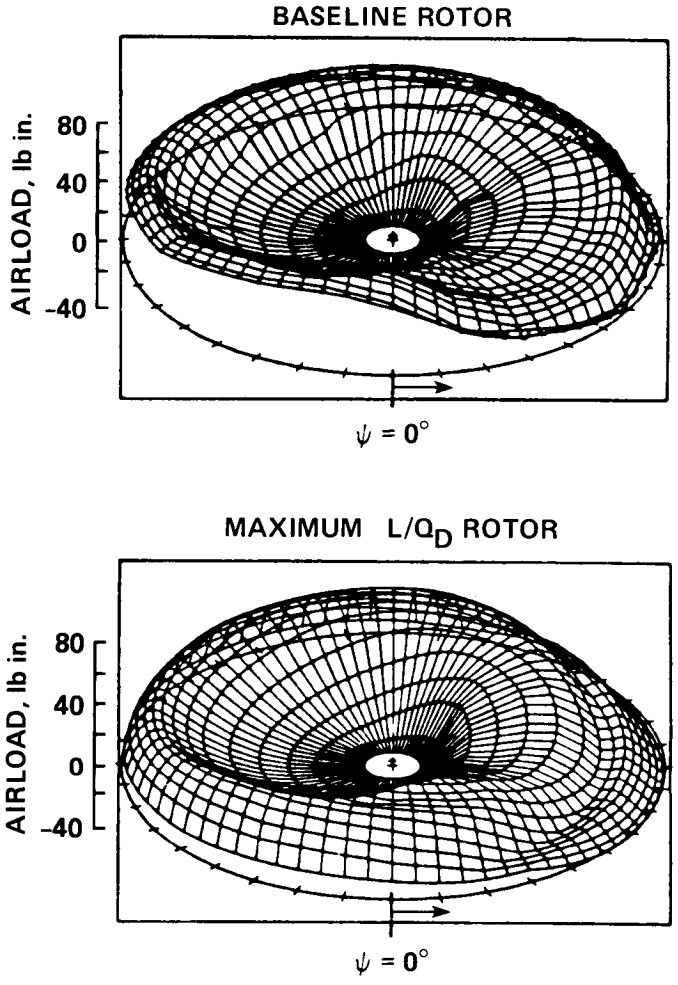

Figure 31.- Comparison of baseline and maximum L/Q_D rotor airload distribution using variable inflow; $\mu = 0.3$, $C_L/\sigma = 0.10$ (ref. 97).

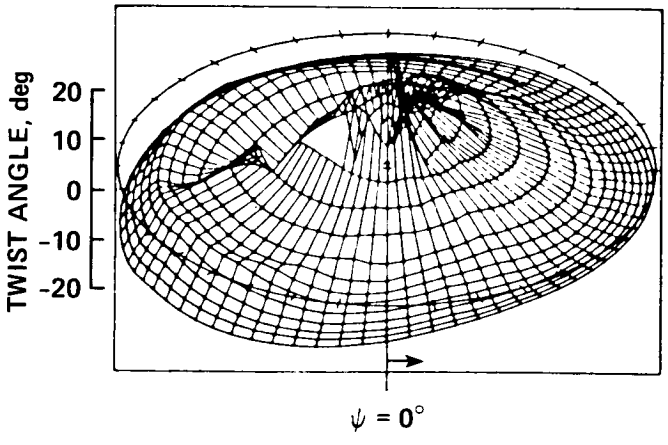

Figure 32.- Twist required to produce maximum L/Q_D; $\mu = 0.3$, $C_L/\sigma = 0.10$ (ref. 97).

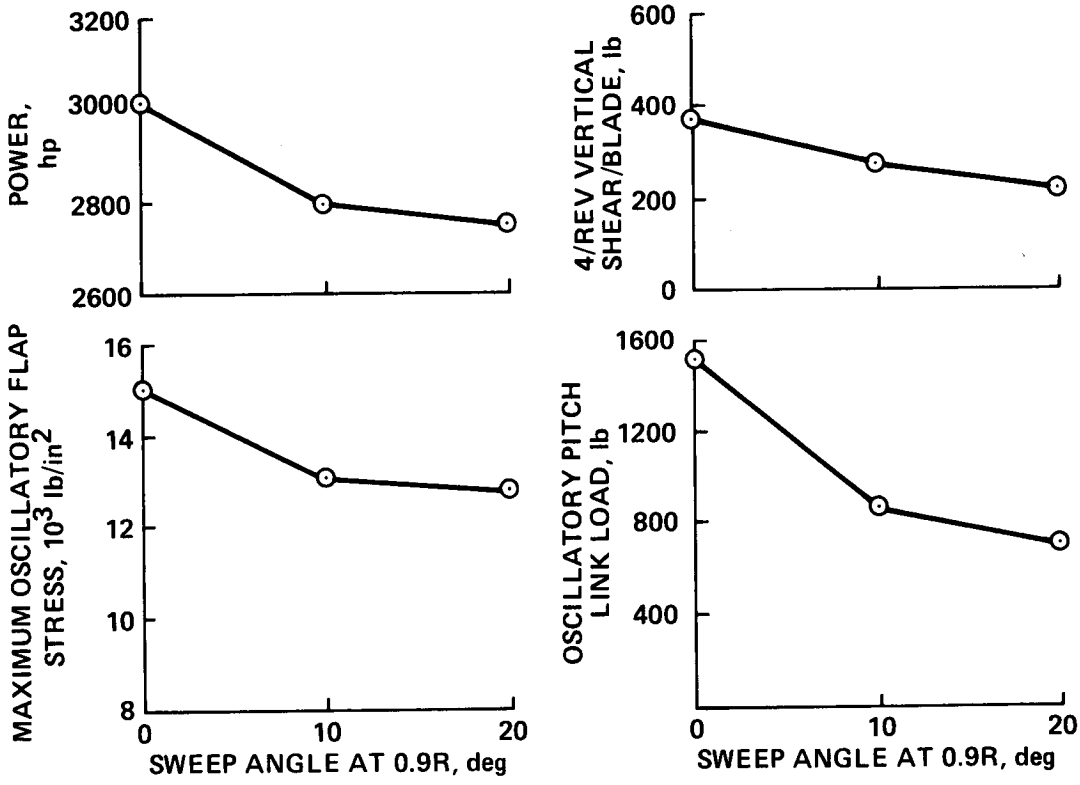

Figure 33.- Variation of power and rotor system loads with sweep angle for conformable rotor; $\mu = 0.4$, $C_L/\sigma = 0.085$ (ref. 97).

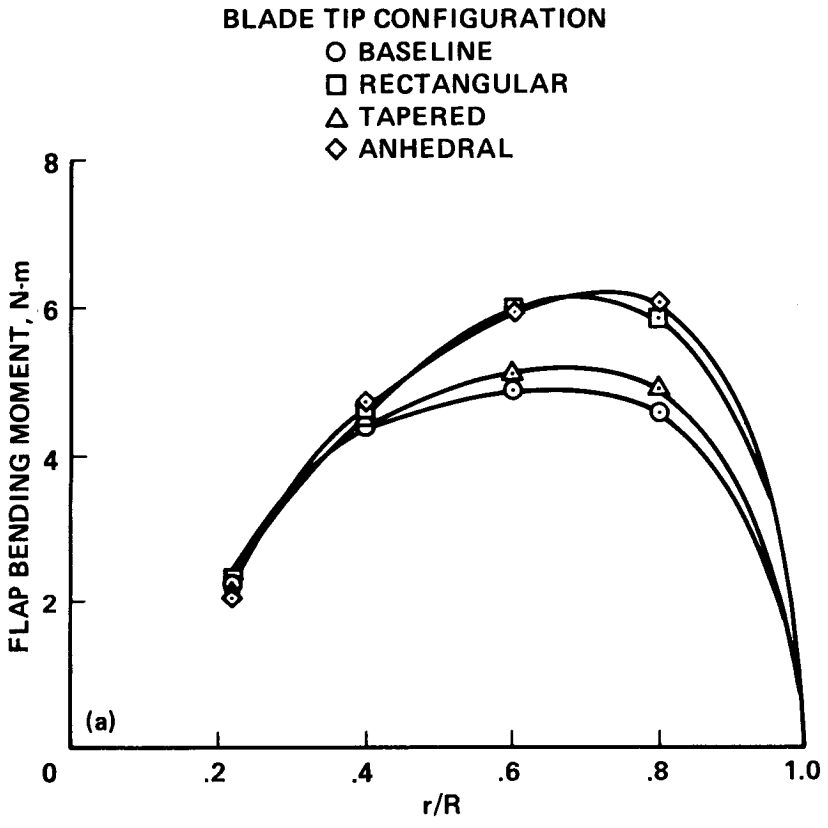

(a) Flap bending moment.

Figure 34.- Oscillatory blade moments for four tip configurations; $\mu = 0.35$, $C_L/\sigma = 0.09$ (ref. 98).

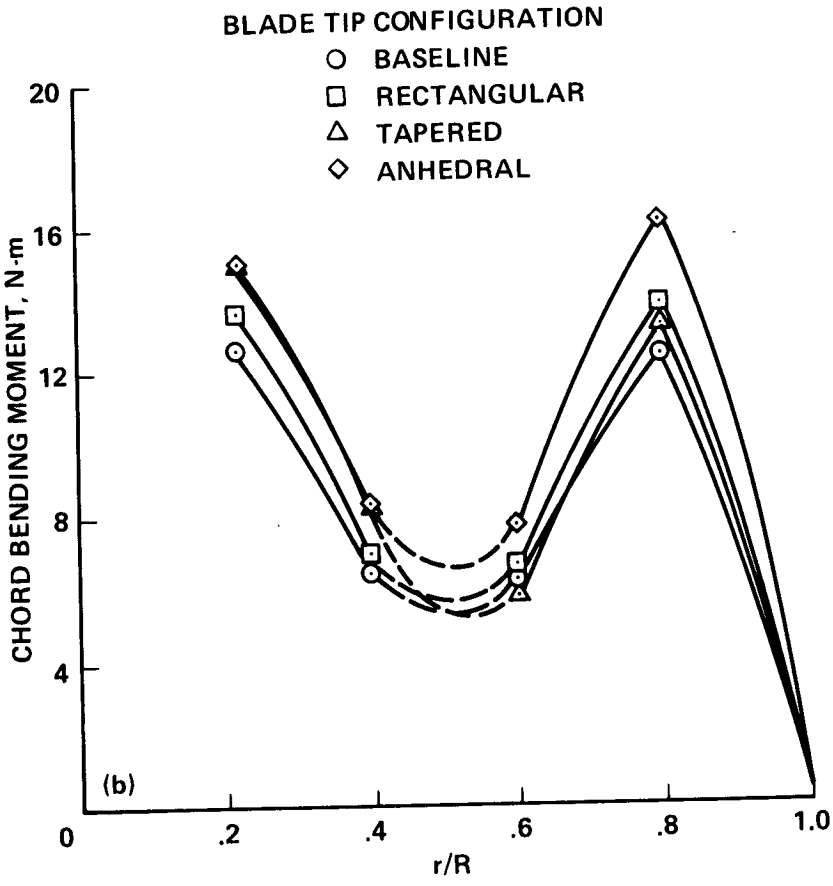

(b) Chord bending moment.

Figure 34.- Continued.

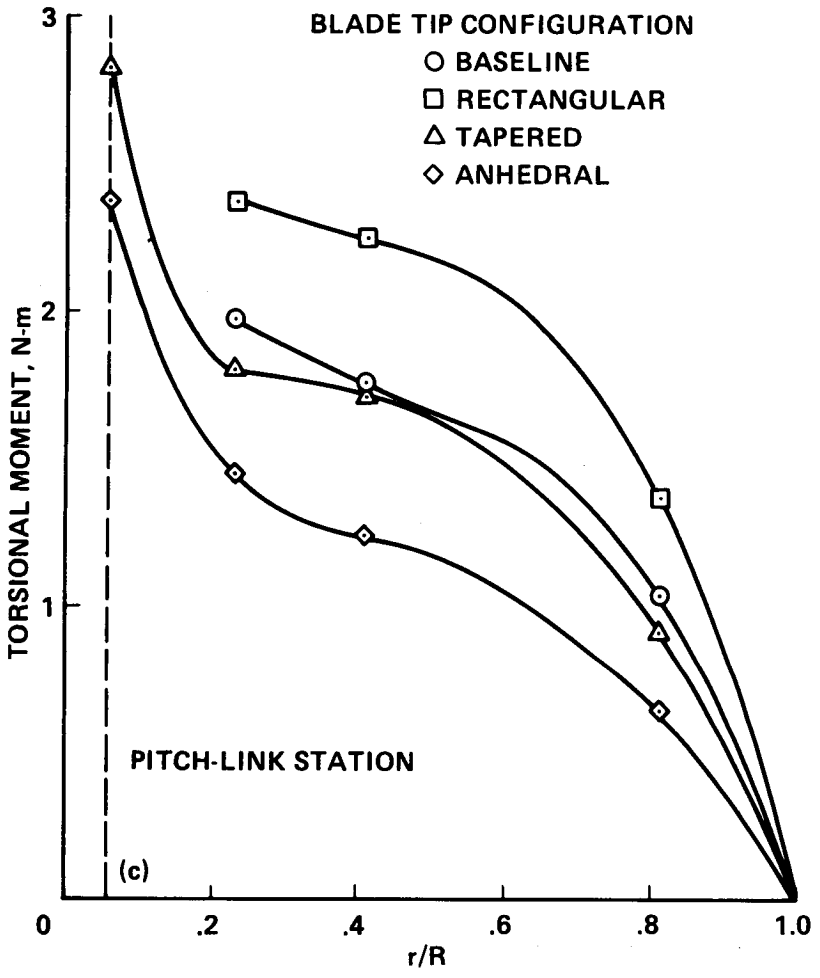

(c) Torsion moment.

Figure 34.- Concluded.

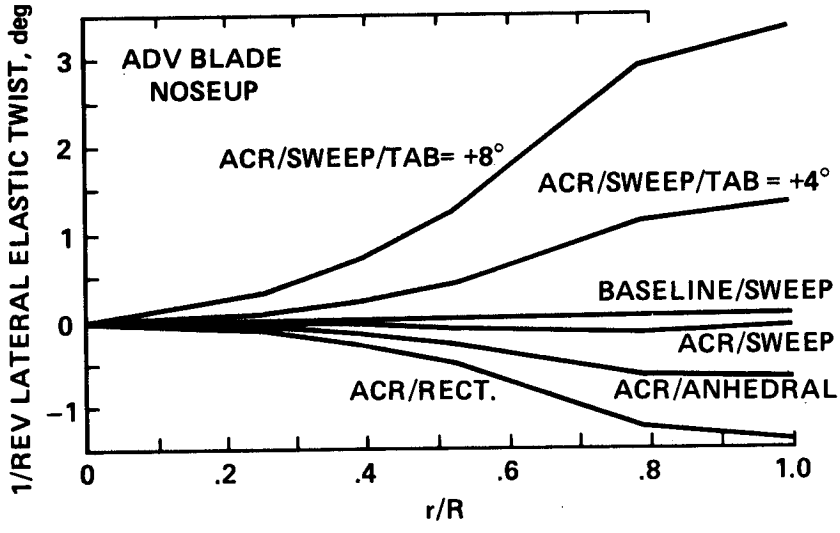

Figure 35.- 1/rev lateral twist of ACR configurations and baseline rotor; $\mu = 0.3$, $C_L/\sigma = 0.08$ (ref. 77).

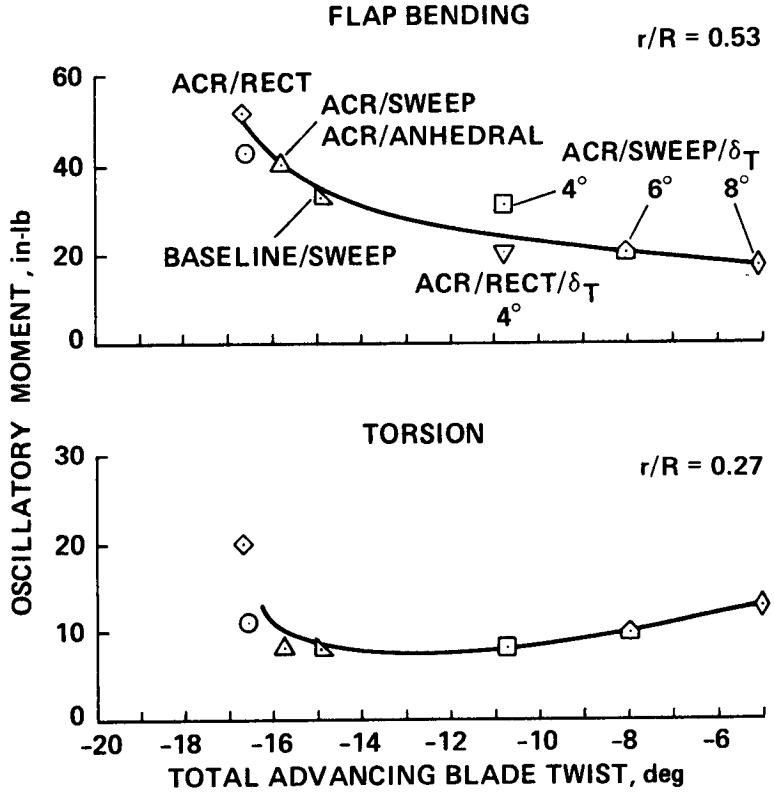

Figure 36.- Oscillatory moments as a function of total twist at $\psi = 90°$; $\mu = 0.3$, $C_L/\sigma = 0.08$ (ref. 77).

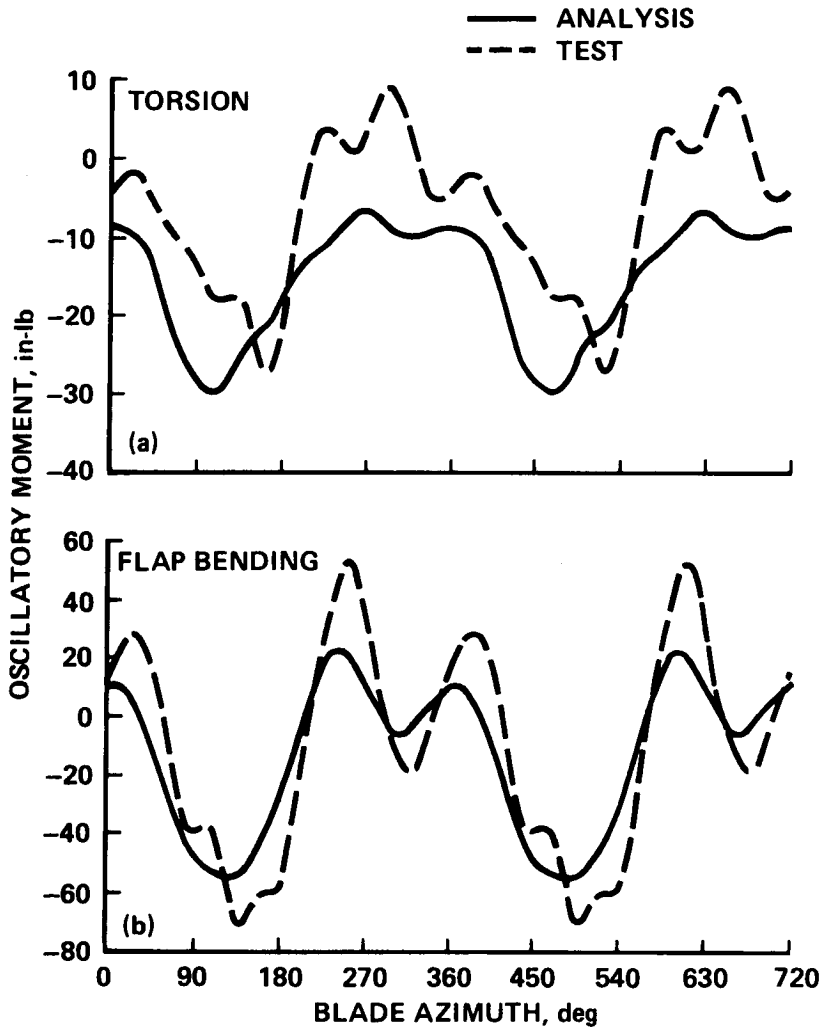

Figure 37.- Comparison of predicted and measured blade moment time histories; $\mu = 0.3$, $C_L/\sigma = 0.08$ (ref. 77). (a) Torsion moment. (b) Flap bending moment.

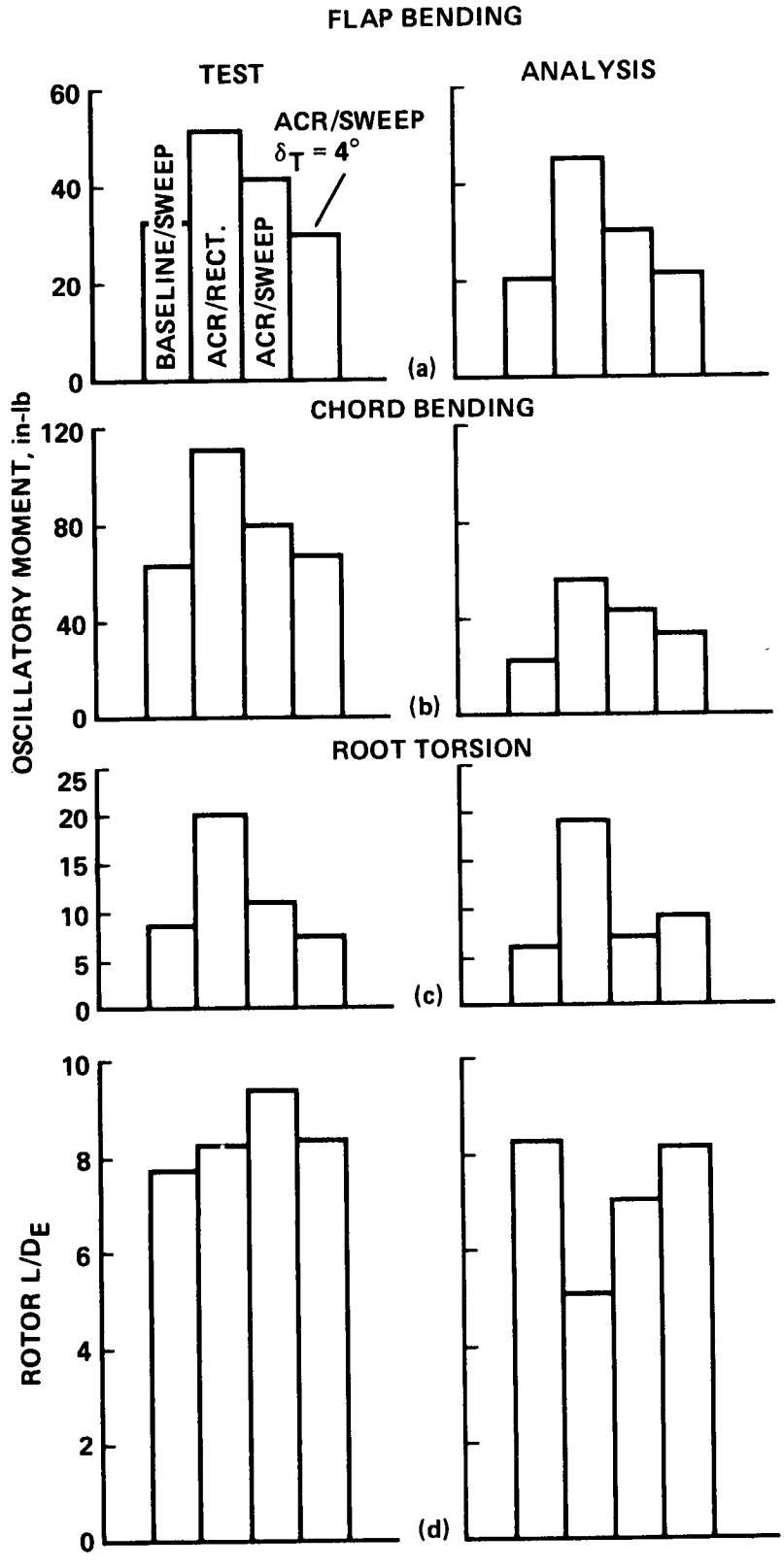

Figure 38.- Correlation of blade loads and rotor L/D_E for four model rotor configurations; $\mu = 0.3$, $C_L/\sigma = 0.08$ (ref. 77). (a) Oscillatory flap bending moment. (b) Oscillatory chord bending moment. (c) Oscillatory root torsion moment. (d) Rotor L/D_E.

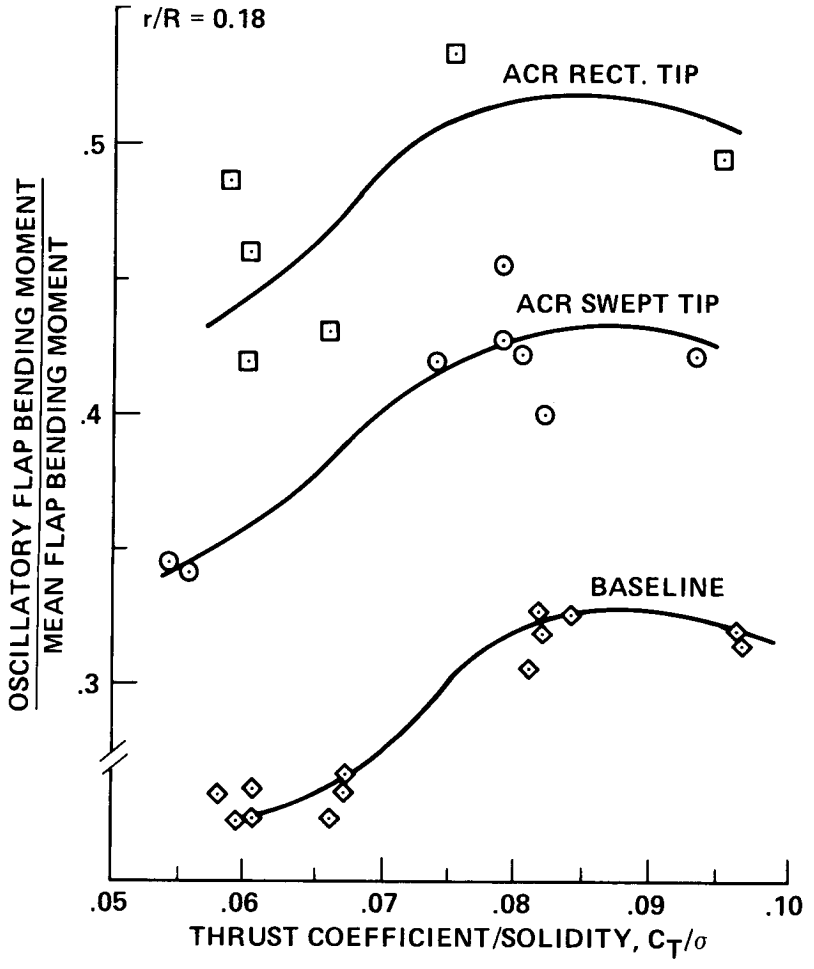

Figure 39.- Ratio of oscillatory flap bending moment to mean for three rotor configurations; $\mu = 0.35$ (ref. 101).

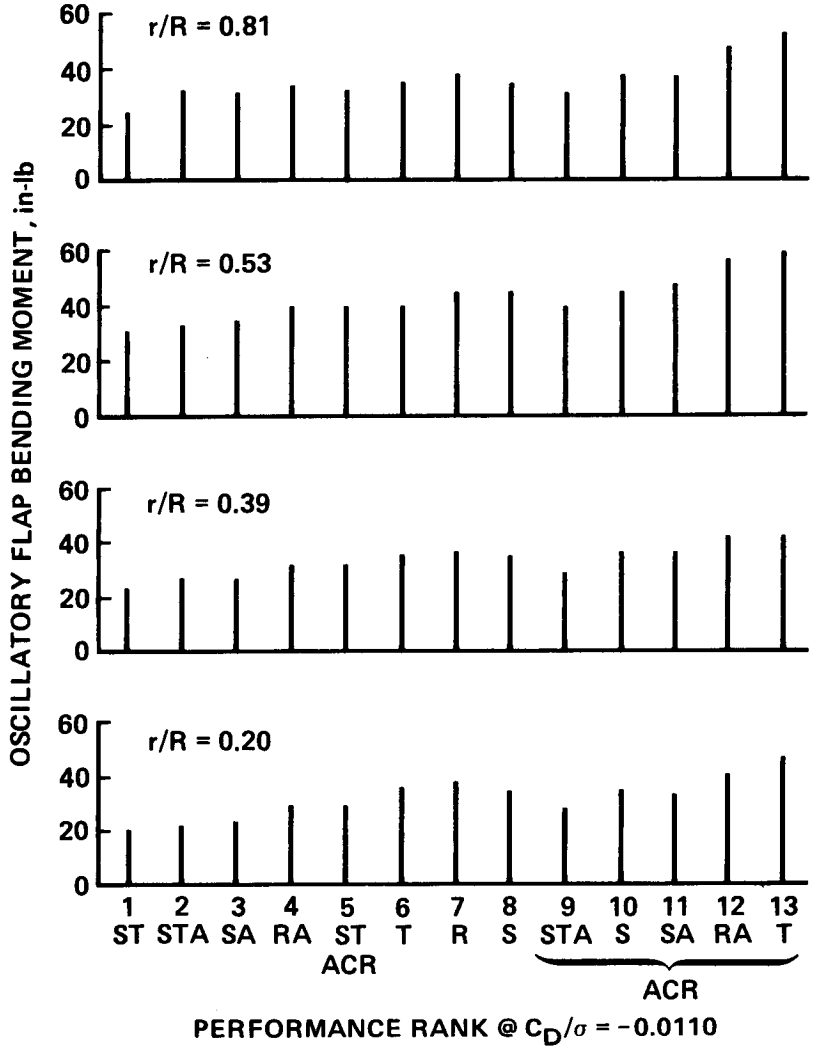

Figure 40.- Oscillatory flap bending moment relative to performance rank; $\mu = 0.35$, $C_L/\sigma = 0.0791$ (ref. 103).

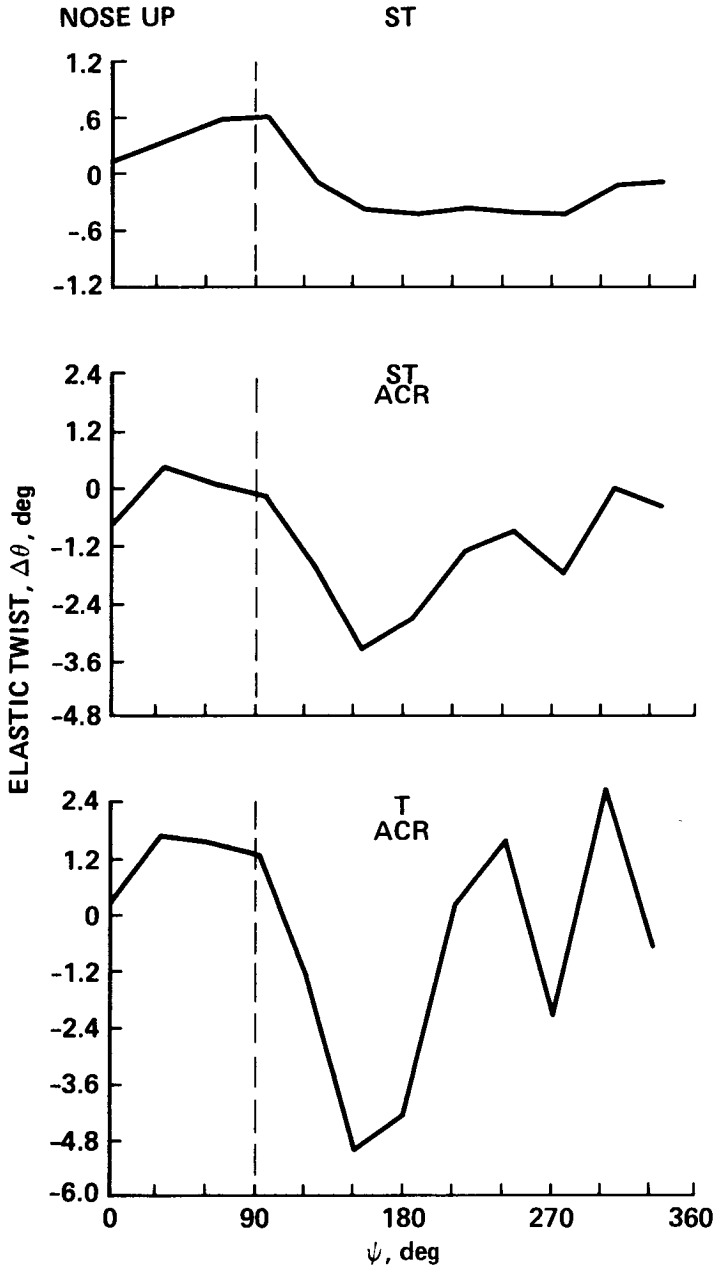

Figure 41.- Elastic twist as a function of azimuth for three rotor configurations; $\mu = 0.35$, $C_L/\sigma = 0.0791$ (ref. 103).

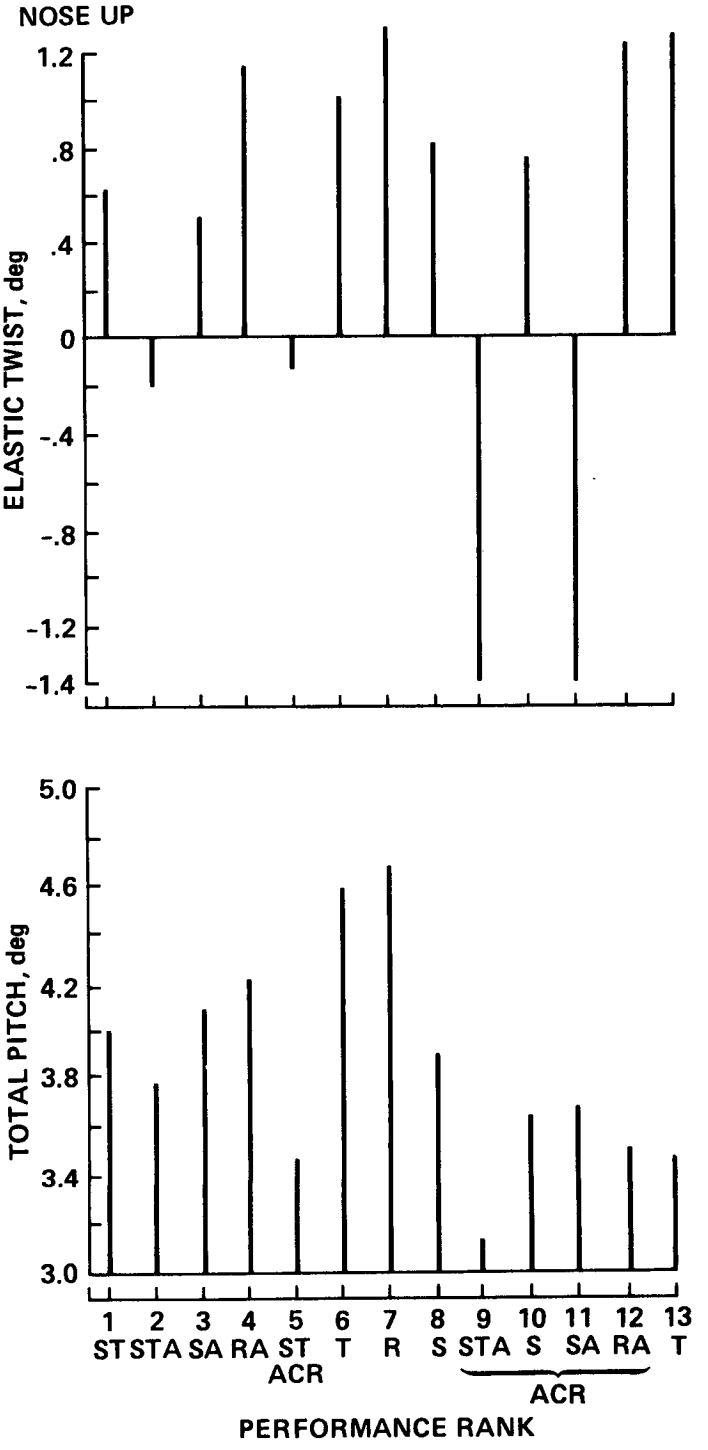

Figure 42.- Elastic twist at $\psi = 90°$ relative to performance rank; $\mu = 0.35$, $C_L/\sigma = 0.0791$ (ref. 103).

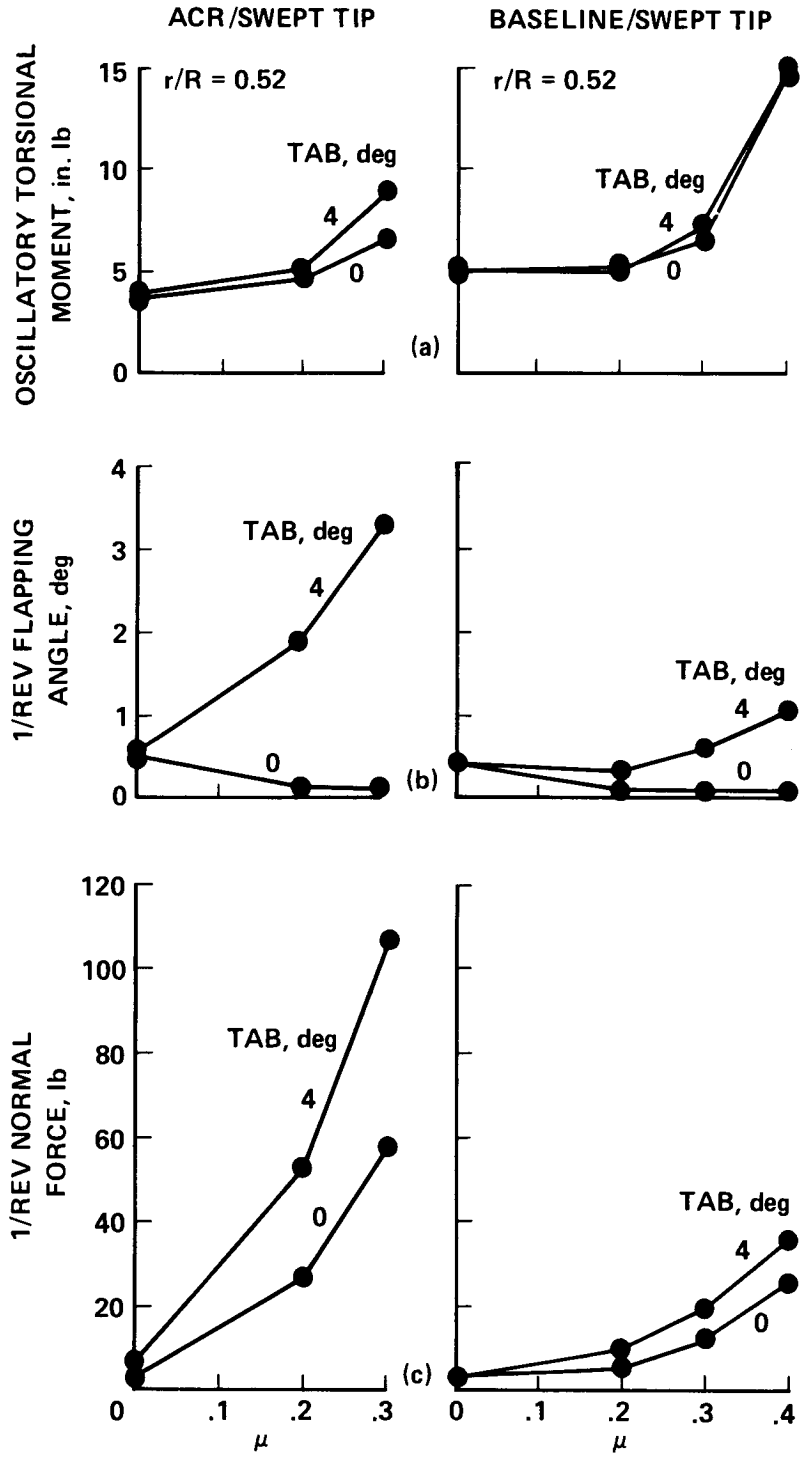

Figure 43.- Effect of tab deflection; C_L/σ = 0.0791 (ref. 103). (a) Oscillatory torsion moment. (b) First harmonic flapping. (c) Fixed system normal loads.

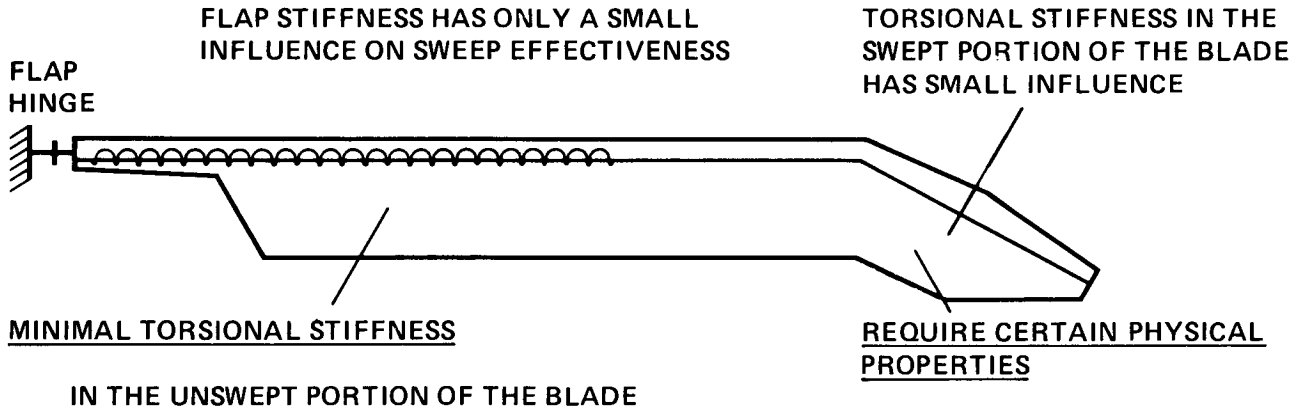

MECHANISM:

AERO/INERTIAL FORCE OF THE SWEPT PORTION OF THE BLADE USED THE SWEEP ARM TO TWIST THE UNSWEPT PORTION OF THE BLADE.

IF THE PHASE AND AMPLITUDE OF THE SWEEP INDUCED ELASTIC TWIST REDUCES THE TIP DOWN TWIST ON THE ADVANCING BLADE AND REDUCES THE HIGHER HARMONIC TWIST FROM OTHER SOURCES, THE 4/REV VERTICAL HUB LOAD IS REDUCED.

Figure 44.- Understanding of hub loads reduction mechanisms (ref. 104).

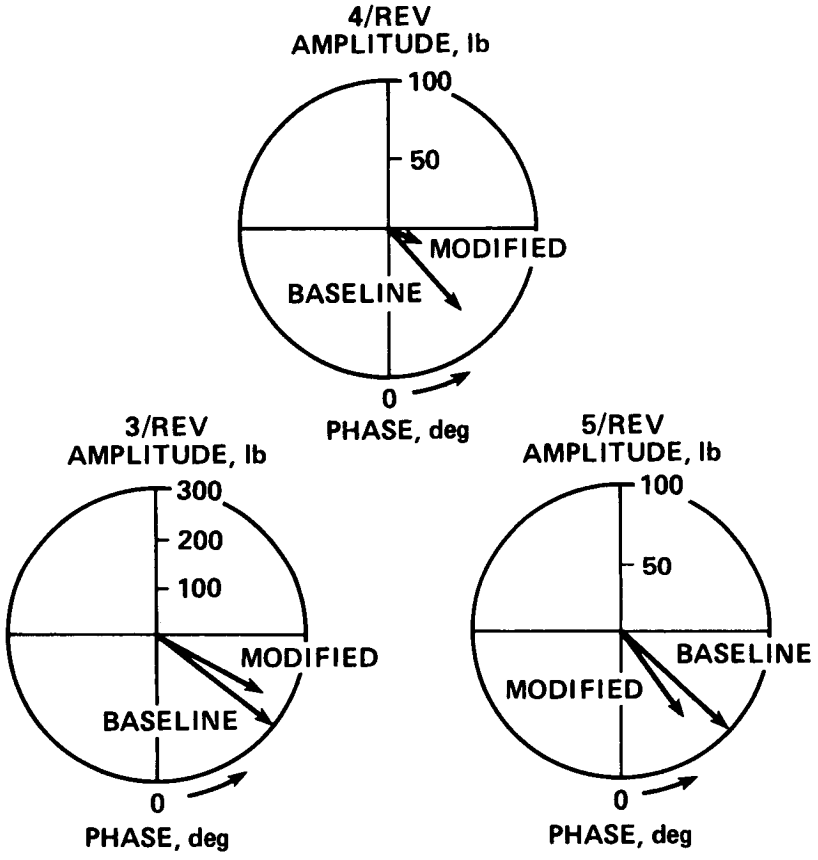

Figure 45.- Predicted reduction in blade root shears (ref. 79).

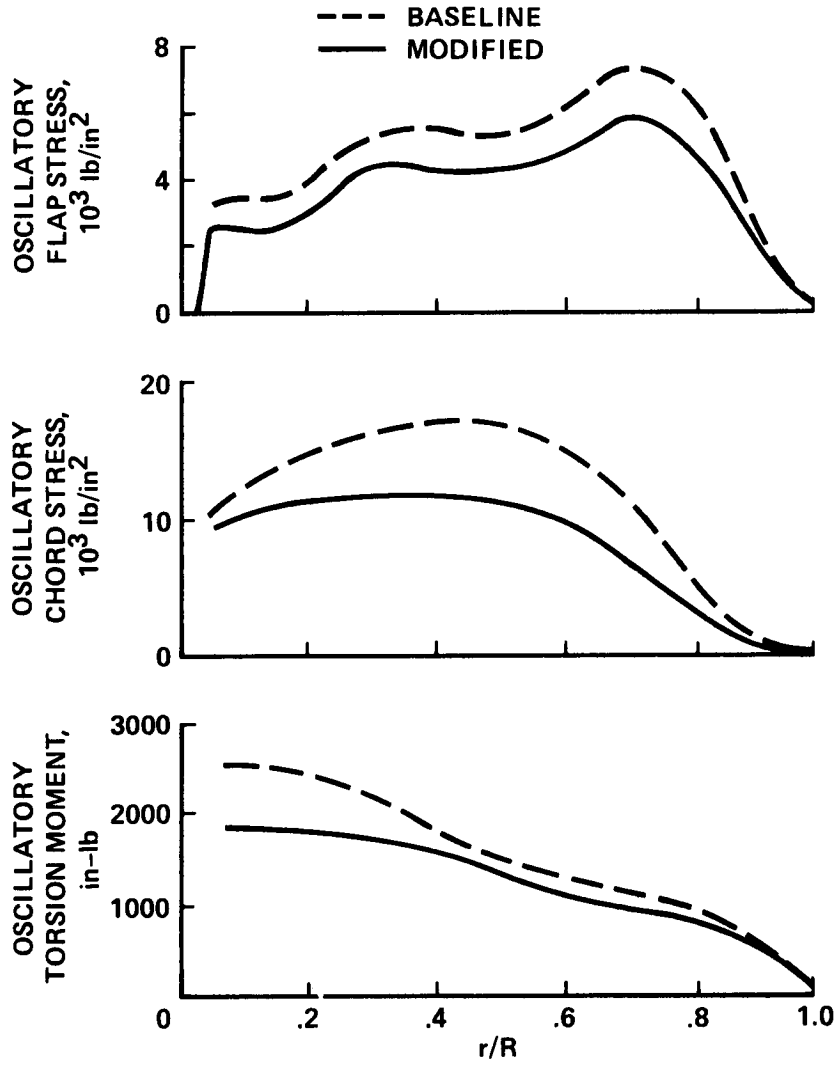

Figure 46.- Predicted reduction in blade stresses (ref. 79).

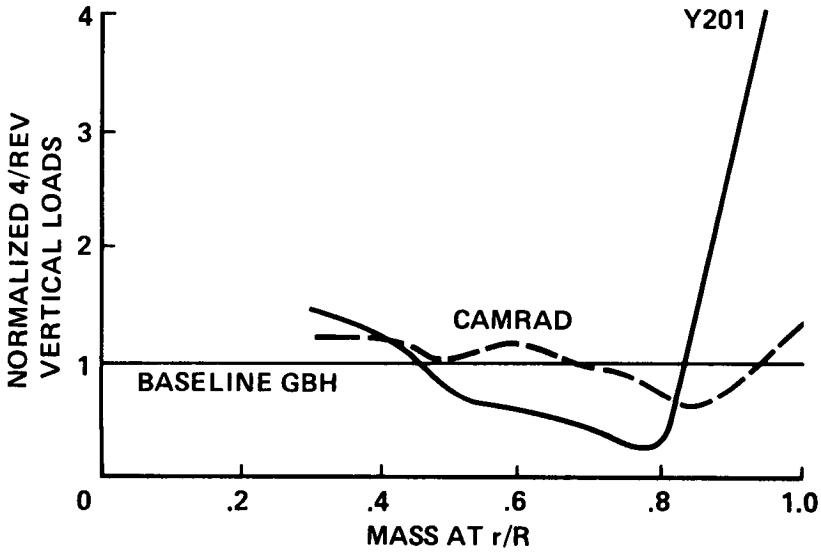

Figure 47.- Predicted 4/rev vertical loads for Growth Black Hawk as mass radial location is varied; $\mu = 0.338$, $C_L = 0.00608$.

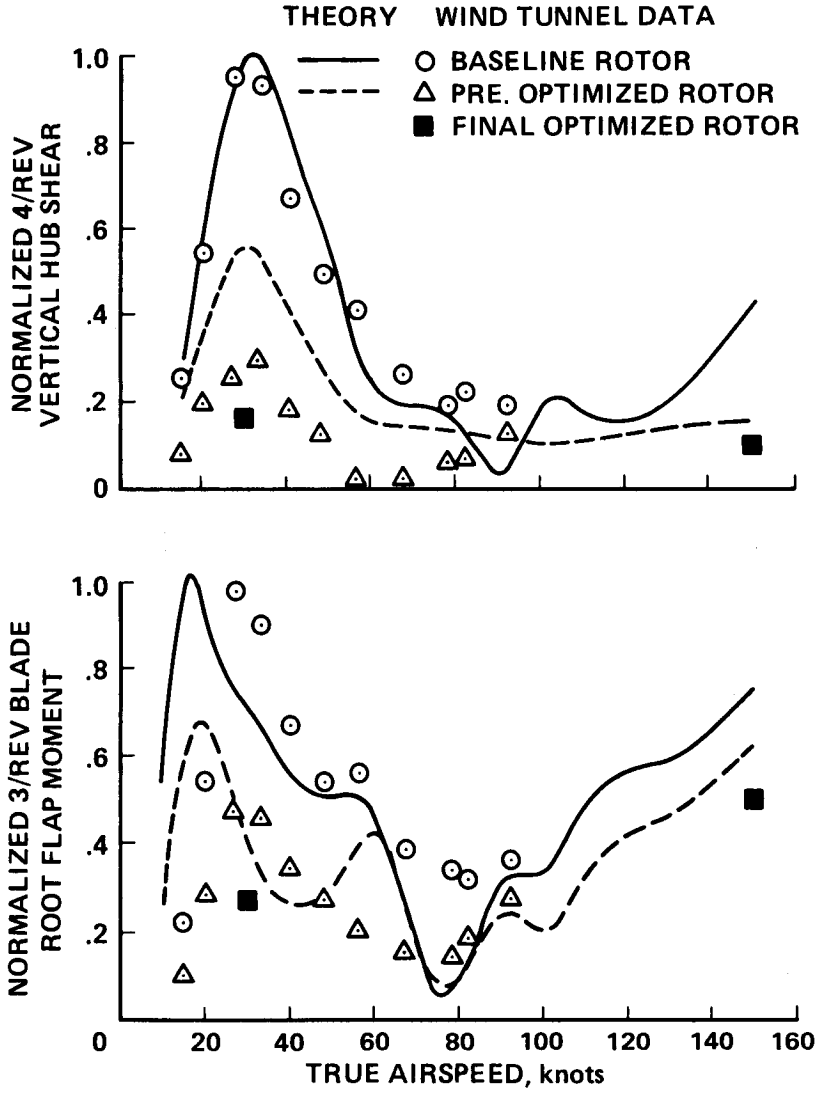

Figure 48.- Normalized 4/rev vertical hub shear and 3/rev blade root flap bending moment as a function of airspeed (ref. 109).

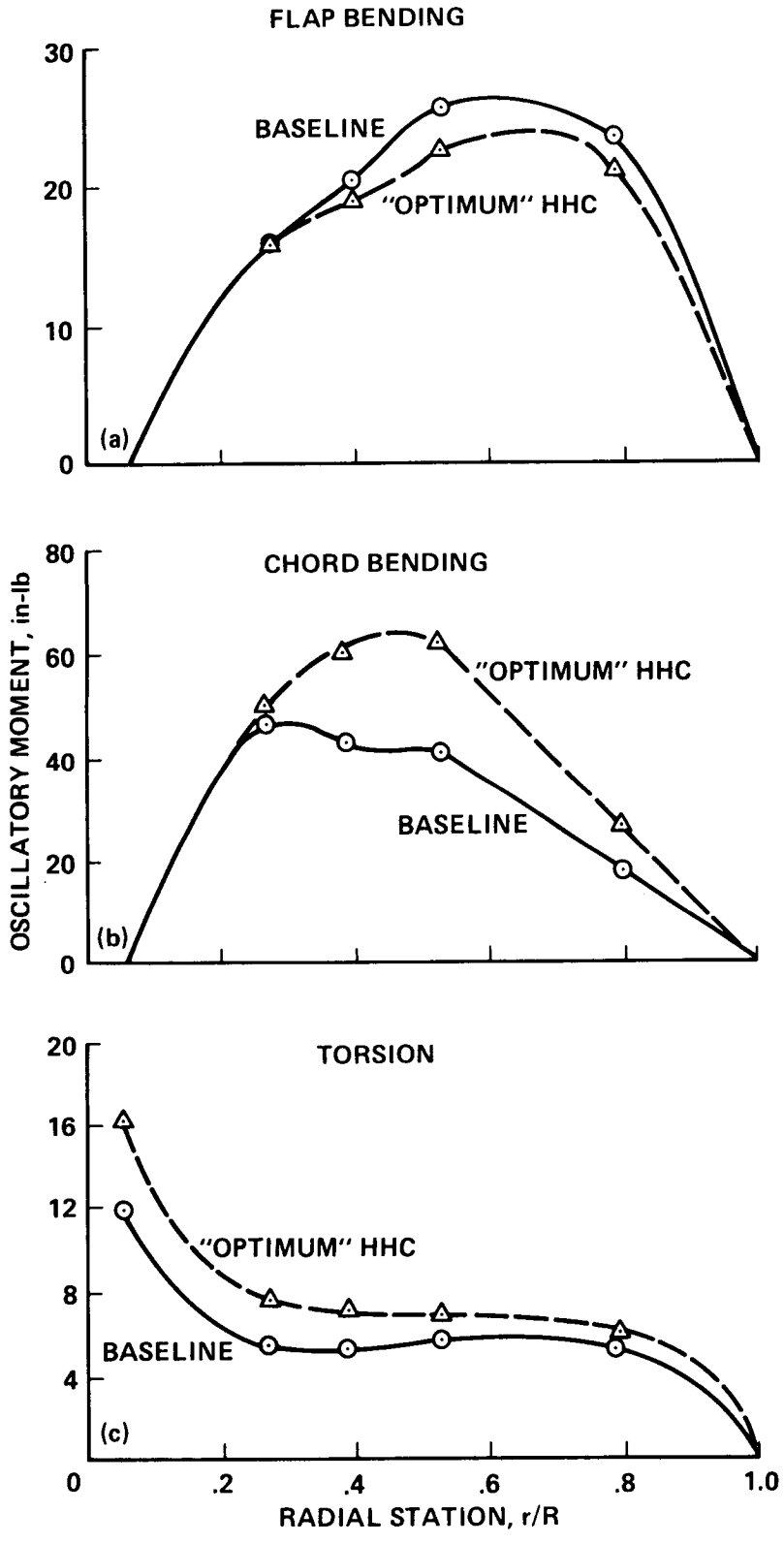

Figure 49.- Blade oscillatory loads with HHC; $\mu = 0.3$ (ref. 110). (a) Flap bending moment. (b) Chord bending moment. (c) Torsion moment.

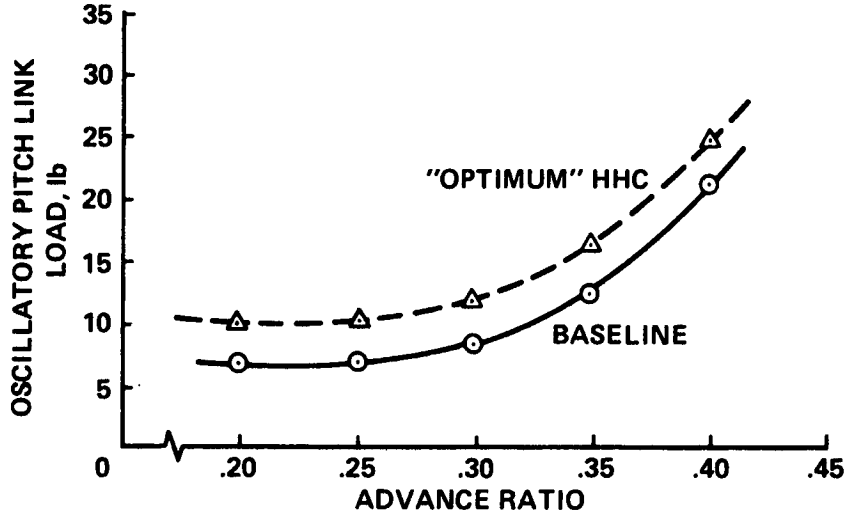

Figure 50.- Oscillatory pitch link loads with HHC (ref. 110).

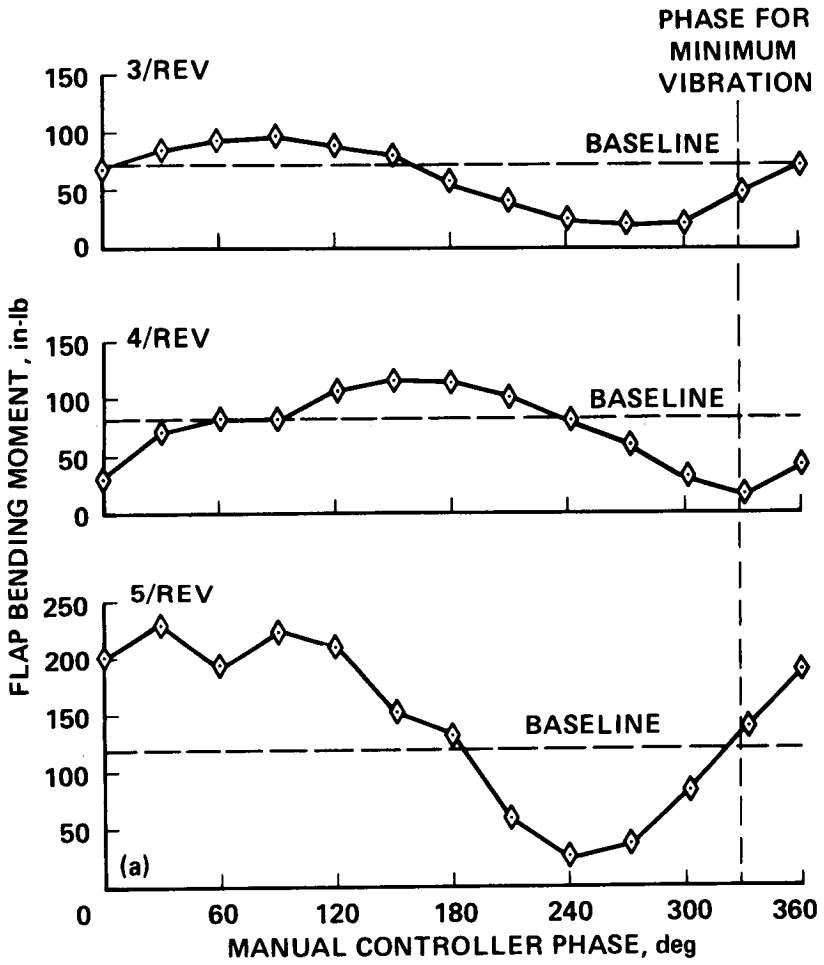

(a) Flap bending moment; r/R = 0.15.

Figure 51.- Effect of HHC on 3, 4, and 5/rev components of blade moments; V = 70 knots (ref. 111).

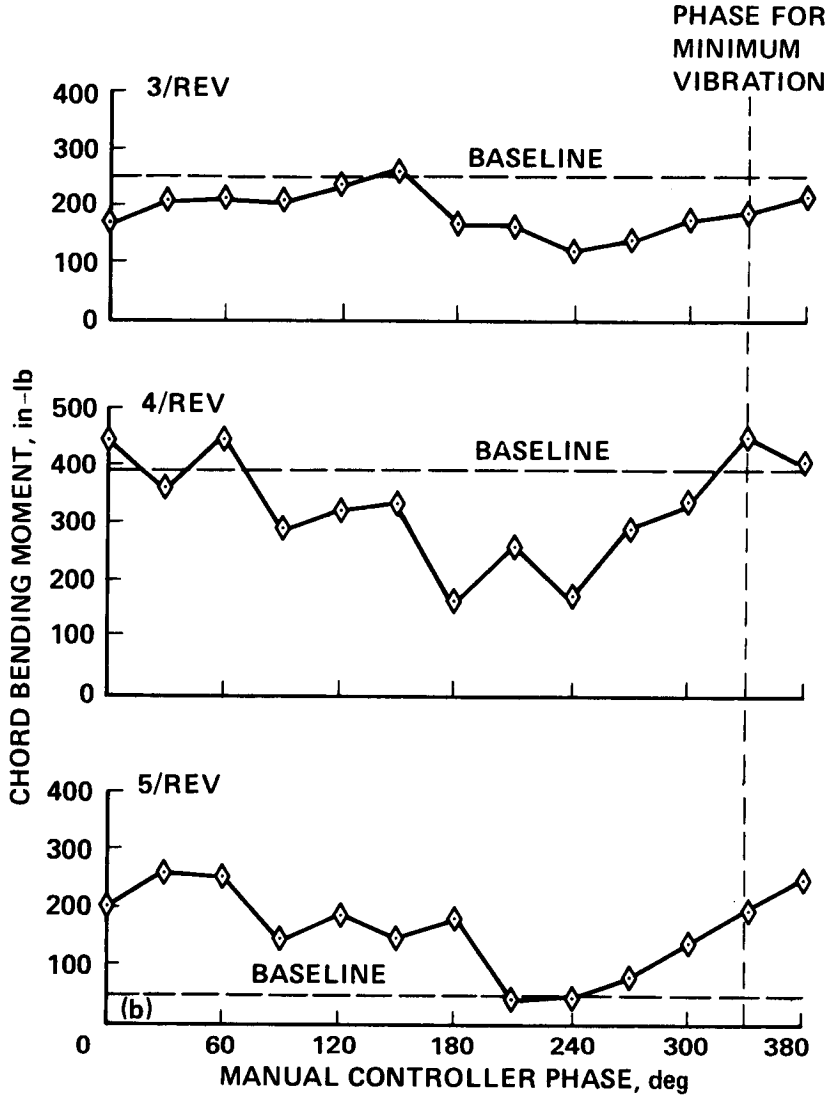

(b) Chord bending moment; r/R = 0.17.

Figure 51.- Continued.

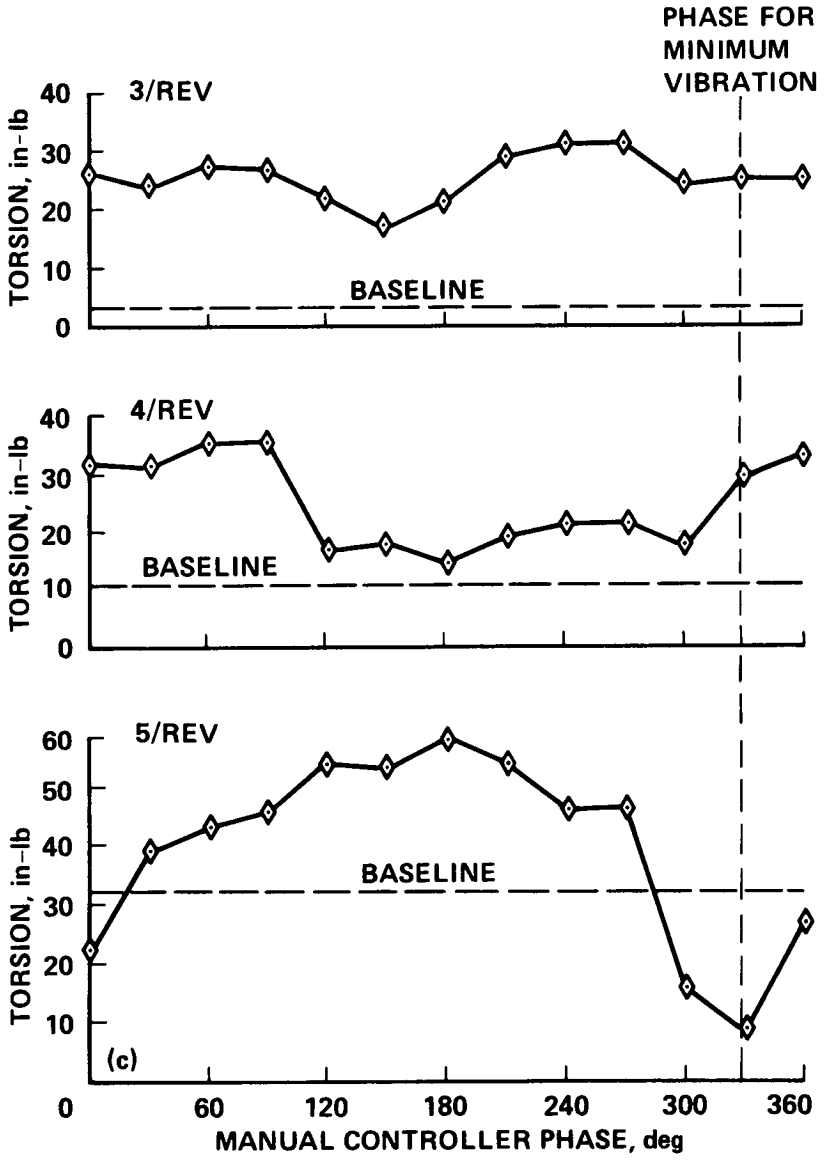

(c) Torsion moment; r/R = 0.17.

Figure 51.- Concluded.

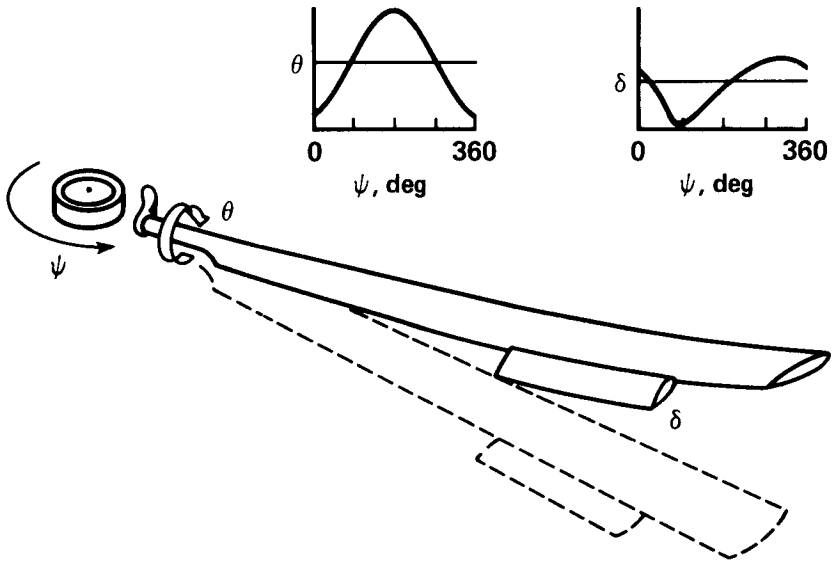

Figure 52.- Controllable twist rotor (CTR) schematic (ref. 112).

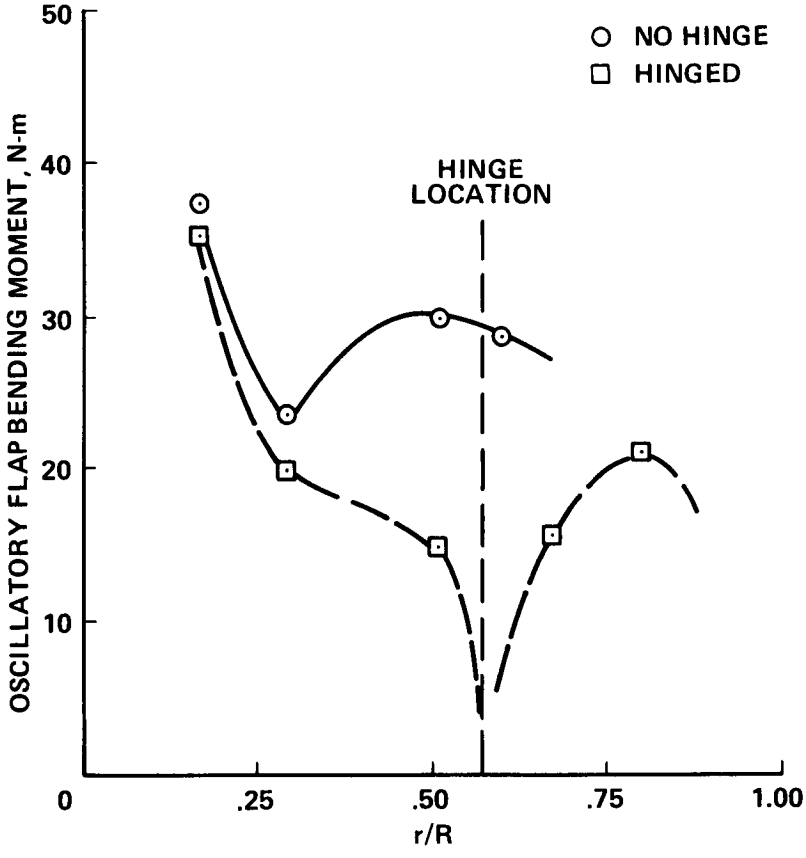

Figure 53.- Effect of mid-span hinge on teetering rotor blade oscillatory flap bending moment; $\mu = 0.35$, $C_L/\sigma = 0.025$ (ref. 113).

C-4

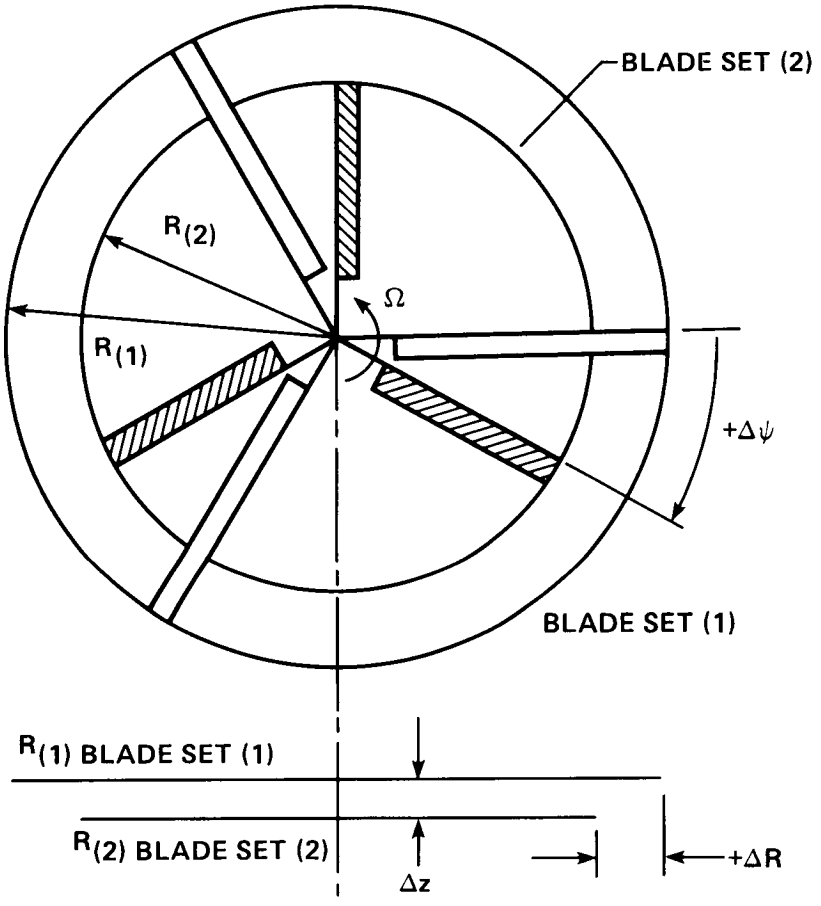

Figure 54.- Variable geometry rotor (VGR) parameters (ref. 114).

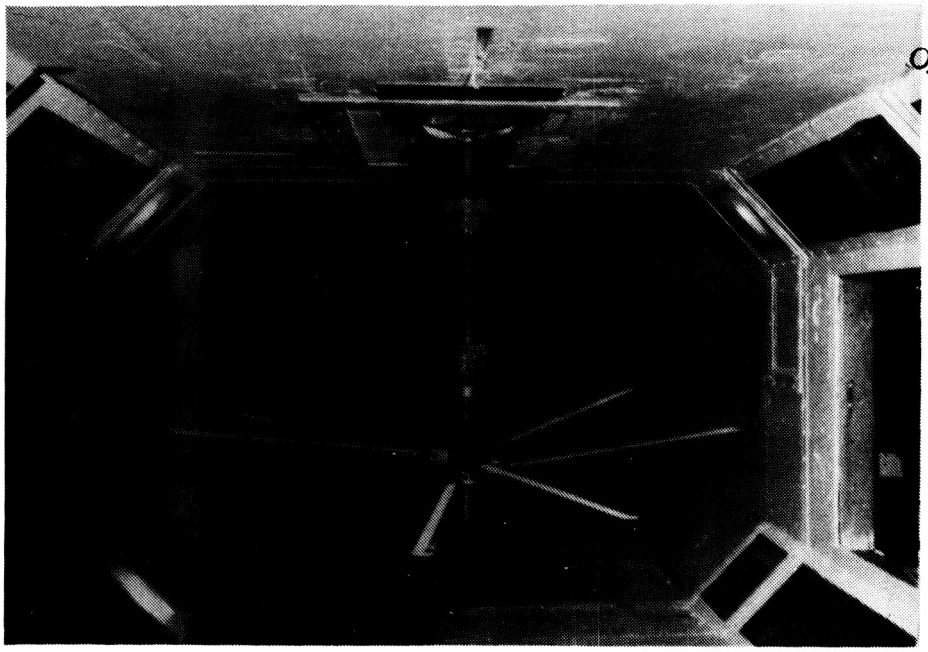

Figure 55.- Variable geometry rotor (VGR) in UTRC wind tunnel (ref. 116).

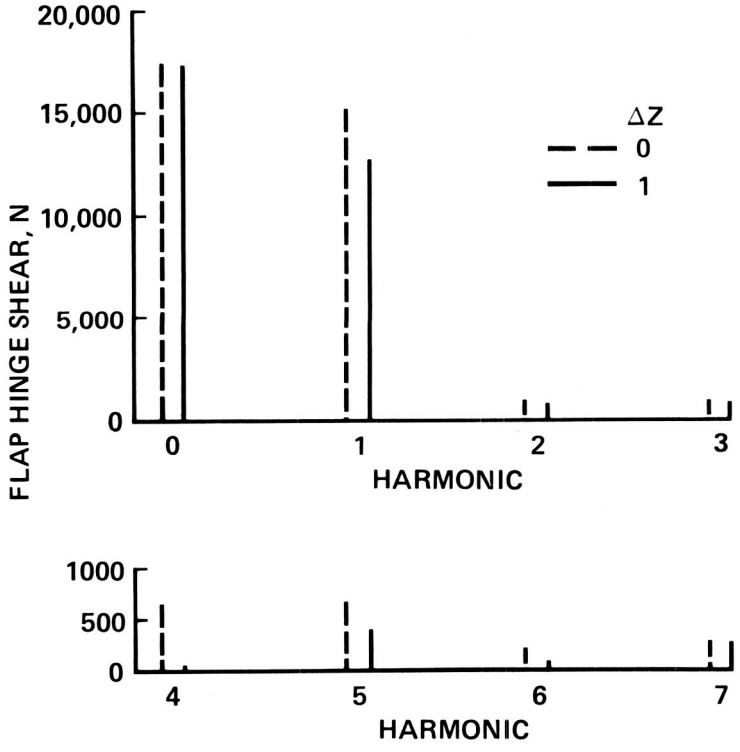

Figure 56.- Calculated upper rotor flap shears for VGR; $\mu = 0.2$ (ref. 117).

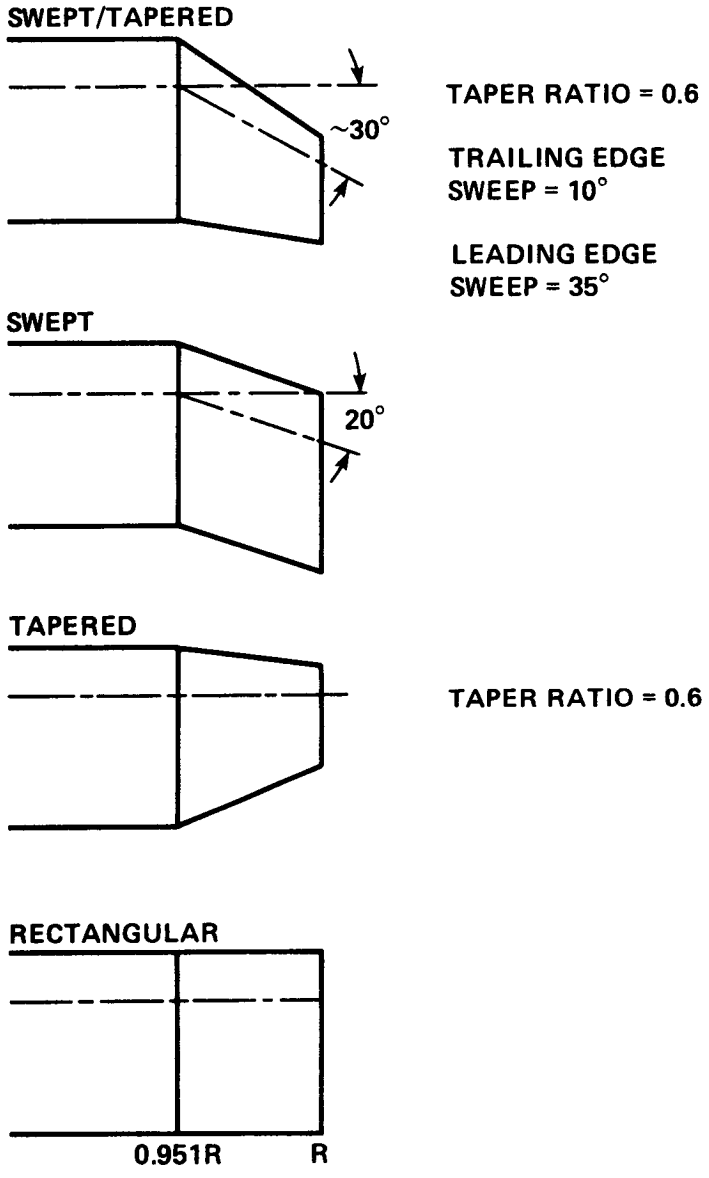

Figure 57.- Tip planform geometry (ref. 67).

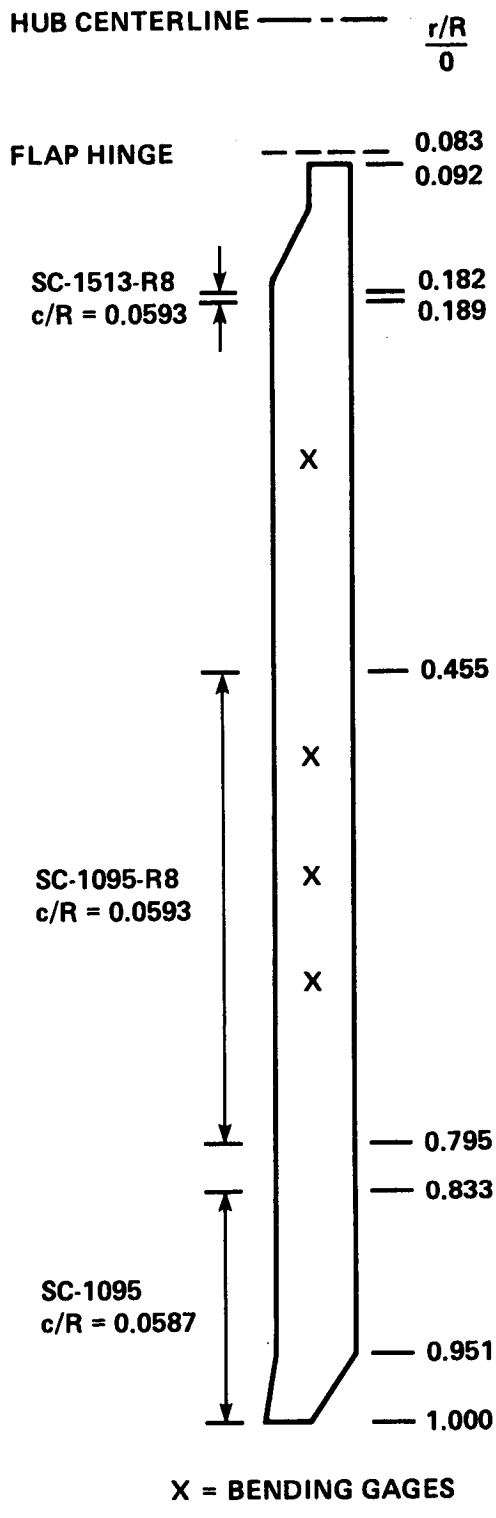

Figure 58.- Rotor blade geometry (ref. 67).

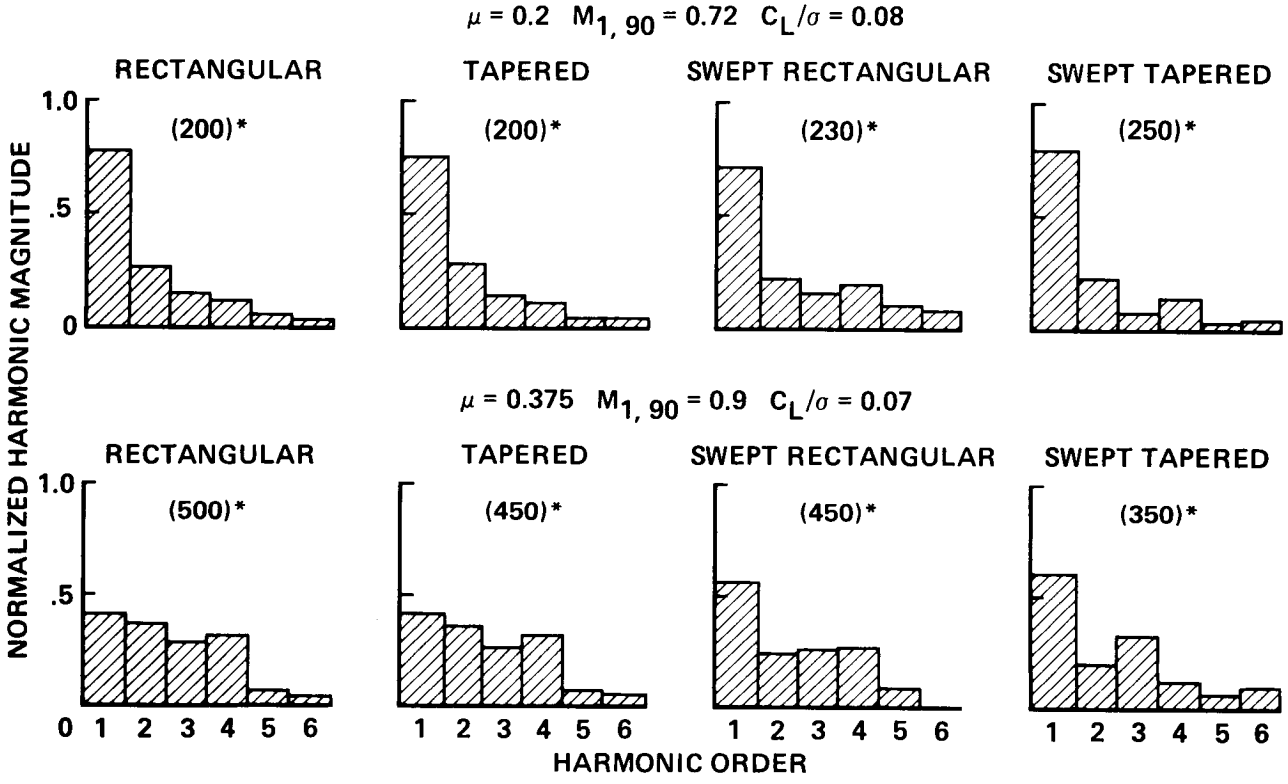

Figure 59.- Normalized measured control load harmonics for four blade tips (ref. 119).

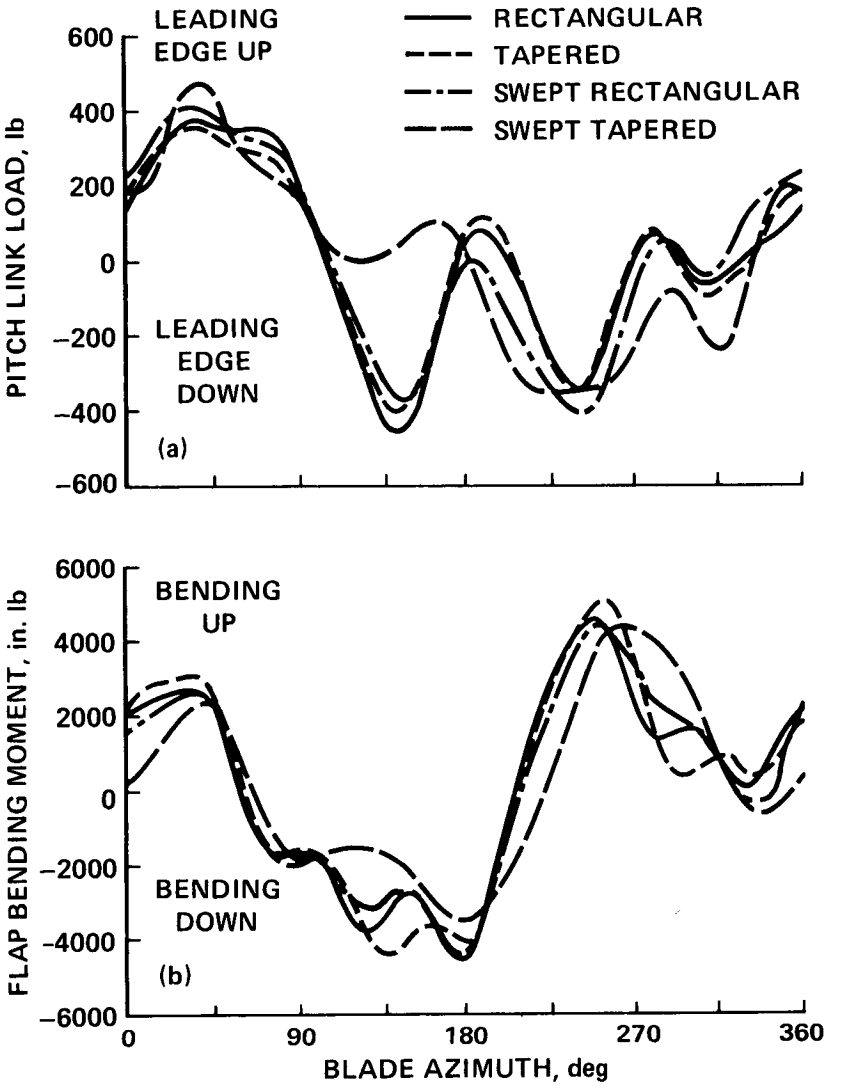

Figure 60.- Rotor loads as a function of blade azimuth for four blade tips; $\mu = 0.38$, $C_L/\sigma = 0.086$ (ref. 119). (a) Pitch link load. (b) Flap bending moment; $r/R = 0.6$.

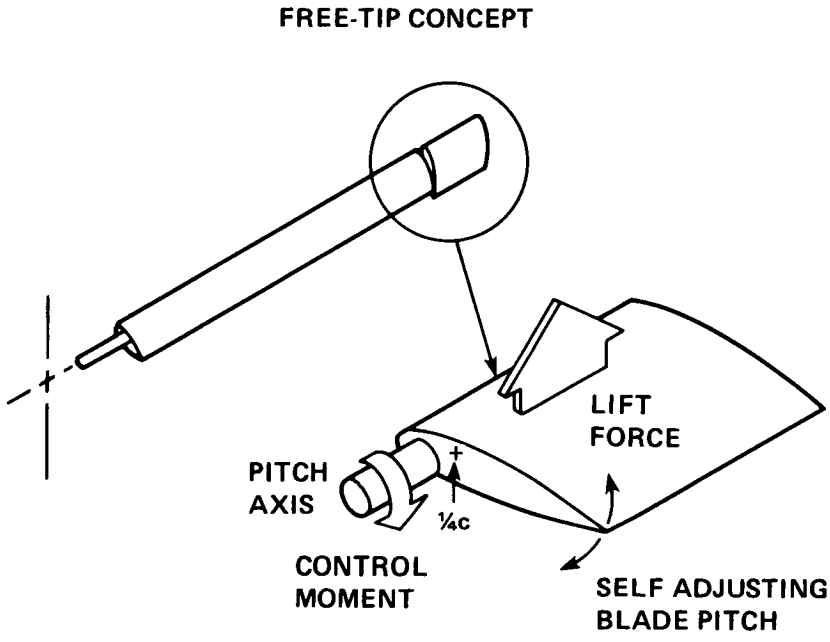

Figure 61.- Free-tip rotor schematic (ref. 120).

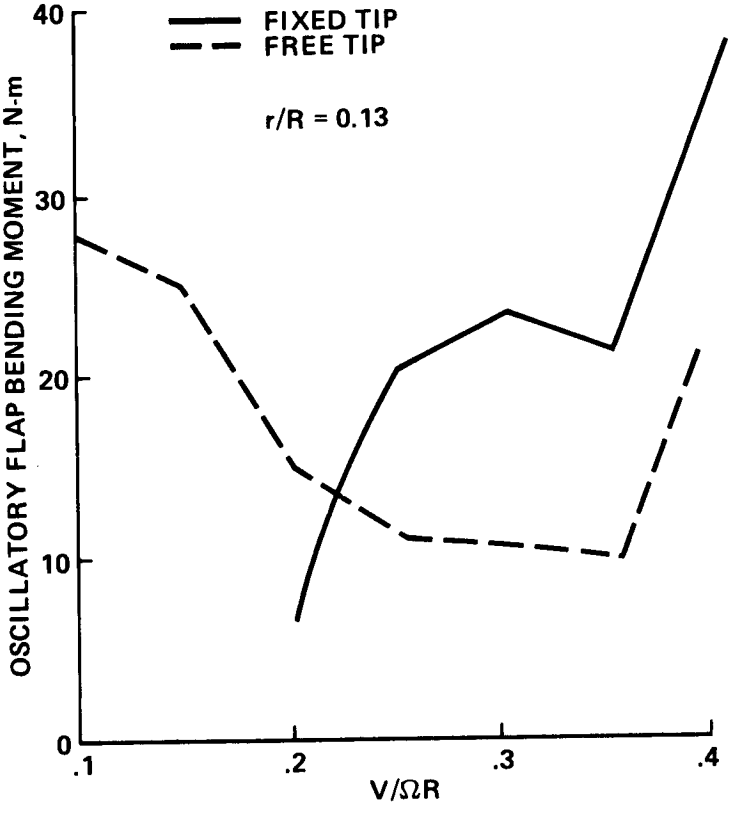

Figure 62.- Effect of free-tip on oscillatory flap bending moments; $C_L/\sigma = 0.07$ (ref. 120).

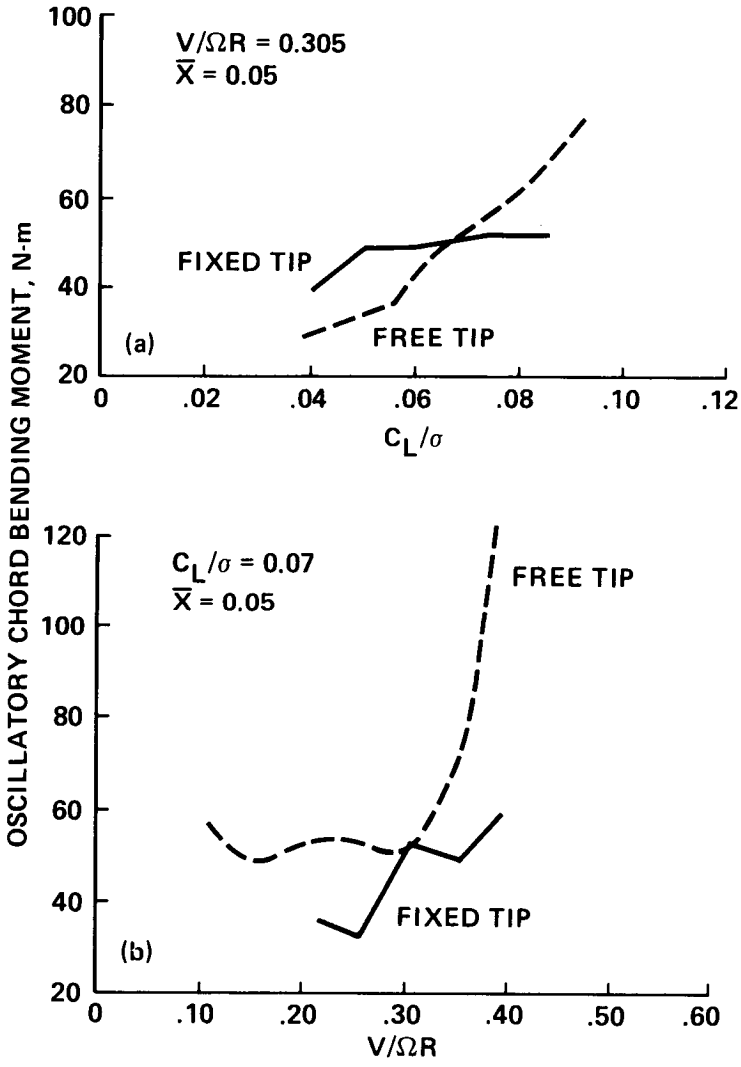

Figure 63.- Effect of free-tip on oscillatory chord bending moments (ref. 120). (a) Chord bending as a function of rotor lift; $\mu = 0.305$. (b) Chord bending as a function of advance ratio; $C_L/\sigma = 0.07$.

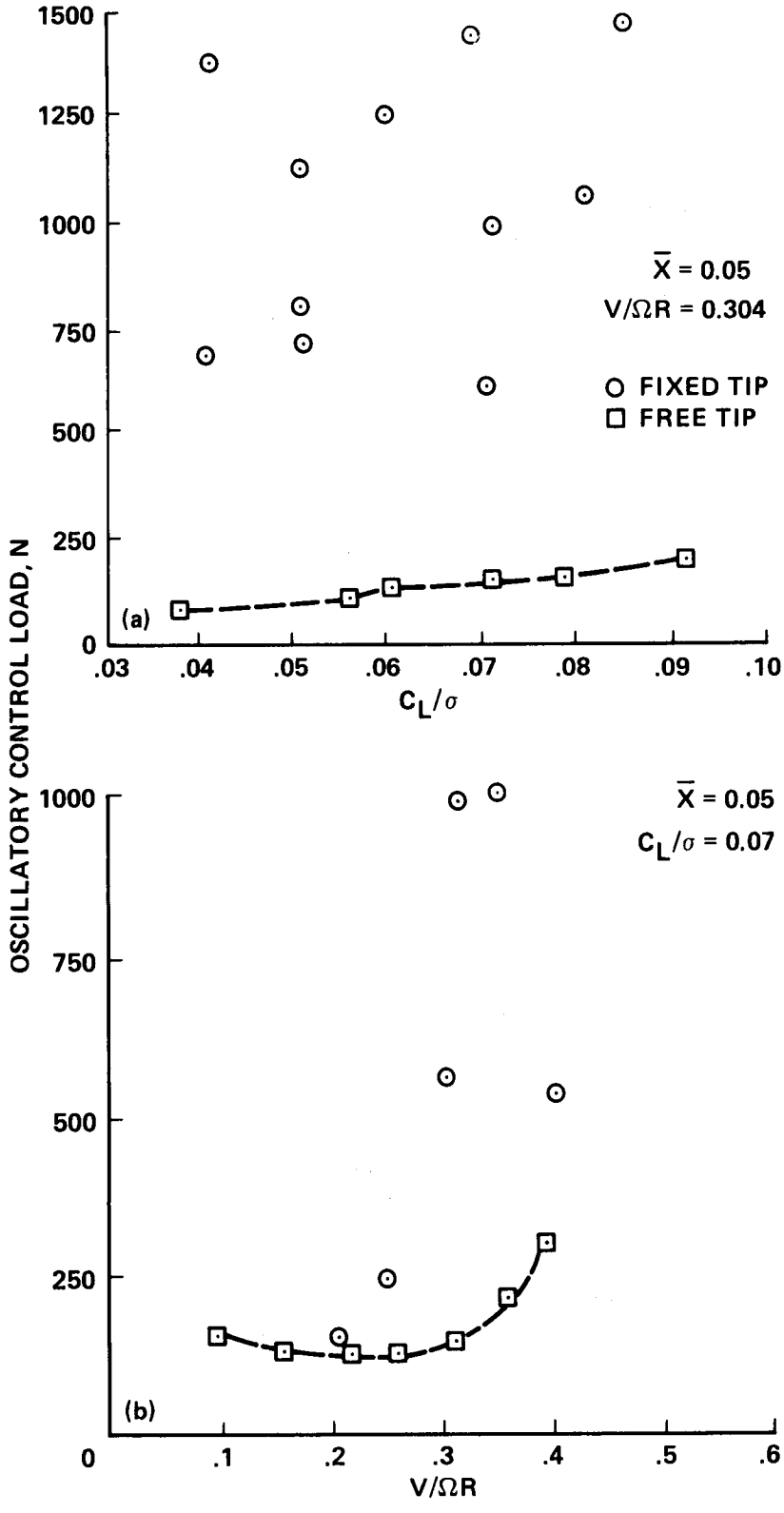

Figure 64.- Effect of free-tip on oscillatory pitch link loads (ref. 120). (a) Oscillatory control load as a function of rotor lift coefficient; $\mu = 0.304$. (b) Oscillatory control load as a function of advance ratio; $C_L/\sigma = 0.07$.

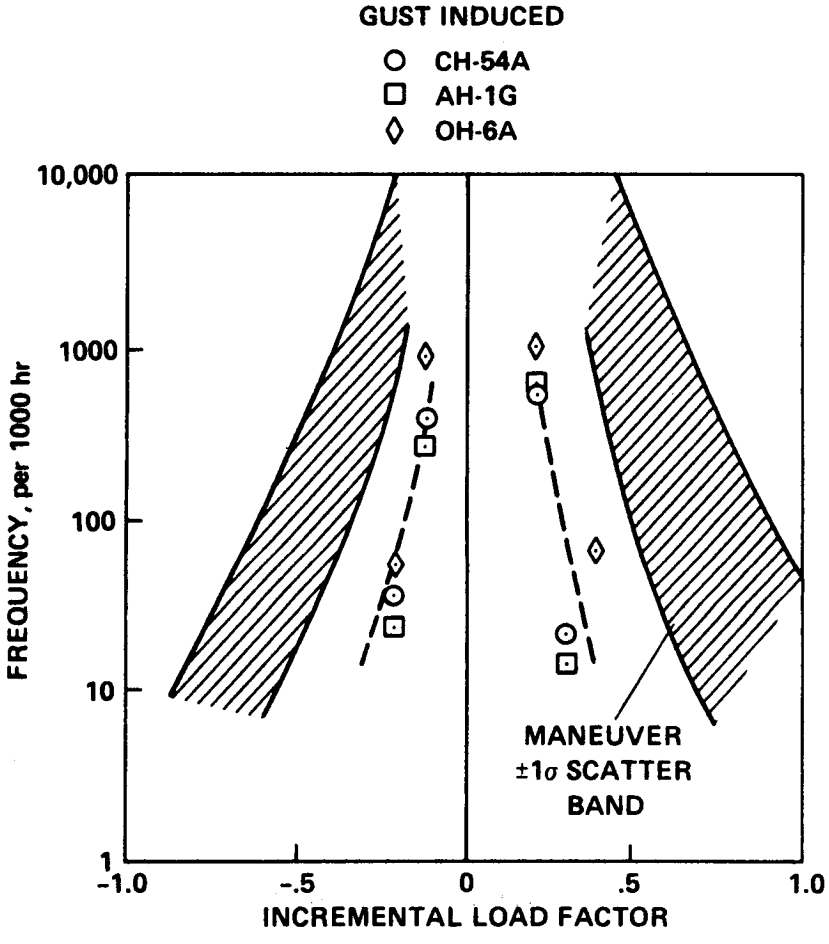

Figure 65.- Comparison of gust and maneuver induced loads (ref. 124).

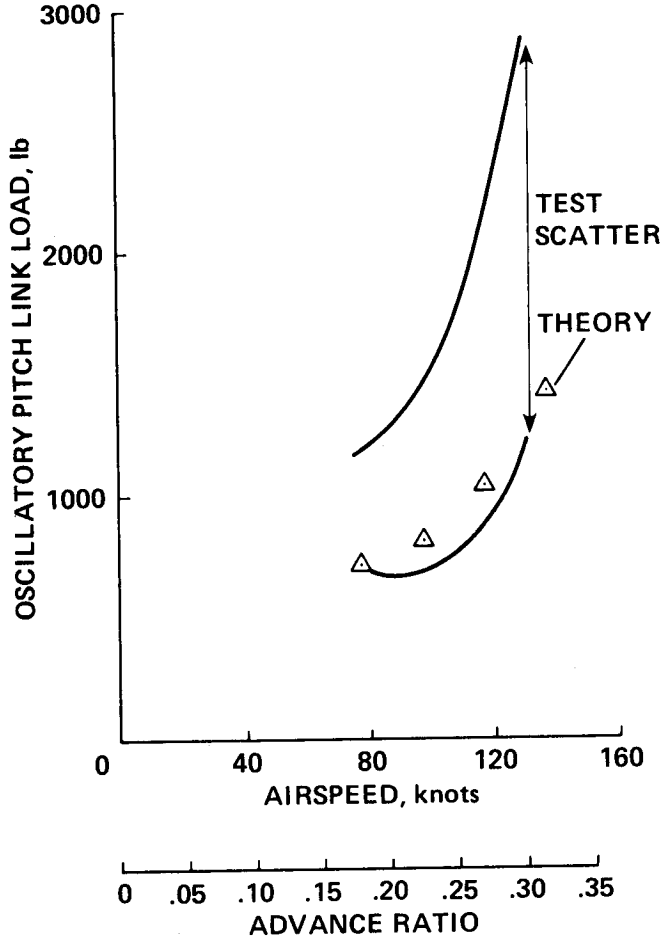

Figure 66.- Oscillatory pitch link load variation over five test flights for CH-47C; C_T/σ = 0.102 (ref. 133).

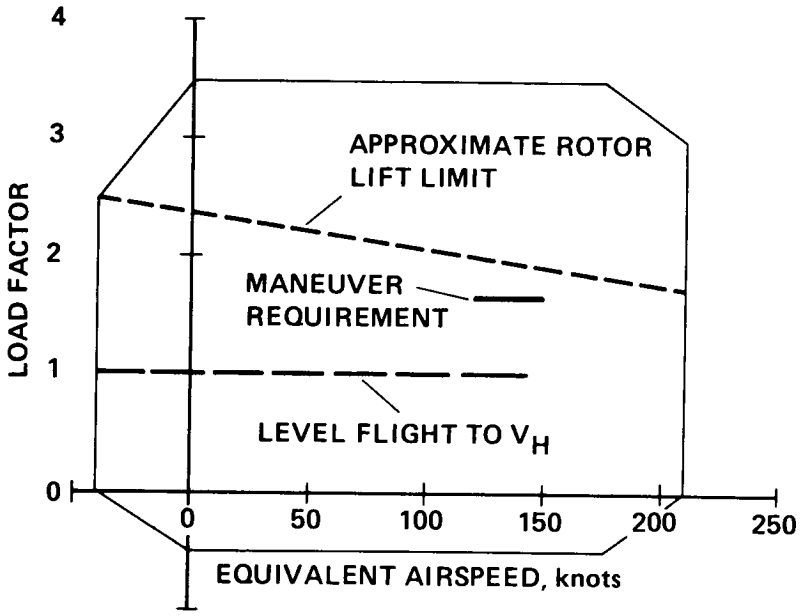

Figure 67.- V-n diagram for military helicopter. Approximate rotor lift limit from ref. 134.

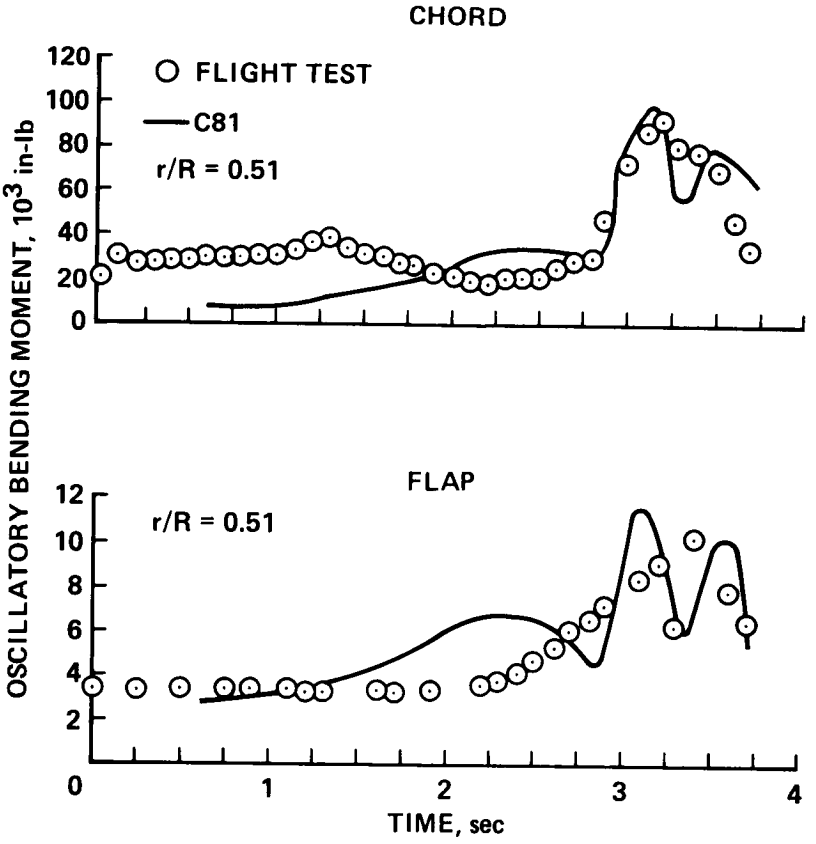

Figure 68.- Comparison of C81 predictions with measured oscillatory bending moments for AH-1G during a 2 g pull-up (ref. 136).

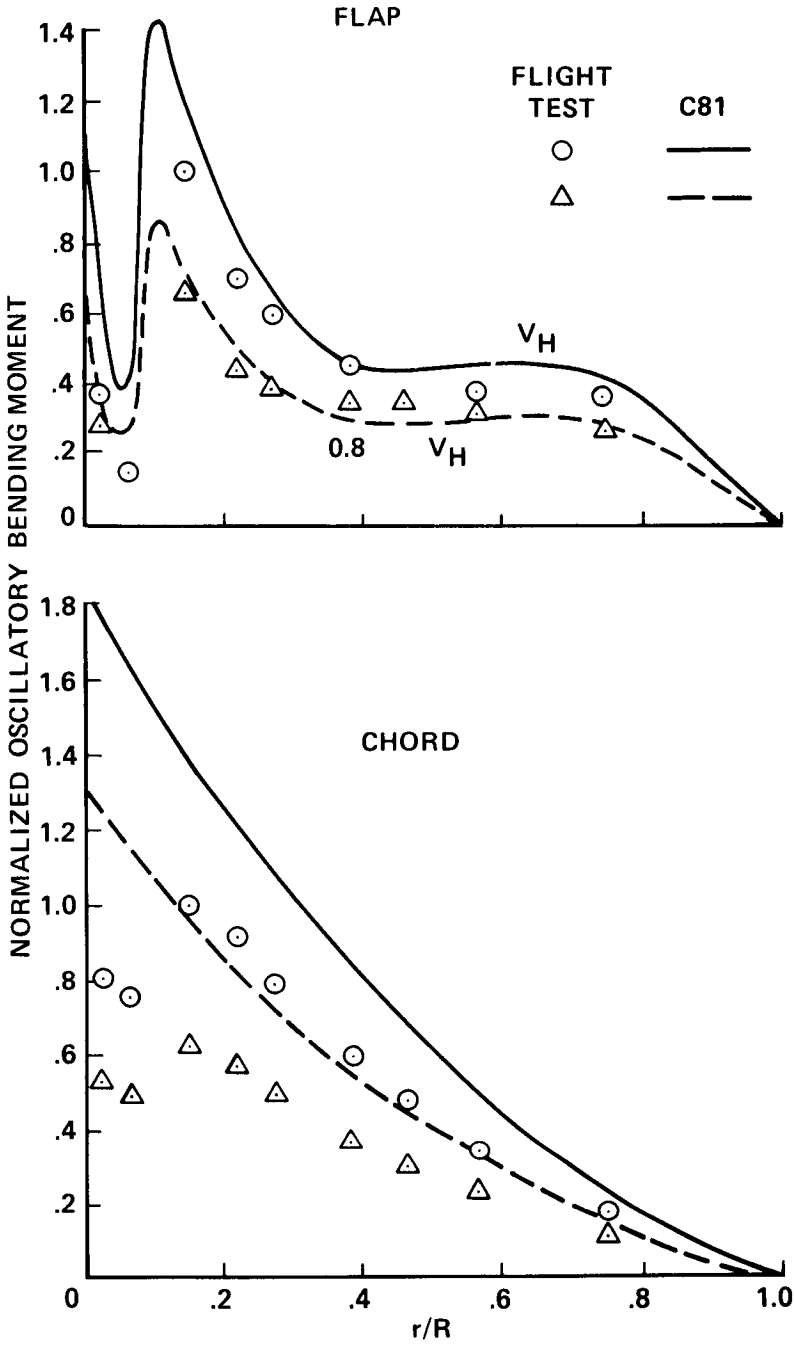

Figure 69.- Comparison of C81 and flight test oscillatory bending moments for a two-bladed teetering rotor. Bending moments normalized by oscillatory moment at r/R = 0.15 and V_H (ref. 13).

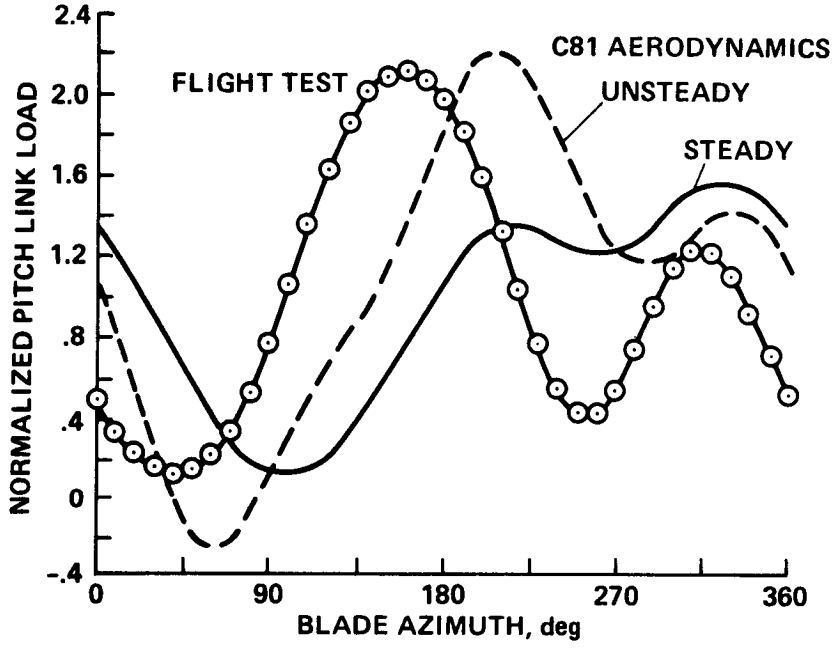

Figure 70.- Comparison of C81 and flight test measured pitch link load for two-bladed teetering rotor at V_H. Pitch link load normalized by measured mean load (ref. 13).

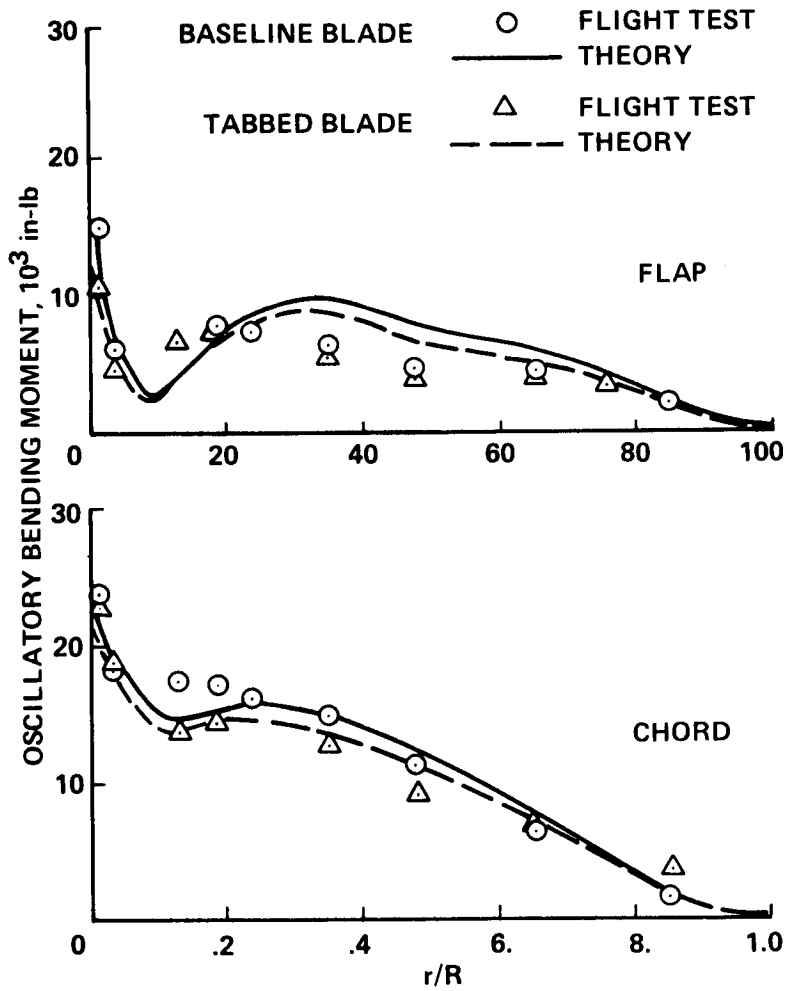

Figure 71.- Comparison of C81 with oscillatory bending moment distributions for a four-bladed rotor; $\mu = 0.282$, $t_c = 0.17$ (ref. 154).

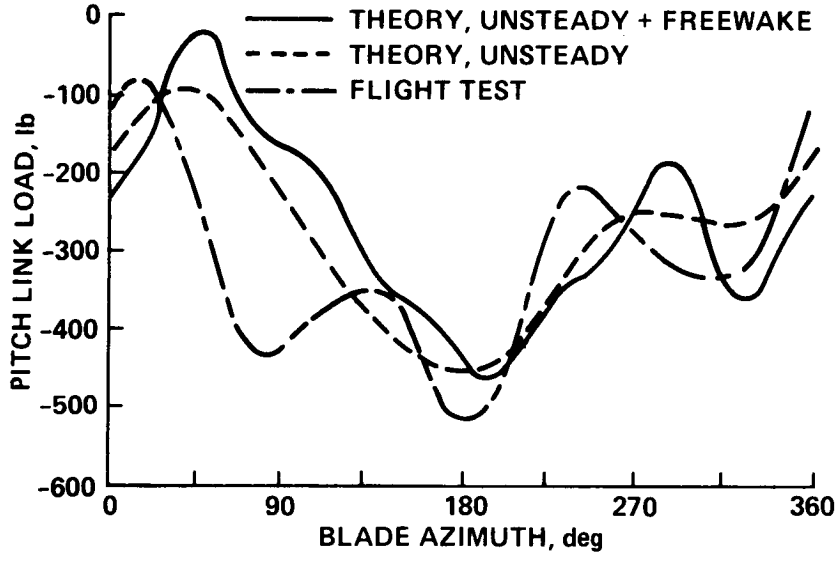

Figure 72.- Comparison of C81 with pitch link time history; $\mu = 0.282$, $t_c = 0.17$, tabbed blade (ref. 154).

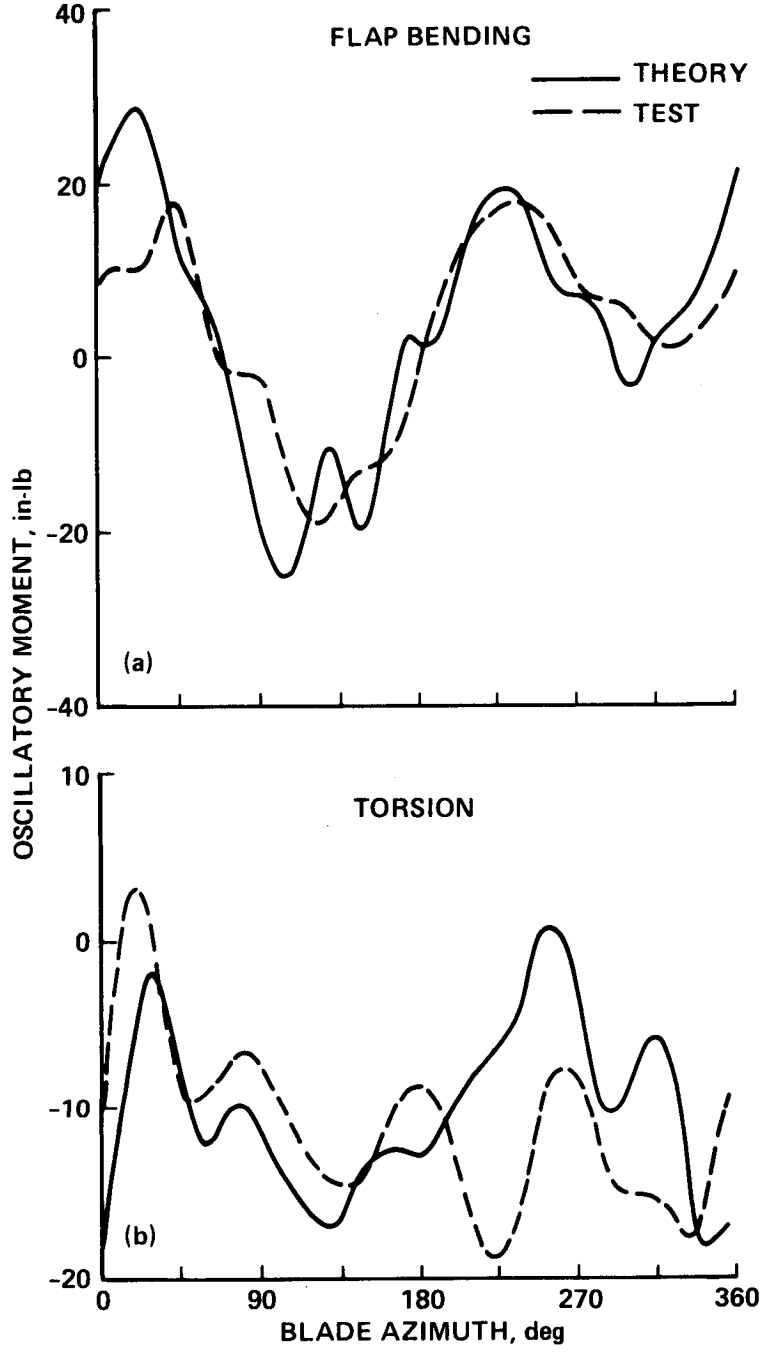

Figure 73.- Comparison of C-60 with midspan flap bending and torsion moments for an articulated model rotor; $\mu = 0.40$, $C_T/\sigma = 0.107$ (ref. 155).

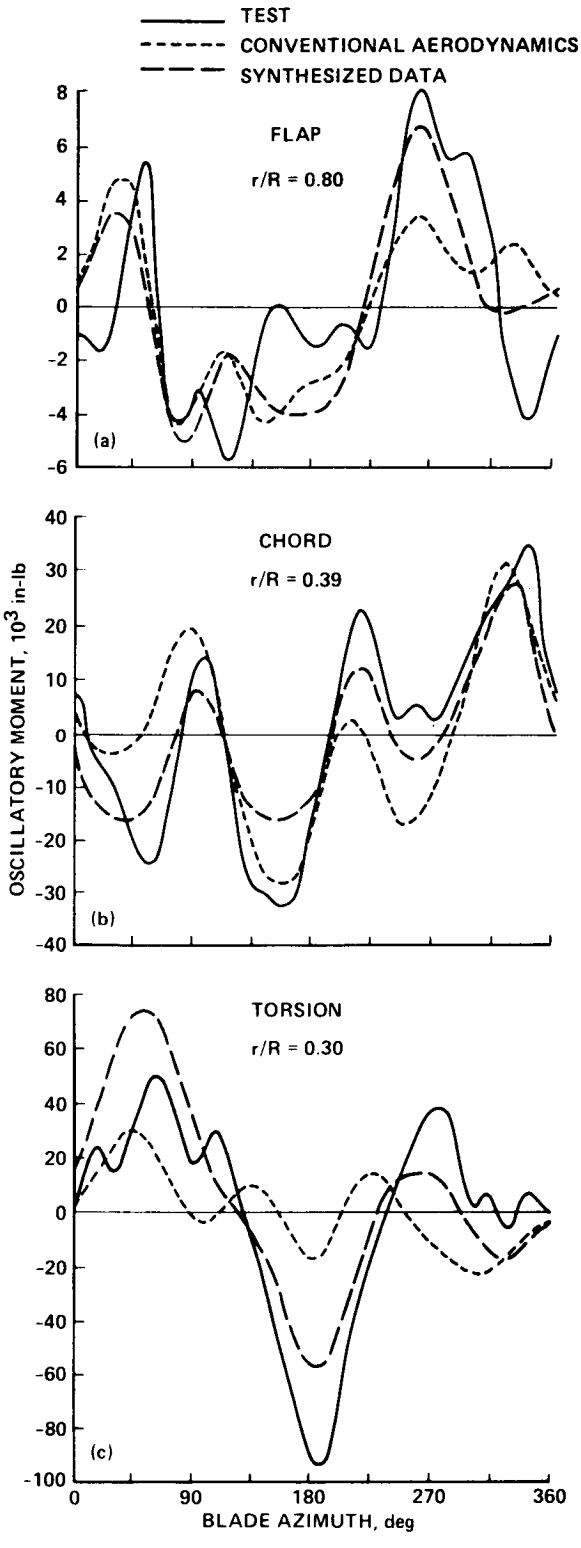

Figure 74.- Comparison of RAVIB with AH-1G OLS blade moment data; V = 142 knots (ref. 32). (a) Flap bending moment; r/R = 0.80. (b) Chord bending moment; r/R = 0.39. (c) Torsion moment; r/R = 0.30.

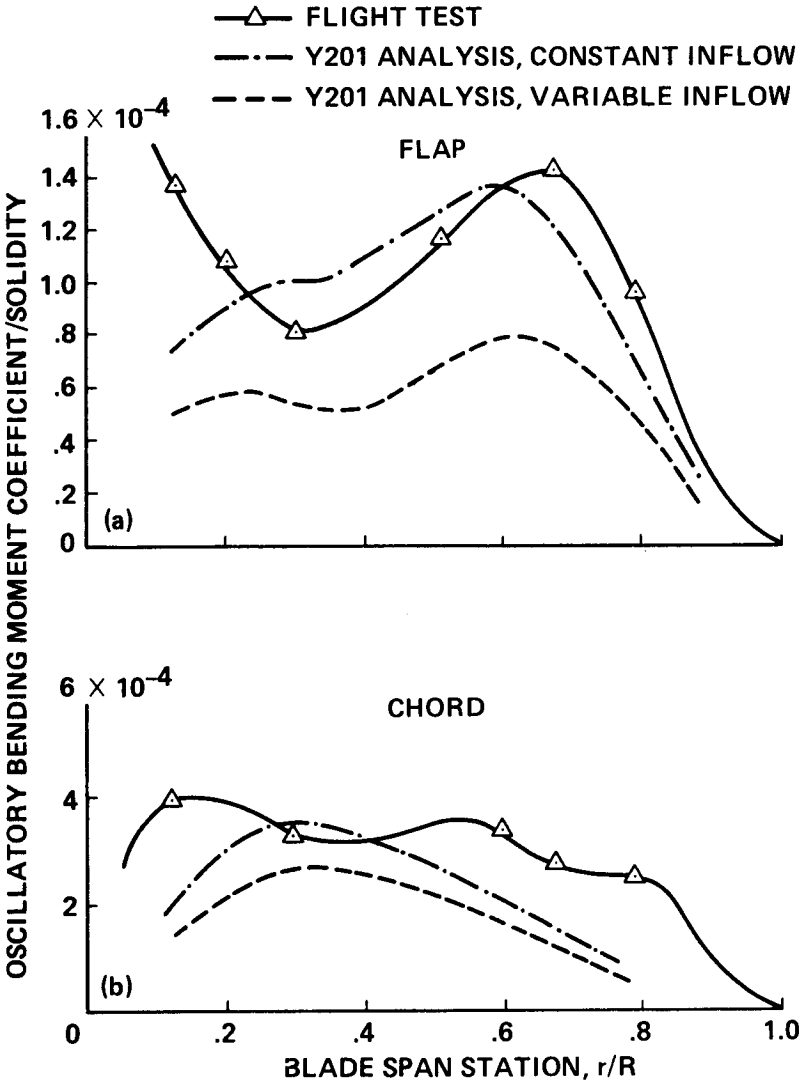

Figure 75.- Comparison of Y201 with radial distribution of flap and chord bending moments for S-76; μ = 0.338, GW = 8,200 lb (ref. 66). (a) Flap bending moment. (b) Chord bending moment.

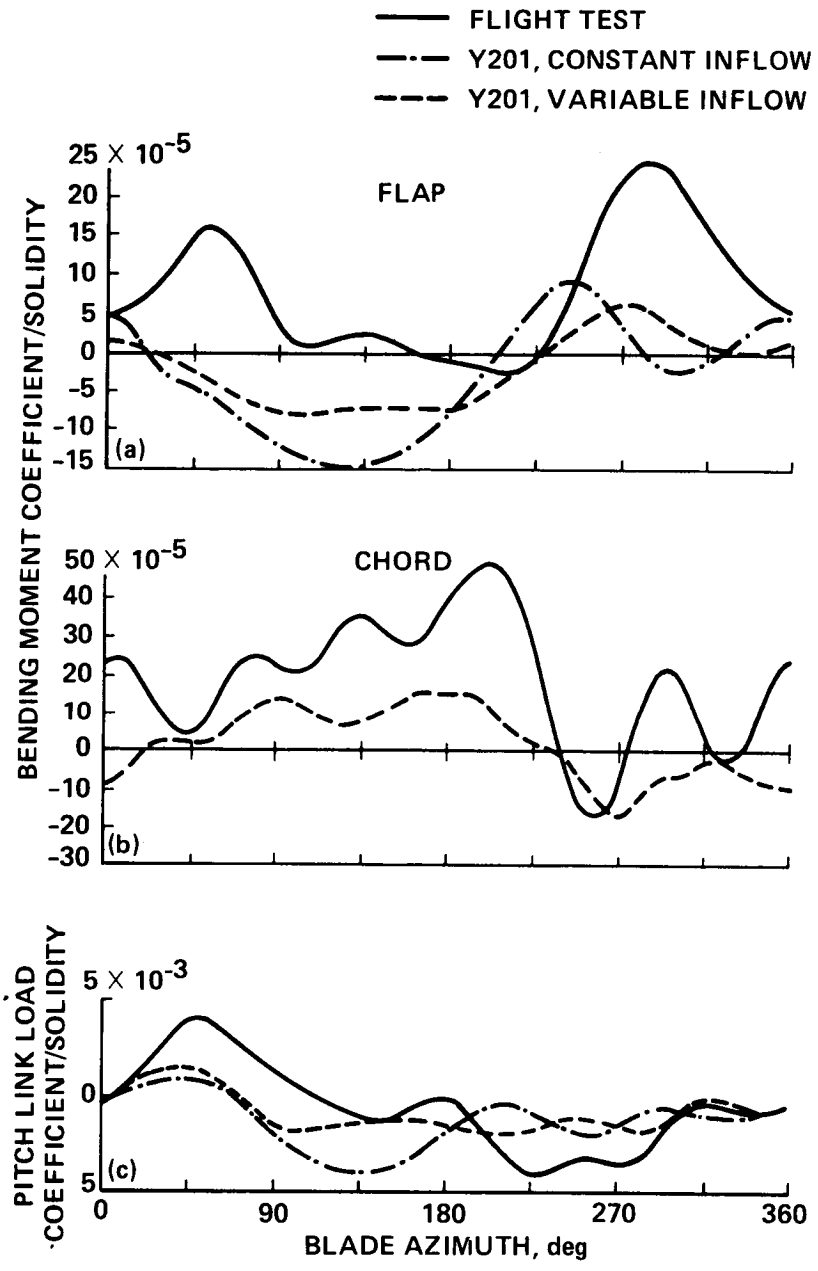

Figure 76.- Comparison of Y201 with flap and chord bending moment and pitch link load waveforms for S-76; μ = 0.338, GW = 8,200 lb (ref. 66). (a) Flap bending moment. (b) Chord bending moment. (c) Pitch link load.

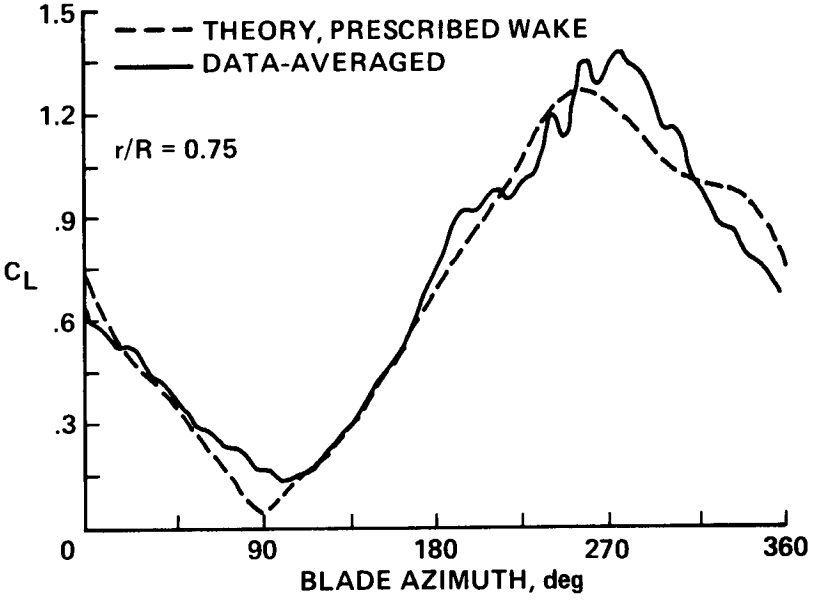

Figure 77.- Comparison of CAMRAD with SA 349-2 blade lift coefficient; $\mu = 0.36$, $C_T/\sigma = 0.071$ (ref. 50).

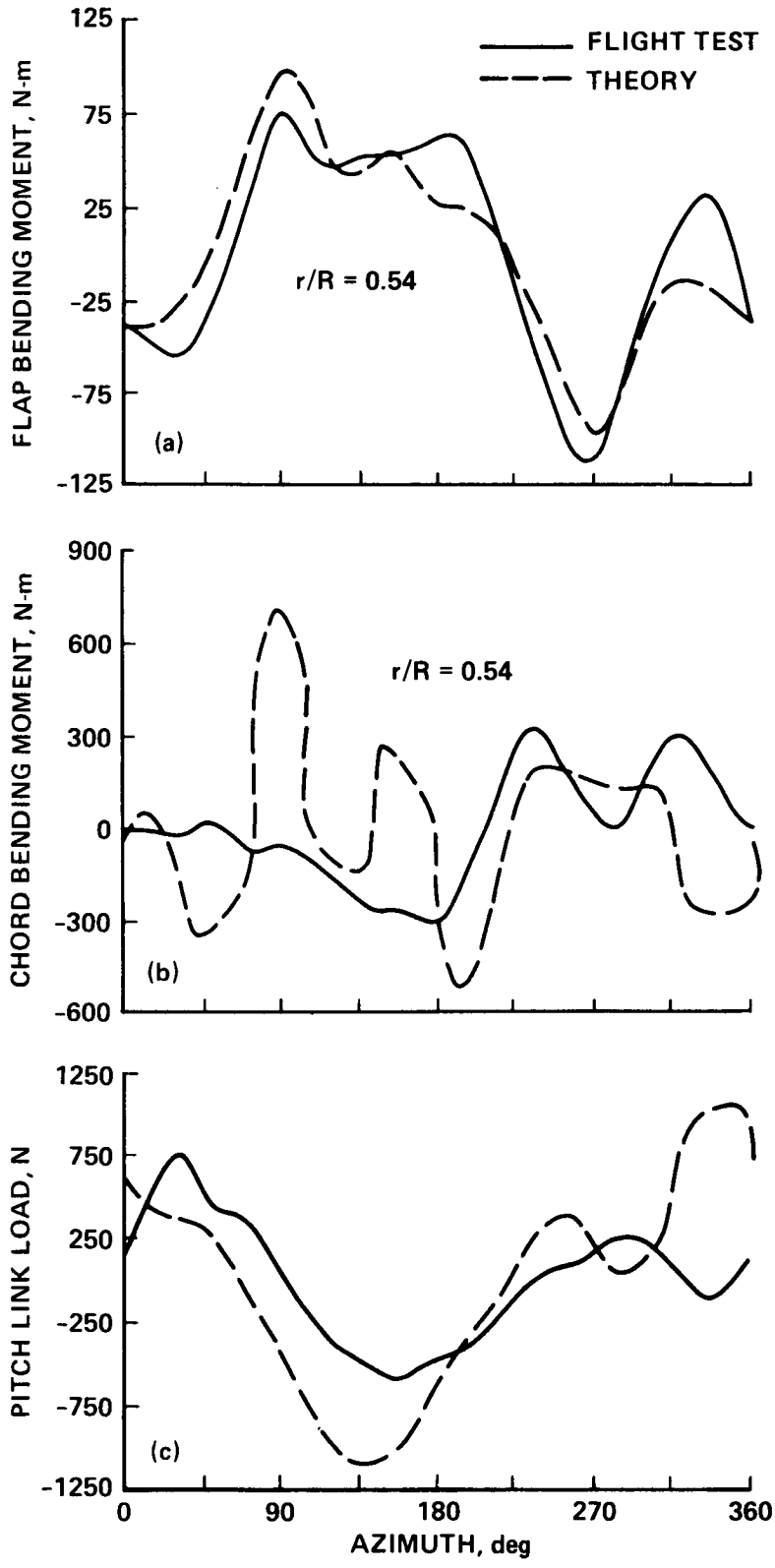

Figure 78.- Comparison of CAMRAD with SA 349-2 blade bending moments and pitch link load; $\mu = 0.36$, $C_T/\sigma = 0.071$ (ref. 50). (a) Flap bending moment; r/R = 0.54. (b) Chord bending moment; r/R = 0.54. (c) Pitch link load.

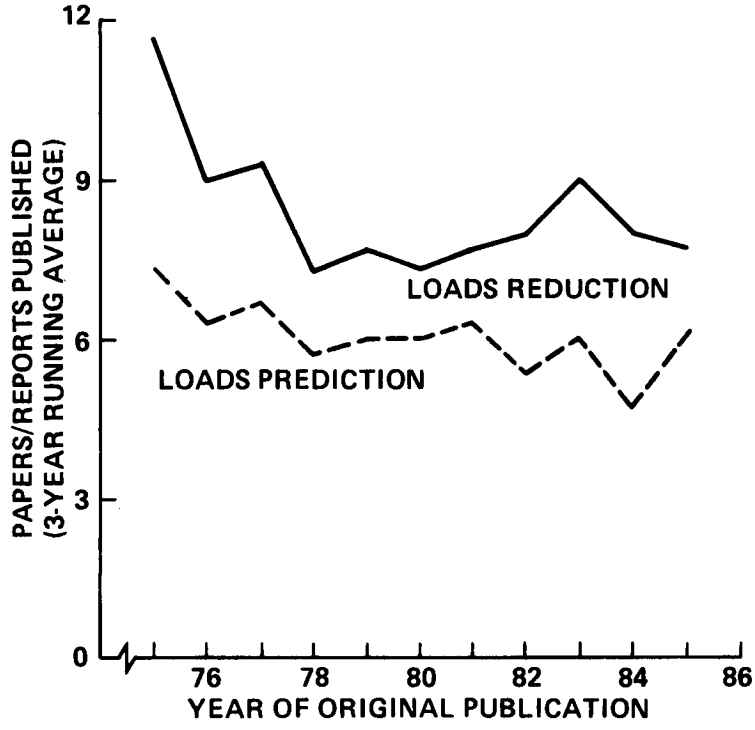

Figure 79.- Rotor loads research papers published per year.